LUANA LUCAS DUTRA

AVALIAÇÃO DE ANTIVIRAIS CONTRA *Acute bee paralysis virus* E AVALIAÇÃO DA INFECÇÃO DE *Apis mellifera* SOB DIFERENTES TEMPERATURAS

Dissertação apresentada à Universidade Federal de Viçosa, como parte das exigências do Programa de Pós-Graduação em Bioquímica Aplicada, para obtenção do título de *Magister Scientiae*.

VIÇOSA
MINAS GERAIS-BRASIL
2019

Ficha catalográfica preparada pela Biblioteca Central da Universidade Federal de Viçosa - Câmpus Viçosa

T
D978a
2019

Dutra, Luana Lucas, 1994-
Avaliação de antivirais contra *Acute bee paralysis virus* e avaliação da infecção de *Apis mellifera* sob diferentes temperaturas / Luana Lucas Dutra. – Viçosa, MG, 2019.
viii, 81 f. : il. (algumas color.) ; 29 cm.

Texto em português e inglês.
Inclui anexo.
Orientador: Tiago Antônio de Oliveira Mendes.
Dissertação (mestrado) - Universidade Federal de Viçosa.
Inclui bibliografia.

1. *Apis mellifera*. 2. *Acute bee paralysis virus*.
3. Temperatura - Efeito fisiológico. I. Universidade Federal de Viçosa. Departamento de Bioquímica e Biologia Molecular. Programa de Pós-Graduação em Bioquímica Aplicada. II. Título.

CDD 22. ed. 595.799

LUANA LUCAS DUTRA

AVALIAÇÃO DE ANTIVIRAIS CONTRA *Acute bee paralysis virus* E AVALIAÇÃO DA INFECÇÃO DE *Apis mellifera* SOB DIFERENTES TEMPERATURAS

Dissertação apresentada à Universidade Federal de Viçosa, como parte das exigências do Programa de Pós-Graduação em Bioquímica Aplicada, para obtenção do título de *Magister Scientiae*.

APROVADA: 12 de julho de 2019.

Weyder Cristiano Santana
(Coorientador)

Poliane Alfenas-Zerbini
(Coorientadora)

Gilza Barcelos de Souza

Tiago Antônio de Oliveira Mendes
(Orientador)

AGRADECIMENTOS

Agradeço a minha irmã Mariana, por estar comigo desde o primeiro dia na escola até o primeiro almoço no RU, e minha irmã Amanda, a razão pela qual quero ser melhor a cada dia. Aos meus pais pelo carinho e suporte durante toda minha vida acadêmica.

Agradeço muito ao meu parceiro Cleyton, que mesmo contrariado me buscava no laboratório as 2:00 da manhã. Meu companheiro diário nos estudos, no trabalho e na vida. Sem nossas longas conversas pela reta sobre a vida, o universo e tudo mais sei que este trabalho não teria sido feito.

Agradeço aos meus amigos Diego, Kaori, Mariana, Thaís, Carla e Leticinha, pela amizade que começou na graduação e que ainda continua. Aos amigos da 6162 Grandville, a melhor casa de Vancouver. Pessoas de todos os cantos do mundo que tive o prazer de conhecer e compartilhar os momentos de alegria e também de saudades de casa. Aos colegas Gustavo, Edgard e Breno, por todas as risadas e por matar minha saudade de falar em português.

Agradeço a todos os colegas de laboratório do LBM e LBSMSB pelos ensinamentos e colaborações. Aos colegas do Foster Lab, em especial Sofia, Lola e Jenny, e todos os profissionais que tive a honra de dividir uma bancada, mesmo que por apenas alguns dias.

Agradeço aos meus professores Tiago, Leonard, Weyder, Poliane, João Paulo e Sergio, pelas orientações e pela paciência. Foi o talento de vocês que me permitiu concluir mais esta etapa da jornada acadêmica.

Agradeço também à Universidade Federal de Viçosa (sempre linda); à agência de fomento FAPEMIG; ao Canadian Bureau for International Education e à University of British Columbia.

A todos que me mandaram notícias sobre abelhas, ou se orgulhavam em contar sobre este projeto, ou apenas ouviram atentos quando eu falava sobre ele: muito obrigada!

RESUMO

DUTRA, Luana Lucas, M.Sc., Universidade Federal de Viçosa, julho de 2019. **Avaliação de antivirais contra *Acute bee paralysis virus* e avaliação da infecção de *Apis mellifera* sob diferentes temperaturas.** Orientador: Tiago Antônio de Oliveira Mendes. Coorientadores: João Paulo Vianna Leite, Poliane Alfenas-Zerbini e Weyder Cristiano Santana.

As abelhas ocidentais *Apis mellifera* são animais de grande valor econômico e ambiental. Sua importância se dá principalmente pelo serviço de polinização, tanto de espécies vegetais silvestres quanto de culturas agrícolas de valor comercial. Nos últimos anos tem ocorrido grandes perdas em colônias ao redor do mundo. Mortes massivas após rigorosos invernos e o desaparecimento de operárias, sem uma ameaça aparente, tem chamado a atenção de pesquisadores e governos. Não existe uma causa específica para estas perdas, trata-se da ação conjunta de fatores como patógenos, mudanças climáticas, nutrição e exposição à pesticidas. Dentre estes fatores destaca-se o *Acute bee paralysis virus* (ABPV). Este patógeno é transmitido pela saliva e fezes dentro da colônia e normalmente provoca uma infecção assintomática. Porém, em altas concentrações o ABPV se torna altamente letal, provocando tremores, escurecimento, paralisia e morte de operárias em poucos dias. A presença do ácaro *Varroa destructor* está associada a infecções sintomáticas de ABPV, dado que o ácaro transmite este vírus diretamente na hemolinfa da abelha através da mordida. Assim, neste trabalho foram avaliadas as mudanças fisiológicas provocadas pelo ABPV sob diferentes temperaturas e propôs-se um antiviral sintético capaz interromper a multiplicação viral. Observou-se que a defesa do hospedeiro contra o ABPV não é mediada pela imunidade humoral ou celular. Abelhas infectadas sob à temperatura normal da colônia (32 ±2ºC) apresentaram maior expressão de ABPV, porém as alterações fisiológicas características da infecção por Dicistrovírus foram observadas no grupo infectado a uma temperatura subótima (26 ±2ºC). Observou-se ainda maior expressão de proteínas da via de choque térmico (HSP) no grupo a 32 ±2ºC, o que indica que a maior concentração do vírus nesta temperatura foi resultado do metabolismo mais ativo do hospedeiro e que a resposta antiviral pode ser mediada por HSPs. Para a busca por um antiviral contra o ABPV utilizou-se o modelo estrutural da cisteíno protease produzida pelo vírus como alvo para potenciais inibidores. A estrutura do alvo foi construída computacionalmente e, após a triagem de 175 moléculas, foram selecionados os cinco ligantes que apresentaram melhor afinidade pelo sítio ativo da enzima. Após o tratamento de operárias infectadas artificialmente com estas moléculas, classificadas como xantenonas, o Composto 2 apresentou significativa redução da

expressão do vírus. Além disso, observou-se que proteínas envolvidas no transporte vesicular de neurotransmissores são *down*-reguladas na presença do vírus. Esta alteração fisiológica não foi observada após o tratamento com o Composto 2, que também aumentou o metabolismo energético da abelha. Assim, neste trabalho foram obtidas novas informações sobre a infecção por ABPV e as alterações que ele provoca no hospedeiro. O antiviral proposto apresentou resultados promissores e estudos futuros serão necessários para confirmar o mecanismo de ação.

ABSTRACT

DUTRA, Luana Lucas, M.Sc., Universidade Federal de Viçosa, July, 2019. **Evaluation of antivirals against *Acute bee paralysis virus* and evaluation of *Apis mellifera* infection under different temperatures.** Adviser: Tiago Antônio de Oliveira Mendes. Co-advisers: João Paulo Vianna Leite, Poliane Alfenas-Zerbini and Weyder Cristiano Santana.

Western bees *Apis mellifera* present high economic and environmental value. Its importance is mainly due to the pollination service that provides for both wild species and crops of commercial value. In recent years significant losses have occurred in colonies around the world. Mass losses after severe winters and the disappearance of workers without an apparent threat have drawn the attention of researchers and governments. There is no specific cause for these losses; it is the joint action of environmental factors such as pathogen, climate change, nutrition, and exposure to pesticides. Among these factors is the *Acute bee paralysis virus* (ABPV). This pathogen is transmitted by saliva and feces inside the colony and usually causes an asymptomatic infection. However, in high concentrations, ABPV becomes highly lethal, causing tremblings, darkening, paralysis, and death of workers in a few days. The presence of the *Varroa destructor* mite is associated with symptomatic ABPV infections, as the mite transmits this virus directly into the honey bee's hemolymph through the bite. Thus, in this work, were evaluated the physiological changes caused by ABPV under different temperatures and proposed a synthetic antiviral capable of interrupting the virus replication. The host defense against ABPV was not mediated by humoral or cellular immunity. Worker bees infected under current colony temperature (32 ±2°C) had high ABPV expression, but the physiological changes characteristic of Dicistrovirus infectionwere observed in the infected group at a suboptimal temperature (26 ±2°C). There was a higher expression of the heat shock proteins (HSP) in the group at 32ºC, which indicates that the higher virus concentration at this temperature could be a result of the more active metabolism of the host and that HSPs could mediate the antiviral response. For the search for an antiviral against the ABPV, were used the structural model of the cysteine protease produced by the virus as a target for potential inhibitors. The target structure was constructed computationally and, after screening for 175 molecules, were selected the five ligands that showed the best affinity for the active site of the enzyme. After treatment of artificially infected worker bees with these molecules, classified as xanthenones, Compound 2 showed a significant reduction of virus expression. Also, the proteins involved in the vesicular transport of neurotransmitters are down-regulated in the presence of the

virus. This physiological change was not observed after treatment with Compound 2, which also increased the energy metabolism of the worker bees. Therefore, this work describe new information on ABPV infection and the changes that it causes in the host. The proposed antiviral presented promising results, and future studies will be needed to confirm the mechanism of action.

SUMÁRIO

1. Introdução geral

Abelhas ocidentais: sua relevância e principais ameaças

As abelhas *Apis mellifera*, também chamadas de abelhas européias ou simplesmente abelhas, são animais fascinantes, em razão de seu comportamento e organização social tão sofisticados. As castas que compõe uma colônia são um interessante caso de polifenismo em resposta à dieta. A alimentação com geleia real desencadeia uma cascata hormonal que leva a formação do fenótipo de rainha, que difere das operárias em tamanho, funcionamentos de alguns órgãos e no comportamento (EVANS e WHEELER, 2001). Estes insetos pertencem à ordem Hymenoptera, que inclui cerca de 100.000 espécies de insetos e realizam partenogênese arrenótoca, onde machos haploides se originam dos ovos não fertilizados e fêmeas diploides se originam dos fertilizados. As abelhas se destacam dos demais insetos especialmente por apresentam grande habilidade cognitiva, sendo capazes de memorizar a localização do alimento e se comunicar através de movimentos denominados de danças (HBGC, 2006).

De acordo com o trabalho publicado em 2006 pelo Consórcio de Sequenciamento do Genoma de Abelhas (The Honeybee Genome Sequencing Consortium), o genoma da *A. mellifera* difere dos demais insetos pelo alto conteúdo de A+T e CpG, porém não apresenta grande parte das famílias de transposons. Além disso, em comparação à *Drosophila* e *Anopheles,* seu genoma possui menos genes relacionados à imunidade inata, enzimas de detoxificação, proteínas de cutícula e receptores gustativos e mais genes para receptores de odor e manipulação de néctar e pólen, o que condiz com sua ecologia e organização social. Apresenta ainda grande similaridade com genes de vertebrados relacionados ao ritmo circadiano, RNA de interferência, metilação de DNA, entre outros.

As abelhas têm ainda um papel crucial como polinizadores de culturas comerciais e espécies selvagens. O impacto da polinização por animais sobre a produção agrícola global chega a USD 153 bilhões anualmente (CALDERONE, 2012; GALLAI et al., 2009), sendo as abelhas melíferas capazes de aumentar em 96% o rendimento de culturas comerciais (POTTS et al., 2010). Além de seu papel como polinizadores, as *Apis melliferas* sustentam um importante mercado de produtos apícolas. No Brasil cerca de USD 444 milhões foram arrecadados com a produção de mel em 2016, garantindo ao país a 9ª posição no ranking mundial de exportadores deste produto (Instituto Brasileiro de Geografia e Estatística, IBGE).

Nas últimas décadas, o crescente número de perdas de colônias despertou o interesse de pesquisadores e governos. Nos EUA, 59% das colônias de *Apis mellifera* foram perdidas no período de 1947 a 2005 e na Europa central houve perda de 25% entre 1985 e 2005 (GOULSON et al., 2015). Apesar destas perdas serem muitas vezes relatadas como casos de CCD (*Colony Collapse Disorder*), este fenômeno ocorreu apenas na América do Norte como uma das causas de perdas após o inverno (MCMENAMIN e GENERSCH, 2015). Os sintomas de CCD são bastante característicos: súbita perda de operárias adultas, principalmente em relação a grande quantidade de prole; notável falta de operárias mortas no interior ou ao redor da colônia, possivelmente devido ao comportamento higiênico de operárias doentes que abandonam a colônia; invasão tardia de pragas ou abelhas vizinhas às colônias enfraquecidas. A infestação pelo ácaro *Varroa destructor*, infecção por *Nosema ceranae* e outros patógenos e a exposição a pesticidas provocam o enfraquecimento das colônias durante o inverno, porém nenhum destes fatores pode até o momento ser apontado como causa principal do CCD (vanENGELSDORP et al., 2009).

As perdas massivas de abelhas tem sido decorrente de um conjunto de fatores, dentre eles as mudanças climáticas e seu impacto sobre a disponibilidade de alimento. Goulson e colaboradores (2015) relacionaram a exposição crônica a pesticidas em doses subletais, em especial os neonicotinoides, com a baixa variabilidade de flores (dieta monótona que leva à maior exposição a inseticidas naturais) como fatores de supressão do sistema imune das abelhas, tornando-as mais suscetíveis a infecções e pragas.

Flores e colaboradores (2019) utilizaram uma tecnologia de monitoramento *in situ* para avaliar o efeito das mudanças climáticas sobre as colônias em região de clima temperado mediterrâneo durante o período de floração em 2016 e 2017. Avaliando parâmetros como peso dos indivíduos, desenvolvimento da prole e quantidade de reservas de mel e pólen, pode-se observar que variações climáticas em regiões quentes, incluindo períodos de seca, ondas de calor e mudanças no período de floração, também promovem danos às abelhas, assim como nas regiões de invernos rigorosos.

Como apresentado anteriormente, as mortes de abelhas estão relacionadas a um conjunto de fatores. Em geral, doenças virais são consideradas as maiores ameaças para as abelhas domesticadas ao redor do mundo. Mais de 20 vírus já foram identificados infectando *A. mellifera* e a maior parte destes apresentam uma fita simples de RNA genômico com polaridade positiva (ssRNA) (TEHEL, BROWN e PAXTON, 2016). Os mais comuns são *Black queen cell virus*

(BQCV), *Israeli acute paralysis virus* (IAPV), *Kashmir bee virus* (KBV), *Acute bee paralysis virus* (ABPV), membros da família *Dicistroviridae*; *Deformed wing virus* (DWV), *Kakugovirus*, *Varroa destructor virus-1/DWV-B*, *Sacbrood virus* (SBV), *Slow bee paralysis virus* (SBPV), que pertencem à família *Iflaviridae*; *Chronic bee paralysis virus* (CBPV) e *Lake Sinai viruses* (LSVs), que não apresentam classificação taxonômica; *Bee macula-like virus* (BeeMLV), membro da família *Tymoviridae*; *Apis mellifera rhabdovirus-1* e *2*, descobertos recentemente e apresentam genoma -ssRNA; *Apis mellifera filamentous virus* (AmFV), o único exemplo já encontrado de vírus de dsDNA em abelhas (MCMENAMIN e FLENNIKEN, 2018).

Vírus da paralisia aguda de abelhas

O vírus causador da paralisia aguda de abelhas (*Acute bee paralysis virus*- ABPV) foi inicialmente identificado na Inglaterra por Bailey e colaboradores em 1963 e é um vírus amplamente encontrado em abelhas da espécie *Apis mellifera* (BAILEY e GIBBS, 1964). Este patógeno geralmente causa uma infecção assintomática nas colônias, mas em altas concentrações pode provocar sérios danos neurológicos como tremores, paralisia e morte dos indivíduos em poucos dias (BAILEY, GIBBS e WOODS, 1963; BAILEY e GIBBS, 1964). A doença se manifesta geralmente em colônias infestadas pelo ácaro *Varroa destructor*, um importante vetor deste e de outros parasitas de abelhas (BAILEY e GIBBS, 1964; de MIRANDA, CORDONI, e BUDGE, 2010). Na Figura 1 pode-se observar que a infestação deste ácaro provoca danos tanto a nível individual, por imunossupressão e transmissão de doenças, quanto a nível coletivo, reduzindo a população das colônias afetadas.

Figura 1- Relação entre nutrição, imunidade e carga viral na presença e ausência do ácaro *Varroa destructor*. O impacto causado pelo ácaro está destacado em marrom. Adaptado de DeGRANDI-HOFFMAN e CHEN (2015).

O ABPV também se dissemina pela saliva de indivíduos infectados e pode ser encontrado tanto em adultos quanto na prole, sendo a prevalência dos vírus em hospedeiros adultos decorrente do comportamento sanitário das abelhas, que eliminam a prole doente dificultando a identificação de larvas contaminadas (de MIRANDA, CORDONI, e BUDGE, 2010). O ABPV já foi identificado em diferentes países como Estados Unidos (EVANS e WHEELER, 2001), França (TENTCHEVA et al., 2004), Áustria (BERÉNYI et al., 2006), Brasil (TEIXEIRA et al., 2008), Hungria (FORGÁCH et al., 2008), Reino Unido (BAKER e SCHROEDER, 2008), Argentina (REYNALDI et al., 2010), e Tailândia (CHANPANITKITCHOTE et al., 2018), sendo o vírus de abelha mais comum na Europa e América do Sul (de MIRANDA, CORDONI, e BUDGE, 2010).

Desde sua descoberta o ABPV tem sido relacionado a grandes perdas em colônias de *A. mellifera* infestadas com o ácaro Varroa. Porém este patógeno também foi encontrado em abelhas do gênero *Bombus* (BAILEY e GIBBS, 1964) e recentemente foi identificado em *Apis cerana* e no ácaro *Tropilaelaps mercedesae* na Ásia (CHANPANITKITCHOTE et al., 2018). *A. cerana e A. mellifera* são as principais espécies de abelhas domesticadas na Ásia e constantemente compartilham espaços naturais e fontes de alimento, favorecendo a transmissão de patógenos entre as espécies (CHANPANITKITCHOTE et al., 2018). O ABPV foi o único vírus encontrado em colônias enfraquecidas de abelhas brasileiras sem ferrão *Melipona scutellaris*, sendo a alimentação artificial de abelhas sem ferrão com produtos apícolas produzidos por *A. mellifera* a provável forma de disseminação do vírus entre as espécies (UEIRA-VIEIRA et al., 2015).

Tendo em vista que as abelhas européias são um conhecido exemplo de insetos eusociais, estes animais apresentam diferentes estratégias para evitar a disseminação de doenças na colônia, como a remoção de larvas doentes, uso de materiais antimicrobianos na construção dos favos, higiene da colônia, entre outros (EVANS et al., 2006). Além dos comportamentos higiênicos, os insetos sociais apresentam mecanismos morfológicos e moleculares de defesa contra patógenos. A resposta imune inata de insetos como *A. mellifera* e *Drosophila* são bem descritas para infecções bacterianas e fúngicas. Em geral a resposta humoral em abelhas é mediada por homólogos das vias Toll e Imd, e a resposta celular é realizada por células especializadas na hemolinfa (hemócitos) (EVANS et al., 2006; AZZAMI et al., 2012). Já a resposta antiviral em insetos ocorre principalmente via RNA de interferência, ativada pela detecção de dsRNA exógeno formado durante a replicação viral (DeGRANDI-HOFFMAN e CHEN, 2015).

O ABPV é formado por um segmento de RNA poliadenilado de 9470 nucleotídeos (GenBank AF150629) contendo duas ORFs (*open reading frame*) codificadoras das enzimas RNA polimerase dependente de RNA (RdRp), helicase e cisteíno peptidase (ORF1), e das quatro proteínas estruturais do capsídeo (ORF2), separadas por uma região de reconhecimento do ribossomo (*Intergenic Ribosome Entry Site*- IRES) (Figura 2) (GOVAN et al., 2000; BONNING, 2009; de MIRANDA, CORDONI, e BUDGE, 2010). Atualmente, o ABPV está classificado na família *Dicistriviridae*, gênero *Aparavirus* (International Committee on Taxonomy of Viruses- ICTV, 2019). Esta família foi reconhecida em 2002 e seus membros apresentam um único segmento de +ssRNA discistrônico e, assim como outros *picorna-like* vírus, possui capsídeo icosaédrico não envelopado, porém a poliproteína estrutural está localizada na extremidade 3' do RNA (BONNING, 2009).

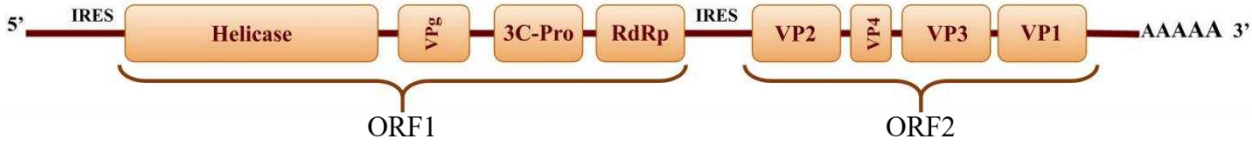

Figura 2- Representação esquemática do genoma de ABPV.

Membros importantes desta família incluem os vírus *Cricket paralysis virus* (CrPC) e *Drosophila C virus*, ambos parasitas de *Drosophila* e modelos bem conhecidos de estudo de interação patógeno-hospedeiro. Nesta família também se encontram os parasitas de abelhas *Israeli acute paralysis virus* (IAPV) e *Kashmir bee virus* (KBV) (KEER e JAN, 2016).

Os Discistrovírus apresentam duas sequências especializadas de RNA denominada IRES, uma na região intergênica (*Intergenic region*- IGR) e outra na extremidade UTR 5', sendo esta responsável por proteger o segmento de RNA da maquinaria de degradação de nucleotídeos da célula hospedeira e permitir a tradução do genoma viral de modo independente de Cap 5' (BONNING, 2009). Ao contrário da IRES presente na extremidade 5', a IGR IRES é altamente estruturada e conservada entre os membros da família *Dicistroviridae*. Esta região possui 3 pseudo-nós (PKI, PKII e PKIII) que juntos formam um domínio de ligação ao ribossomo capaz de manipular todo o processo de ligação e translocação ribossomal sem a presença de fatores de iniciação ou do anti códon AUG, mimetizando o passo fundamental para a tradução no hospedeiro e burlando as rígidas etapas de regulação deste processo, o que favorece o metabolismo do RNA viral em detrimento dos mRNAs do hospedeiro (KEER e JAN, 2016).

O capsídeo viral é composto de 60 capsômeros, cada um formado pelas proteínas estruturais VP1, VP2 e VP3. A proteína VP4 se posiciona na face interna do capsômeros e permite o contato entre a cápsula viral e o genoma. Em Picornavirus observa-se a formação de cânions na superfície da proteína VP1, que não estão presentes nos dicistrovírus, sugerindo um mecanismo de reconhecimento celular diferente entre estas duas famílias virais. A entrada do vírus ocorre via endocitose mediada por clatrina, resultando na liberação do RNA viral no citoplasma e remodelamento do complexo de Golgi para formação de vesículas, que se associam ao RNA viral durante sua replicação (BONNING, 2009).

A expressão do ABPV gera duas poliproteínas que são clivadas pela cisteíno protease viral (3C-Pro). Esta classe de enzimas, responsáveis pela hidrólise da ligação peptídica, está presente nos mais diversos organismos e participa de diferentes processos fisiológicos como inflamação e doenças degenerativas; além de apresentarem papel crucial na virulência de patógenos (ZHAI et al., 2015; VIEIRA, SANTOS e FERREIRA, 2018), tornando-as alvos atrativos para o desenvolvimento de novas drogas.

Modelagem molecular de proteínas

A predição de estrutura tridimensional ou modelagem molecular de proteínas é uma importante área da bioinformática que tem atraído a atenção de pesquisadores, tanto pela necessidade de dados estruturais em aplicações terapêuticas e biotecnológicas, quanto pelo crescente avanço da capacidade de processamento computacional, que possibilita predições cada vez mais acuradas (DU et al., 2015; RAMACHANDRAN, KESAVAN e RAJKUMAR, 2016; WEITZNER et al., 2017).

Tendo em vista que os modelos tridimensionais são gerados a partir da sequência primária, a compreensão do processo de enovelamento de proteínas é essencial para o desenvolvimento de métodos de modelagem molecular eficientes. Com seu notável trabalho, Anfinsen e colaboradores (1961) foram pioneiros nesta área, estabelecendo a relação entre a sequência de aminoácidos e a estrutura nativa de proteínas baseada em princípios termodinâmicos.

Inicialmente, os métodos de predição de estrutura de proteínas eram divididos de acordo com a disponibilidade de informações estruturais em bancos de dados experimentais. Estes podiam ser classificados como modelagem comparativa, predição de enovelamento ou predição por primeiros princípios (*ab initio*). Entretanto os novos métodos podem ser colocados em mais de uma destas

categorias, sendo mais intuitiva a seguinte classificação: métodos independentes de estrutura molde (*template-free*) ou métodos dependentes de estrutura molde (*template-based*) (Figura 3) (VERLI, 2014, p. 162).

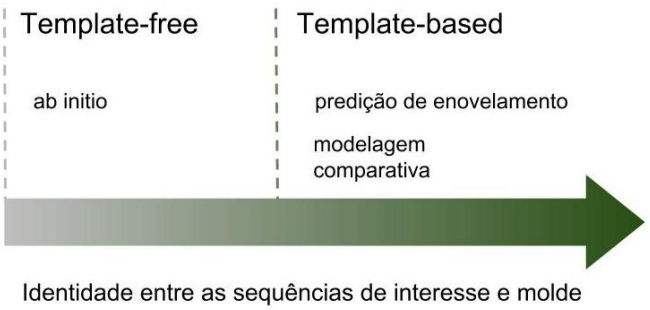

Figura 3- Classificação de métodos de predição de estrutura de proteínas (VERLI, 2014, p. 162).

A modelagem independente de moldes é mais adequada para pequenas proteínas (<200 resíduos) e apesar da acurácia destes métodos de predição terem melhorado nos últimos anos, estes não são eficientes para modelagem de grandes estruturas proteicas (KINCH et al, 2015; MOULT et al, 2016). Entretanto, a modelagem *ab initio* é amplamente utilizada em métodos híbridos, para determinação de regiões da sequência de interesse que não apresentam homologia com estruturas disponíveis, e também para predição de regiões de *loop*. Estas regiões têm papel crucial na interação proteína-alvo e a predição acurada destas estruturas é essencial para estudos como designer de anticorpos, modelagem de canais iônicos, refinamento de estruturas, entre outros (LÓPEZ-BLANCO et al, 2016).

De acordo com a comunidade CASP (*Critical Assessment of Structure Prediction*), um experimento comunitário de larga escala realizado a cada dois anos com o objetivo de avaliar a eficiência dos métodos de modelagem de proteínas (MOULT, 2005), a modelagem baseada em moldes (*template-based*) é a mais utilizada e seu princípio básico desenvolvido nos anos 1970 e 1980 ainda é aplicado (Figura 4) (MODI et al., 2016).

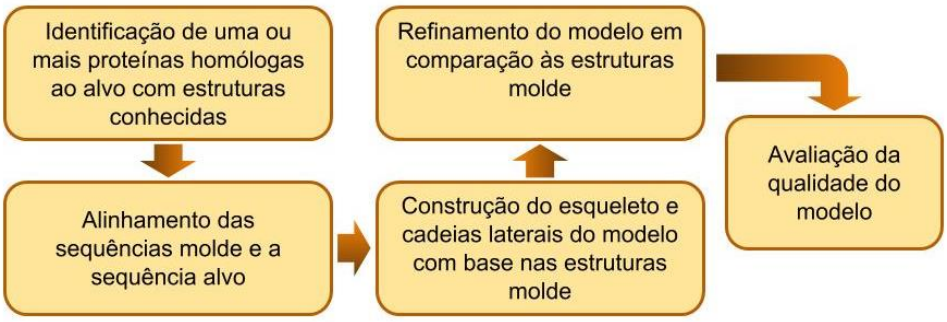

Figura 4- Princípio básico de métodos de modelagem de proteínas *template-based* (MODI et al., 2016).

Nas últimas 7 avaliações realizadas pela comunidade CASP, o servidor I-Tasser foi classificado como servidor número 1 para a predição de estruturas de proteínas (ZHANG, 2008; ROY, KUCUKURAL, ZHANG, 2010; YANG et al., 2015). Neste método, a construção do modelo é feita pela combinação de fragmentos da sequência de interesse com estruturas conhecidas de bancos de dados, incorporando também a função biológica das proteínas molde. O processo de modelagem *template-based* realizado pelo servidor I-Tasser pode ser descrito em três passos: identificação de modelos estruturais na biblioteca do banco de dados PDB (*Protein Data Bank*) pelo alinhamento com fragmentos da sequência de interesse; montagem do modelo com fragmentos de estruturas retiradas dos moldes e construção das regiões sem alinhamento pelo método *ab initio*; agrupamento das estruturas geradas a fim de determinar os estados de baixa energia livre; repetição da simulação, para o refinamento dos modelos de cada grupo e incorporação das informações funcionais das proteínas molde (YANG e ZHANG, 2015).

O I-Tasser apresenta diferentes parâmetros internos de qualidade do modelo gerado, que incorporam informações do modelo final e das etapas da simulação. Os principais parâmetros são: *Z-score* (indica a confiabilidade do alinhamento modelo-molde, os modelos gerados pelo I-Tasser são ordenados de acordo com este parâmetro), *C-score* (indica a precisão global do modelo e varia de -5 < *C-score* < 2]) e *TM-score* (avalia a similaridade entre as estruturas alinhadas e deve variar entre 0,5 < *TM-score* < 1,0) (ZHANG, 2008; YANG e ZHANG, 2015). Entretanto existem também programas de avaliação de qualidade de modelos (MQAPs, do inglês *Model Quality Assessment Programs*), que analisam o modelo final em relação à bancos de dados de estruturas resolvidas experimentalmente (Tabela 1).

Tabela 1- Descrição de programas de avaliação de qualidade de modelos (MQAPs)

MQAPs	Descrição	Acesso online	Referência
Verify 3D	Determina a compatibilidade entre a sequência de aminoácidos e a estrutura tridimensional do modelo, avaliando o ambiente químico de cada resíduo e comparando com estruturas experimentais de qualidade.	http://servicesn.mbi.ucla.edu/Verify3d/	Bowie et al. (1991), Luethy et al. (1992)
PROCHECK	Avalia a qualidade estereoquímica do modelo, analisando a geometria global e resíduo por resíduo e gerando um gráfico de Ramachandran para o modelo analisado.	http://servicesn.mbi.ucla.edu/PROCHECK/	Laskowski et al. (a 1993, b 1996)
ERRAT	Calcula a probabilidade das interações não-covalentes entre os átomos do modelo, baseado nas interações de estruturas cristalográficas de qualidade, gerando um gráfico entre a função de erro e a posição do átomo em uma janela de 9 resíduos e uma avaliação geral do modelo, que deve ser superior a 95%.	http://servicesn.mbi.ucla.edu/ERRAT/	Colovos e Yeates (1993)

Existem algumas abordagens de refinamento de alta resolução que visam vencer os obstáculos entre molde e modelo como rearranjo de regiões de *loop*, modificações de estruturas secundárias ou reagrupamentos de resíduos em regiões específicas, minimizando a energia livre da estrutura e tornado-a mais realista (KRIEGER et al., 2009). Um exemplo de servidor online para este fim é o YASARA Minimization (KRIEGER, KORAIMANN e VRIEND, 2002), que promove a otimização da estrutura sem detrimento dos ângulos e comprimentos das ligações.

Ancoragem molecular: *docking* e *virtual screening*

Ancoragem molecular (ou *docking*) é uma ferramenta amplamente utilizada para a predição computacional do modo de ligação de uma molécula à um receptor de interesse (pose) e da afinidade de ligação molécula-hospedeiro, uma técnica interdisciplinar que envolve conhecimentos de diferentes áreas como bioinformática, biologia molecular, biotecnologia, matemática e ciência da computação (GUPTA, SHARMA, e KUMAR, 2018; LI et al., 2016).

Os fundamentos utilizados nos programas de *docking* para a predição do comportamento de moléculas foram determinados por Karplus, Levitt e Warshel na década de 1970, o que garantiu a estes químicos o Prêmio Nobel de Química em 2013 (FERSHT, 2013). Hoje esta ferramenta tem atraído o interesse de pesquisadores principalmente da área de desenvolvimento de fármacos, pois

a aplicação desta técnica na triagem de novas moléculas torna o processo mais rápido, racional e menos oneroso (GUPTA, SHARMA, e KUMAR, 2018).

A aplicação de estudos *in silico* na área de química medicinal tem sido cada vez mais recorrente, dado o avanço das técnicas de caracterização de biomoléculas e também dos métodos computacionais de análise destes dados. Neste contexto, os métodos computacionais utilizados no desenvolvimento de novos fármacos podem ser divididos em duas categorias: aqueles baseados na estrutura do alvo biológico (*structure-based drug design*- SBDD) e aqueles baseados nas estruturas e informações de atividade biológica de pequenas moléculas, referidas como ligantes (*ligand-based drug design*- LBDD) (Figura 5) (FERREIRA et al., 2015).

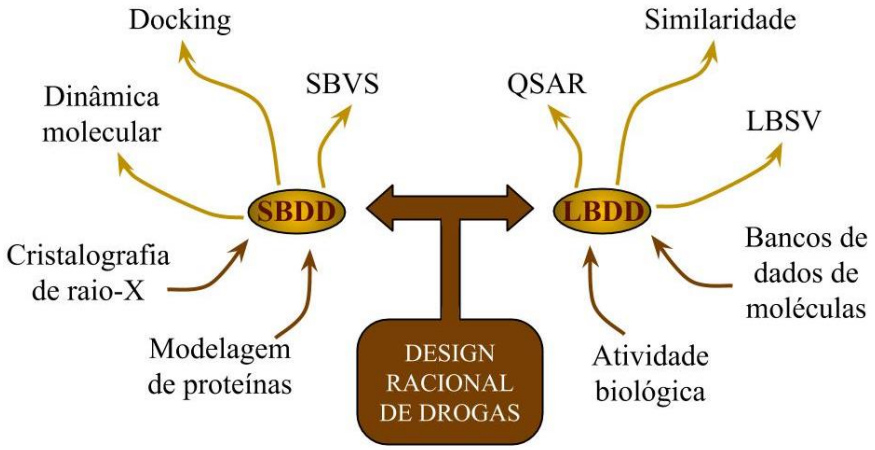

Figura 5- Design racional de drogas se divide em duas categorias: métodos baseados na estrutura do alvo, SBDD, que utiliza estruturas experimentais ou modelos computacionais de proteínas como alvo e seleciona os ligantes por meio de triagem virtual (SBVS), docking ou dinâmica molecular; e os métodos baseados no ligante, LBDD, que utilizam informações de bancos de dados de pequenas moléculas ou dados da literatura sobre a atividade biológica de um conjunto de compostos para estudos de relação estrutura-atividade (QSAR), triagem virtual (LBVS) ou análise de similaridade entre os ligantes.

A ancoragem molecular é o método mais usado na triagem de potenciais fármacos baseado na estrutura do alvo (*structure-based virtual screening*- SBVS), seguido de outros processos computacionais para a seleção dos melhores candidatos (*hits*) como dinâmica molecular, determinação de farmacóforos baseados no receptor ou métodos baseados na estrutura do ligante (LBDD) (Figura 6). Após a identificação das moléculas mais promissoras é necessária a validação experimental dos resultados, seja por testes de atividade biológica ou até a resolução do complexo proteína-ligante por cristalografia de raio-X. Estes dados são usados para guiar os próximos passos, com base na estrutura do alvo modificada pela interação com o ligante ou nas características

estruturais e químicas dessas moléculas, levando a uma nova etapa de síntese e triagem de compostos (FERREIRA et al., 2015; VIEIRA, SANTOS e FERREIRA et al., 2018).

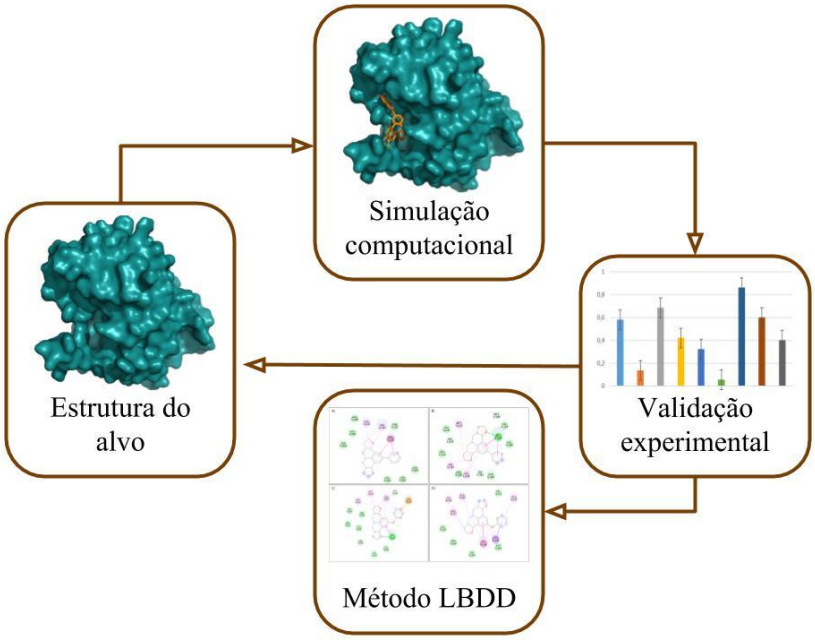

Figura 6- Fluxograma geral de desenvolvimento de drogas baseado na estrutura do alvo. Após a simulação computacional, como *docking* por exemplo, deve ser feita a validação experimental dos compostos mais promissores e em seguida pode-se refazer simulação utilizando a estrutura experimental do complexo alvo-ligante ou aplicar métodos de LBDD, como predição de mapas farmacofóricos, para guiar a síntese de novos compostos.

Gupta e colaboradores (2018) avaliaram os uso de *softwares* de *docking* em publicações no período de 2000 a 2017, sendo AutoDock, Gold e Glide os programas mais citados, com 34%, 20% e 17% respectivamente.

Um típico programa de docking aplica um algoritmo capaz de gerar um conjunto de poses para cada ligante e uma pontuação (função *score*) que ordena estas poses de acordo com a afinidade de ligação da molécula com o alvo (LI et al., 2016).

O Autodock Vina, desenvolvido por Trott e Olson (2010), apresenta melhor desempenho que sua versão anterior, AutoDock4, por ser mais rápido e de maior acurácia. Além de apresentar uma performance de qualidade, este software é bastante popular entre os pesquisadores por ser de fácil utilização e gratuito.

Apesar desta ser uma técnica amplamente empregada em *virtual screening*, a análise dos resultados pode variar de um estudo para o outro. Mugumbate e colaboradores (2013) identificaram

19 moléculas da base de dados ZINC como potenciais inibidores da enzima falcipaína-2 (cisteíno protease de *Plasmodium falciparum*, agente causador da malária) através de *virtual screening* baseado na estrutura do alvo e também na seleção de ligantes com propriedades específicas (*drug-like*). Os *hits* foram selecionados a partir de inspeção visual com software PyMol, escolhendo aqueles que interagiram com o sítio ativo do alvo e com resíduos importantes para a atividade biológica. Porém, apesar do composto mais ativo contra o parasita apresentar atividade inibitória também da enzima, esta foi 50 vezes menor, o que sugere que a falcipaína-2 não é o alvo primário deste composto. Já no trabalho de Wiggers e colaboradores (2013) o composto 2-acetamido tiofeno-3-carboxamida foi identificado como um inibidor não-covalente da cruzaína, cisteíno protease que tem sido um importante alvo na busca de drogas contra doença de Chagas. Neste trabalho foram utilizados métodos de *virtual screening* baseados tanto na estrutura da enzima alvo quanto nas atividades biológicas apresentadas pelos ligantes analisados. Os testes *in vitro* e a resolução do complexo ligante-enzima validaram a predição computacional.

O presente trabalho buscou desenvolver um tratamento antiviral que pudesse ser de fácil aplicação e baixo risco para a saúde das abelhas e qualidade dos produtos apícolas. Aplicando um método racional de desenho de drogas, foi realizada uma busca por compostos em banco de dados de produtos naturais (Grupo de Pesquisa BIOPROS- Universidade Federal de Viçosa) e sintéticos (Grupo de Química Supramolecular e Biomimética- GQSB- Universidade Federal de Viçosa) que tivessem ação inibitória sobre a protease viral. O alvo foi modelado computacionalmente a partir da sequência do genoma definida no banco de dados National Center for Biotechnology Information (NCBI) como região da protease-C3G (NP_066241.1). Após o *docking* e seleção dos melhores ligantes foram realizados testes *in vivo* para a avaliação da atividade antiviral dos compostos.

Neste trabalho também buscou-se avaliar o efeito da temperatura sobre a resposta à infecção artificial por ABPV. Para isso abelhas recém nascidas foram infectadas por alimentação e colocadas em três diferentes temperaturas (26ºC, 33ºC e 36ºC). A diferença de expressão de genes relacionados ao sistema imune, bem como a quantidade de ABPV em cada tratamento foram mensurados por RT-qPCR em um trabalho prévio do grupo de pesquisa (estes dados foram publicados em conjunto com os resultados produzidos no presente trabalho). Com base nestes resultados, buscou-se avaliar os efeitos fisiológicos através da quantificação de proteínas totais,

utilizando cromatografia líquida acoplada a espectrometria de massas (LC-MS/MS). Os resultados obtidos serão apresentados nas próximas seções.

Referências

ANFINSEN, C. B; HABER, E; SELA, M; WUITE, F. H. Jr. The kinetics of formation of native ribonuclease during oxidation of the reduced polypeptide chain. **Proceedings of the National Academy of Sciences**, v. 15, n. 47, p. 1309-1314, 1961.

AZZAMI, K; RITTER, W; TAUTZ, J; BEIER, H. Infection of honey bees with *Acute bee paralysis virus* does not trigger humoral or cellular immune responses. **Archives of Virology**, v. 157, n. 4, p. 689-702, 2012.

BAILEY, L; GIBBS, A. J. Acute infection of bees with paralysis virus. **Journal of Insect Pathology**, v. 6, n. 4, 1964.

BAILEY, L; GIBBS, A. J; WOODS, R. D. Two Viruses from adult honey bees (*Apis mellifera* Linnaeus). **Virology**, v. 21, p. 390-395, 1963.

BAKER, A; SCHROEDER, D. Occurrence and genetic analysis of picorna-like viruses infecting worker bees of *Apis mellifera* L. populations in Devon, South West England. **Journal of Invertebrate Pathology,** v. 98, p. 239-242, 2008.

BERÉNYI, O; BAKONYI, T; DERAKHSHIFAR, I; KÖGLBERGER, H; NOWOTNY, N. Occurrence of six honeybee viruses in diseased Austrian apiaries. **Invertebrate Microbiology**, v. 72, p. 2414-2420, 2006.

BONNING, B. C. The *Dicistroviridae*: an emerging family of invertebrate viruses. **Virologica Sinica**, v. 24, n. 5, p. 415-427, 2009.

CALDERONE, N. W. Insect pollinated crops, insect pollinators and US agriculture: Trend analysis of aggregate data for the period 1992-2009. **PLoS ONE**, v. 7, n. 5, p. e37235, 2012.

CHANPANITKITCHOTE, P; CHEN, Y; EVANS, J. D; LI, W; LI J; HAMILTON, M; CHANTAWANNAKUL, P. *Acute bee paralysis virus* occurs in the Asian honey bee *Apis cerana* and parasitic mite *Tropilaelaps mercedesae*. **Journal of Invertebrate Pathology**, v. 151, p. 131-136, 2018.

de MIRANDA, J. R; CORDONI, G; BUDGE, G. The *Acute bee paralysis virus-Kashmir bee virus-Israeli acute paralysis virus* complex. **Journal of Invertebrate Pathology**, v. 103, p. S30-S47, 2010.

DeGRANDI-HOFFMAN, G; CHEN, Y. Nutrition, immunity and viral infections in honey bees. **Current Opinion in Insect Science**, v. 10, p. 170-175, 2015.

DU, H; BRENDER, J. R; ZHANG, J; ZHANG, Y. Protein structure prediction provides comparable performance to crystallographic structures in docking-based virtual screening. **Methods**, v. 71, p. 77-84, 2015.

EVANS, J. D. and WHEELER, D. E. Gene expression and the evolution of insect polyphenisms. **BioEssays**, v. 21, 2001.

EVANS, J. D; ARONSTEIN, K; CHEN, Y. P; HETRU, C; IMLER, J. L; JIANG, H; KANOST, M; THOMPSON, G. J; ZOU, Z; HULTMARK, D. Immune pathways and defence mechanisms in honey bees *Apis mellifera*. **Insect Molecular Biology**, v. 15, p. 645-656, 2006.

FERREIRA, L. G; dos SANTOS, R. N; OLIVIA, G; ANDRICOPULO, A. D. Molecular docking and structure-based drug design strategies. **Molecules**, v. 20, p. 13384-13421, 2015.

FERSHT, A. R. Profile of Martin Karplus, Michael Levitt, and Arieh Warshel, 2013 Nobel laureates in chemistry. **Proceedings of the National Academy of Sciences**, v. 110, n. 49, p. 19656-19657, 2013.

FLORES, J. M; GIL-LEBRERO, S; GÁMIZ, V; RODRÍGUES, M. I; ORTIZ, M. A; QUILES, F. J. Effect of the climate change on honey bee colonies in a temperate Mediterranean zone assessed through remote hive weight monitoring system in conjunction with exhaustive colonies assessment. **Science of the Total Environment**, v. 653, p. 1111–1119, 2019.

FORGÁCH, P; BAKONYI, T; TAPASZTI, Z; NOWOTNY, N; RUSVAI, M. Prevalence of pathogenic bee viruses in Hungarian apiaries: Situation before joining the European Union. **Journal of Invertebrate Pathology**, v. 98, n. 2, p. 235-238, 2008.

GALLAI, N; SALLES, J. M; SETTELE, J; VAISSIÈRE, B.E. Economic valuation of the vulnerability of world agriculture confronted with pollinator decline. **Ecological economics**, v.6, n. 8, p. 810-821, 2009.

GOULSON, D; NICHOLLS, E; BOTÍAS, C; ROTHERAY, E. L. Bee declines driven by combined stress from parasites, pesticides, and lack of flowers. **Science**, v. 347, n. 6229, 2015.

GOVAN, V. A; LEAT, N; ALISOPP, M; DAVISON, S. Analysis of the complete genome sequence of *Acute bee paralysis virus* shows that it belongs to the novel group of insect-infecting RNA viruses. **Virology**, v. 277, p. 457-463, 2000.

GUPTA, M; SHARMA, R; KUMAR, A. Docking techniques in pharmacology: how much promising? **Computational Biology and Chemistry,** v. 76, p. 210-217, 2018.

Honeybee Genome Sequencing Consortium. Insights into social insects from the genome of the honeybee *Apis mellifera*. **Nature***,* v. 443, p. 931–949, 2006.

KERR, C. H; JAN, E. Commandeering the ribosome: lessons learned from *Dicistroviruses* about translation. **Journal of Virology**, v. 90, n. 12, p. 5538-5540, 2016.

KINCH, L. N; LI, W; MONASTYRSKYY, B; KRYSHTAFOVYCH, A; GRISHIN, N. V. Evaluation of free modeling targets in CASP11 and ROLL. **Proteins**, v. 34, p. 51-66, 2015.

KRIEGER, E; JOO, K; LEE, J; LEE, J; RAMAN, S; THOMPSON, J; TYKA, M; BAKER, D; KARPLUS, K. Improving physical realism, stereochemistry, and side-chain accuracy in homology modeling: four approaches that performed well in CASP8. **Proteins**, v. 77, p. 114-122. 2009.

KRIEGER, E; KORAIMANN, G; VRIEND, G. Increasing the precision of comparative models with YASARA NOVA-a self-parameterizing force field. **Proteins**, v. 47, n. 3, p. 393-402, 2002.

LI, H; LEUNG, K. S; WONG, M. H; BALLESTER, P. J. Correcting the impact of docking pose generation error on binding affinity prediction. **BCM Bioinformatics**, v. 17, p. 13-25, 2016.

LÓPEZ-BLANCO, J. R; CANOSA-VALLS, A. J; LI, Y; CHACÓN, P. RCD+: Fast loop modeling server. **Nucleic Acids Research**, v. 44, p. W395-W400, 2016.

MCMENAMIN, A. J; FLENNIKEN, M. L. Recently identified bee viruses and their impact on bee pollinators. **Current Opinion in Insect Science**, v. 26, p. 120-129, 2018.

MCMENAMIN, A. J; GENERSCH, E; Honey bee colony losses and associated viruses. **Current Opinion in Insect Science**, v. 8, p. 121-129, 2015.

MODI, V; XU, Q; ADHIKARI, S; DUNBRACK, R. L. Jr. Assessment of template-based modeling of protein structure in CASP11. **Proteins**, v. 84, p. 200-220, 2016.

MOULT, J. A decade of CASP: progress, bottlenecks and prognosis in protein structure prediction. **Current Opinion in Structural Biology**, v. 15, p. 285-189, 2005.

MOULT, J; FIDELIS, K; KRYSHTAFOVYCH, A; SCHWEDE, T; TRAMONTANO, A. Critical assessment of methods of protein structure prediction: progress and new directions in round XI. **Proteins**, v. 84, p. 4-14, 2016.

MUGUMBATE, G; NEWTON, A. S; ROSENTHAL, P. J; GUT, J; MOREIRA, R; CHIBALE, K; GUEDES, R. C. Novel anti-plasmodial hits identified by virtual screening of the ZINC database. **Journal of Computer-Aided Molecular Design**, v. 27, p. 859-871, 2013.

POTTS, S. G; BIESMEIJER, J. C; KREMEN, C;NEUMANN, P;SCHWEIGER, O. KUNIN, W. E. Global pollinator declines: trends, impacts and drivers. **Trends in Ecology and Evolution**, v. 25, p. 345-353, 2010.

RAMACHANDRAN, B; KESAVAN, S; RAJKUMAR, T. Molecular modeling and docking of small molecule inhibitors against NEK2. **Bioinformation**, v. 12, n. 2, p. 62-68, 2016.

REYNALDI, F. J; SGUAZZA, G. H; PECORARO, M. R; TIZZANO, M. A; GALOSI, C.M. First repost of viral infections that affect argentine honeybees. **Environmental Microbiology Reports**, v. 2, n. 6, p. 749-751, 2010.

ROY, A; KUCUKURAL, A; ZHANG, Y. I-TASSER: a unified platform for automated protein structure and function prediction. **Nature protocols**, v. 5, n. 4, p. 735-738, 2010.

TEHEL, A; BROWN, M. J. F. AND PAXTON, R. J. Impact of managed honey bee viruses on wild bees. **Current Opinion in Virology**, v. 19, p. 16-22, 2016.

TEIXEIRA E. W; CHEN, Y; MESSAGE, D; PETTIS, J; EVANS, J. D. Virus infection in Brazilian honey bees. **Journal of Invertebrate Pathology**, v. 99, p. 117-119, 2008.

TROTT, O; OLSON, A. J. AutoDock Vina: improving the speed and accuracy of docking with a new scoring function, efficient optimization, and multithreading. **Journal of Computational Chemistry**, v. 31, p. 455-491, 2010.

UEIRA-VIEIRA, C; ALMEIDA, L. O; de ALMEIDA, F. C; AMARAL, I. M. R; BRANDEBURGO, M. A. M; BONETTI, A. M. Scientific note on the first molecular detection of the A*cute bee paralysis virus* in Brazilian stingless bees. **Apidologie**, v. 46, n. 5, p. 628-639, 2015.

VanENGELSDORP, D; EVANS, J. D; SAEGERMAN, C; MULLIN, C; HAUBRUGE, E; NGUYEN, B. K; FRAIZER, M; FRAIZER, J; COX-FOSTER, D; CHEN, Y; UNDERWOOD, R; TARPY, D. R; PETTIS, J. S. Colony collapse disorder: a descriptive study. **PLoS ONE**, v. 4, n. 8, 2009.

VERLI, Hugo. Bioinformática: da Biologia à Flexibilidade Molecular. 1ª Edição. São Paulo: Sociedade Brasileira de Bioquímica e Biologia Molecular - SBBq, 2014.

VIEIRA, R. P; SANTOS, V. C; FERREIRA, R. S. Structure-based approaches targeting parasite cysteine proteases. **Current Medicinal Chemistry**, v. 25, p. 1-18, 2018.

WEITZNER, B. D; JELIAZKOV, J. R,, LYSKOV, S; MARZE, N; KURODA, D; FRICK, R; ADOLF-BRYFOGLE, J; BISWAS, N; DUNBRACK, R. L. JR, GRAY, J. J. Modeling and docking of antibody structures with Rosetta. **Nature protocols**, v. 12, n. 2, p. 401-416, 2017.

WIGGERS, H. J; ROCHA, J. R; FERNANDES, W. B; SESTI-COSTA, R; CARNEIRO, Z. A; CHELESKI, J; DA SILVA, A.B; JULIANO, L; CEZARI, M. H; SILVA, J. S; MCKERROW, J. H; MONTANARI, C. A. Non-peptidic cruzain inhibitors with trypanocidal activity discovered by virtual screening and in vitro assay. **PLoS neglected tropical diseases**, v. 7, n.8, 2013.

YANG J; ZHANG, Y. I-TASSER server: new development for protein structure and function predictions. **Nucleic Acids Research**, v. 43, p. W175-W181, 2015.

YANG, J; YAN, R; ROY, A; XU, D; POISSON, J; ZHANG, Y. The I-TASSER Suite: protein structure and function prediction. **Nature methods**, v. 12, 2015.

ZHAI, Y; ZHAO, X; CUI, Z; WANG, M; WANG, Y; LI, L; SUN, Q; YANG, X; ZENG, D; LIU, Y; SUN, Y; LOU, Z; SHANG, L; YIN, Z. Cyanohydrin as an anchoring group for potent and selective inhibitors of *enterovirus* 71 3c protease. **Journal of Medicinal Chemistry**, v. 59, p. 9414-9420, 2015.

ZHANG, Y. I-TASSER server for protein 3D structure prediction. **BMC Bioinformatics**, v. 9, n. 40, 2008.

Title:

2. Increase of honey bee infection by *Acute bee paralysis virus* in warmer condition is associated with efficient virus biosynthesis and reduction of immune response

Authors and affiliations:

Luana Lucas Dutra[1], Ananda Pereira Aguilar[1], Cecília Fausto[1], Amanda Martins da Cruz Souza[2], Dênia Pires de Almeida[3], Isabel Samila Lima Castro[3], Kyung-Mee Moon[4], Poliane Alfenas-Zerbini[5], Leonard Foster[4], Weyder Cristiano Santana[6], Tiago Antônio de Oliveira Mendes[1]*

1 Department of Biochemistry and Molecular Biology, Universidade Federal de Viçosa, Viçøsa, Minas Gerais, Brazil.

2 Department of Biochemistry and Molecular Biology, Universidade Federal de Viçosa, Viçøsa, Minas Gerais, Brazil.

3 Department of General Biology, Universidade Federal de Viçosa, Viçøsa, Minas Gerais, Brazil.

4 Department of Biochemistry and Molecular Biology, University of British Columbia, Vancouver, British Columbia, Canada.

5 Department of Microbiology, Universidade Federal de Viçosa, Viçosa, Minas Gerais, Brazil.

6 Department of Enthomology, Universidade Federal de Viçosa, Viçosa, Minas Gerais, Brazil.

***Correspondent author: tiagoaomendes@ufv.br**

Abstract

The *Acute bee paralysis virus* (ABPV) is a worldwide distributed pathogen that is associated with significant losses of colonies. Infection usually occurs asymptomatically; however, the ABPV may become more virulent and lethal in response to external stressors such as the presence of *Varroa destructor* mite. We used the method of artificial infection of bees by ABPV through feeding in different temperatures and evaluated the expression of genes related to immune response and also the expression of proteins in response to infection on different temperature. We observed that the decrease in temperature could suppress the carbohydrates catabolism and the energy production process. That effect makes the honey bee more susceptible to the physiologic changes

produced by the infection. ABPV depress the metabolism of ATP, deviates the biosynthetic machinery of the host and the typical symptoms of trembling and paralysis could be a result of the modification of protein expression evolved in processes of vesicular transport and muscle system.

Introduction

The influence of animal pollination on global agricultural production reaches USD 153 billion annually (CALDERONE, 2012; GALLAI et al., 2009). Domesticated bees are able to increase crop yields by 96% (POTTS et al., 2010). In addition to their role as pollinators, the trade of honey and other bee products are a valuable business. In Brazil, around USD 95,181 thousand was collected from honey production in 2018, providing the country the 9th position in the world exporter ranking of this product according to International Trade Center (http://www.intracen.org/)

In general, viral diseases are one of the highest threat to domesticated bees. More than 20 viruses have been identified in *Apis mellifera* and most of them have a positive sense single-strands RNA genome (TEHEL, BROWN, and PAXTON, 2016; MCMENAMIN and FLENNIKEN, 2018). The most common bee viruses belong to the families *Dicistroviridae*; *Iflaviridae* and *Tymoviridae*; besides the *Chronic bee paralysis virus* and *Lake Sinai viruses*; that are taxonomically unclassified (MCMENAMIN and FLENNIKEN, 2018).

The *Dicistroviridae* family has some important examples of insect pathogens such as *Cricket paralysis virus* and *Drosophila C virus*, both parasites of Drosophila and well-known models of pathogen-host interaction. In this family, there are also the bee pathogens *Israeli acute paralysis virus*, *Kashmir bee virus* and *Acute bee paralysis virus* (ABPV) (de MIRANDA, CORDONI, BUDGE, 2010).

The ABPV was primarily identified in England by Bailey and coworkers in 1963. This is a virus widely spread in the honey bee *A. mellifera* (BAILEY and GIBBS, 1964) and usually causes an asymptomatic infection in the colonies, but at high quantity can cause serious neurological damage such as tremors, paralysis, and death in a few days (BAILEY, GIBBS and WOODS, 1963; BAILEY and GIBBS, 1964). The disease usually manifests in colonies infested by the *Varroa destructor* mite, an important vector of ABPV and other honey bee viruses (BAILEY and GIBBS, 1964; de MIRANDA, CORDONI, BUDGE, 2010).

ABPV also spreads through saliva of infected individuals and can be found in both adults and offspring (de MIRANDA, CORDONI, BUDGE, 2010). This virus has a worldwide spread

(EVANS and WHEELER, 2001; TENTCHEVA et al., 2004; BERÉNYI et al., 2006; TEIXEIRA et al., 2008; FORGÁCH et al., 2008; BAKER and SCHROEDER, 2008; REYNALDI et al., 2010 and CHANPANITKITCHOTE et al., 2018) and is the most common honey bee virus in Europe and South America (de MIRANDA, CORDONI, BUDGE, 2010).

In general, humoral response in honey bees is mediated by antimicrobial peptides (AMPs) and cellular response is performed by specialized hemolymph cells that work on the process of melanization and phagocytosis (EVANS et al., 2006; AZZAMI et al., 2012). The major homologs components of the Toll, Imd, JNK, and JAK/STAT pathways are present in *A. mellifera* genome and the expression of effector genes like AMPs abaecin, defensin, hymenoptaecin, and the enzymes phenoloxidase and lysozyme are upregulated in response to an immune challenge (EVANS et al., 2006; BRUTSCHER, DAUGHENBAUGH, and FLENNIKEN, 2015). However, the antiviral response in honey bees seems to occur mainly through RNA interference, activated by detection of exogenous dsRNA formed during RNA viruses' replication (DeGRANDI-HOFFMAN and CHEN, 2015).

Climate change is a significant threat to bees. The temperature changes, rainless periods, or severe winter affect the availability of flowers and, consequently, the production of nectar and pollen (REDDY et al., 2012; GOULSON et al., 2015; FLORES et al., 2019). Thermal tolerance has a direct influence on foraging activity, and climate change can also affect bees' physiology and susceptibility to diseases and pests (Le CONTE and NAVAJAS, 2008; REDDY et al., 2012).

This work aims to evaluate the effect of the temperature over the infection by ABPV on honey bee *A. mellifera*. We tested the artificial infection by feeding the honey bees with a viral suspension and maintained them in different temperatures for 24 and 48 hours. After the infection time, we evaluated the viral charge and the expression of the immune-related genes. The physiologic effects of the temperature and the infection were also measured by label-free proteomics.

Material and methods

Identification of the ABPV:

The ABPV was previously identified in symptomatic honey bees from an apiary in Passa Quatro-MG (Brazil) in August 2017 by RT-PCR (SOUZA et al., manuscript in preparation). The

honey bees were kept on ethanol at 4ºC until the following procedures. The total RNA extraction of six honey bees was done with the TRIzol commercial reagent (Invitrogen). The cDNA was then synthesized using MultiScribe Reverse Transcriptase (Applied Biosystems) with the oligo dT primer, according to the manufacturer's instructions. The primers used for PCR reaction were described by Teixeira et al. (2008) and are specific for ABPV identified in Brazil, generating a 500 bp amplicon (ABPV-F 5'-TCTGATGCTGAAGAGAGAAA-3'; ABPV-R 5'- AATCATCATT GCCGGCTCTA-3'). The absence of other common viruses was confirmed in a previously work by RT-PCR (SOUZA et al., manuscript in preparation).

After the PCR amplification, the fragment was purified using GFX PCR DNA and Gel Band Purification kit (Amersham Biosciences) according to the manufacturer's instructions. The 500 bp DNA fragment was cloned into the pGEM-T Easy vector (Promega) according to the manufacturer's instructions. Next, the vector carrying the insert was placed in *E. coli* DH5 competent cells by heat shock transformation. The transformed cells grow on liquid Luria-Bertani (LB) (Fisher) medium for 1 hour at 37° C. After that, the supernatant was discarded and the cells were resuspended in a small volume and plated on solid LB medium containing ampicillin (100 μg/ml), X-gal (80 μg/ml) and 0.5 mM IPTG. The plates were incubated at 37° C for 16 hours and the white colonies were selected and cultured in liquid LB for 14 hours under agitation at 37° C. Plasmids were purified (Wizard® Plus SV Minipreps DNA Purification System, Promega) and sequenced (Myleus Facility) and the fragment sequence was used as a template for the construction of the ABPV-specific RT-qPCR primers (Table 1).

Table 1- Sequence of the primers used for RT-qPCR

Name	Sequence (5'- 3')	Gene (efficiency %)	Reference
β-actin F	TGCCAACACTGTCCTTTCTG	β-actin (76.3%)	Lourenço et al., 2008
β-actin R	AGAATTGACCCACCAATCCA		
ABPV-F	ACTGCGCTTACGGATTTGAC	171pb Amplicon specific for ABPV (100%)	This work.
ABPV-R	TCTTGGTGTCAAAAAGCTTCG		
ABA-F	CAGCATTCGCATACGTACCA	Abaecin (78.4%)	Evans et al., 2006
ABA-R	GACCAGGAAACGTTGGAAAC		
DEF-F	TGTCGGCCTTCTCTTCATGG	Defensin (74.7%)	Yang and Cox-Foster, 2005
DEF-R	TGACCTCCAGCTTTACCCAAA		
HYM-F	CTCTTCTGTGCCGTTGCATA	Hymenoptaecin (73.6%)	Evans et al., 2006
HYM-R	GCGTCTCCTGTCATTCCATT		
PO-F	AATCCATTACCTGAAATTGATGCTTAT		

PO-R	TAATCTTCCAACTAATTCATACGCTCTT	Phenoloxidase (74.0%)	Yang and Cox-Foster, 2005
LYS-F	ACACGGTTGGTCACTGGTCC	Lysozyme (67.7%)	Yang and Cox-Foster, 2005
LYS-R	GTCCCACGCTTTGAATCCCT		

Extraction of ABPV from Passa Quatro-MG (Brazil):

For this step, we collected 10 symptomatic bees from the Passa Quatro-MG apiary and grounded them with 10 mL of the carbon tetrachloride and water (1: 4, v/v). The mixture was filtered on gauze and centrifuged at 3000 rpm for 10 minutes. The organic fraction was discarded (BAILEY, GIBBS, WOODS, 1963).

In order to prepare a suspension with higher viral load, we carried the first infection on honey bees from Viçosa-MG (Brazil). For this, 36 newborn bees were selected from colonies where the absence of ABPV was previously confirmed by RT-PCR. They were anesthetized by chilling on ice, and subsequently, volumes of 1 μL of the aqueous fraction previously described were injected laterally between the second and the third tergite into the hemocoel of each bee, using a capillary glass coupled to a microinjector. The workers were kept in a plastic container coupled to a 2 mL tube containing a 50% sucrose solution and stored at 32° ±2ºC for 4 days. The food was replaced daily.

Every 24 hours, the bees were inspected and those with paralysis and tremors were removed and stored at -20° C. At the end of the fourth day all bees were stored at -20º C. Thereafter, the virus extraction step was performed again and the aqueous phase (ABPV suspension) was used for the artificial infection by feeding.

Artificial infection of workers by feeding:

The worker bees were collected from the same colony described above in the apiary of the Federal University of Viçosa (Brazil), all with the same age (until 12 hours after birth). Initially, we tested three temperatures: 26º ±2ºC, 32º ±2ºC, and 36º ±2ºC. On each test temperature were placed 5 plastic cages with 6 honey bees on each. During the first 48 hours (induction time), all groups got the same diet (50% sucrose solution). After that, the food from the groups at each temperature was replaced by 2 mL of a mixture of 50% sucrose solution and ABPV suspension or 50% sucrose solution and water, in a proportion of 3:1, *ad libitum*. At each temperature, an initial group (0h) was collected, which received only the temperature change treatment during the

induction time, without any infection. The worker bees of each group were divided into triplicates, each pool containing 2 bees, and stored at -20°C after the periods of 0 h, 24 h and 48 h.

Real Time Quantitative PCR (RT-qPCR) of immune genes:

Viral load at different temperatures as well as the expression of immunological response genes were measured by RT-qPCR using the primers described in Table 1. Total RNA extraction from each pool of bees was performed using commercial TRIzol reagent (Invitrogen) according to the manufacturer's instructions. The fraction containing DNA + proteins were stored at -20° C for the subsequent proteomics study. The RNA of two samples from each group was quantified with Qubit RNA Assay kit and the cDNA was synthesized from 1.5 µg of RNA. The qPCR reaction was done in a 96-well plate using the 7500 Real-Time PCR System (Applied Biosystems, Thermo Fisher Scientific, USA) by the standard curve method applying the GoTaq® qPCR kit Master Mix (Promega, Madison, USA). In these reactions, 1 µL of cDNA with a concentration of 20 ng/µL and 0.5 µL of each primer (2 µM) (Table 1) was applied, a total of 10 µL in each reaction. The thermocycler program was started at 95° C for 10 minutes followed by 40 cycles of 95° C for 15 seconds and 60° C for 1 minute.

The amplification results were expressed as the *threshold cycle* (Ct) value. The quantification was done by a standard curve (log_{10}DNA concentration (ng) vs. *threshold cycle* (Ct) value) obtained for each genes described in Table 1. The R^2 and the reaction efficiency ($E = (10^{-1/SLOPE})-1$) was calculated for each primer. The results of ABPV and the immune genes concentration in each sample were normalized by the endogenous gene β-actin (Relative expression) (de SOUZA et al., 2019). The infected group was compared to the control group at the same condition and between the different temperatures by t-test (p-value < 0.05), and the graphs were prepared using the GraphPad Prism 5.0 software (GraphPad Inc.) (de SOUZA et al., 2019).

Proteomic profile:

In order to evaluate the difference of protein expression on each group, we performed a label-free proteomic study. The total protein extraction was performed with commercial TRIzol® reagent (Invitrogen) according to the manufacturer's instructions. Protein pellets were resuspended in 200 µL of solubilization buffer (6M urea / 2M thiourea in 0.1M Tris pH 7.8), vortexed for 10 seconds, sonicated in an ice bath for 5 minutes and vortexed again. After rapid centrifugation

(14000 x g, 15 seconds) the tubes were incubated at room temperature for 30 minutes and then centrifuged again (16000 x g, 10 minutes). The supernatant was transferred to new tubes and the protein content in each sample was determined by Bradford assay (Bio-Rad). Next, the protein samples were diluted in solubilization buffer to the concentration of 1 µg/µl, used in the in solution digestion step. At this step, 15 µg of total proteins were digested with Lys-C and trypsin, and desalted by STAGE tips, as previously described by Foster et al. (2003). Each sample was dried (SpeedVac, Eppendorf, 45 min) and resuspended in 15 µL of 0.1% formic acid. Peptide concentrations were determined using a NanoDrop (Thermo, 280 nm) and the sample was analyzed by liquid chromatography-tandem mass spectrometry (LC-MS/MS).

LC-MS/MS data acquisition and statistical analysis:

Each peptide sample was injected on an EASY-nLC 1000 liquid chromatography system (Thermo) coupled to an Impact II Q-TOF mass spectrometer (Bruker), essentially as previously described by McAfee and collaborators (2017).

Mass spectrometry data were searched using MaxQuant (v1.6.3.3), with the default parameters (TYANOVA, TEMU, and COX, 2018). The protein search database was the *Apis mellifera* gene assembly version 4.5 (Amel 4.5) blasted against the non-redundant protein database for Arthropoda (NCBI ID: GCF_003254395.2) in 2015 plus the manually annotated ABPV proteome from UniProt database release 2019_05 (15314 entries).

Experiments were carried out in three biological replicates. The statistical difference of the normalized LFQ intensity values (COX, et al., 2014) among the samples were calculated by T-test (p-value < 0.05). The fold changed was calculated as the ratio of the mean LFQ intensity values of the groups between different temperatures (group 0h) and infected *vs*. non-infected (24h26ºC; 24h32ºC; 48h26ºC and 48h32ºC). The result was shown as logarithm in base two ($\log_2$ Fold change) versus the negative logarithm of p-value (-log p-value) in a volcano-plot graph created with the software GraphPad Prism 5 (GraphPad Software, Inc, La Jolla, CA, USA). The proteins with p-value less than 0.05 (p-value < 0.05) or negative logarithm of p-value more than 1.30 ($-\log_{10}$ p > 1.30) were considered differentially abundant proteins.

Bioinformatics analysis:

The Gene Ontology (GO) annotations of the process and function of proteins were acquired with the tool AgBase-GOanna (https://agbase.arizona.edu/, McCARTHY, et al. 2006). Then, the Protein-Protein Interaction (PPI) network was generated for the up and down regulated proteins identified in each experimental group using the STRING database version 11.0 (https://string-db.org/, SZKLARCZYK, et al. 2019). The confidence levels of the PPI were evaluated by the PPI enrichment p-value < 0.05 which means that the proteins have more interactions among themselves than what would be expected for a random set of proteins of similar size, drawn from the genome. The proteins network was represented as a Cytoscape graph (v 3.7.1, SHANNON, et al., 2003) and the statistically overrepresented GOs were determined with the tool Bingo (MAERE, HEYMANS, KUIPER, 2005) by a Hypergeometric Test with the Benjamini & Hochberg's FDR correction (q-values < 0.05).

Results and discussion

The effect of temperature in ABPV virulence

The worker bees placed at 26º ±2ºC and 32º ±2ºC survived all the experiment time. The group placed at 36º ±2ºC had a survival rate of 50% and it was excluded from RT-qPCR and proteomic analysis. The remained groups of the infected and non-infected honey bees submitted to 32º C (usual in hives with brood) and 26º C (a suboptimal temperature) during 24h and 48h survived (Figure 1-A).

Viral load was higher at 32º C for both times (Figure 1-B). Viral load was higher at 48h, showing that artificial infection by feeding was efficient. However, the influence of temperature decreased whereas infection progresses. In all experimental conditions any of the classical symptoms of ABPV infection was observed (trembling, paralysis, darkening, loss of hair and death). The asymptomatic infection occurs when the ABPV is transmitted by feeding or spreading (BAILEY, GIBBS and WOODS, 1963; AZZAMI, et al., 2012) and the viral load is kept at low levels.

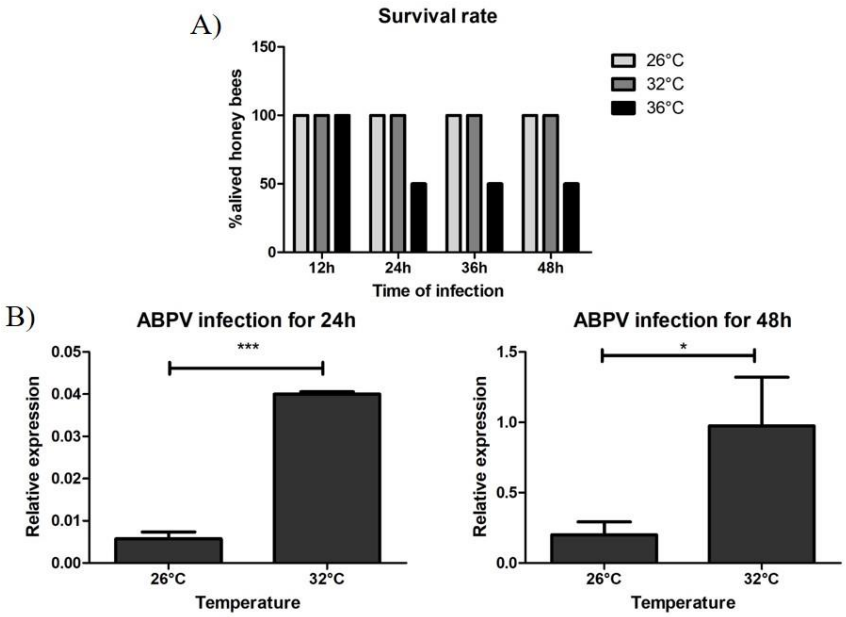

Figure 1- A) Survival of infected honey bees under three different temperature. The cages were inspected every 12 hours. B) Relative expression of ABPV in honey bees after 24 and 48 hours of infection. In each treatment, three pools containing two worker bees each were used.

According to the national survey of managed honey bee 2014–2015 annual colony losses in the USA, commercial beekeepers suffered the highest colony losses during that summer, approximately 50% higher average losses than backyard beekeepers (SEITZ et al., 2016). However, in the winter colony losses were twice as high in backyard beekeepers compared to commercial beekeepers. Usually, the losses are higher during the winter for the backyard beekeepers because of some colony management issues that commercial beekeepers didn't report. The main causes of these summer losses reported by commercial beekeepers could be related to increase of pesticide exposure during pollination events or increase of disease and viral transmission when commercial colonies are transported or placed in large holding yards (SEITZ et al., 2016). The increase of temperature over the ideal (the group at 36º ±2ºC) may have improved the host's susceptible for infections, which justifies the high mortality observed only in this group and the recent increase in loss of colonies during the summer, reported by Seitz et al. (2018). What makes us question whether the low expression of the virus at the lowest temperature results from the decrease of its virulence or it was a consequence of host metabolism and more susceptibility of worker bees?

The effect of temperature and ABPV infection in host immune response

In order to evaluate the effect of temperature and ABPV infection on the immune system of honey bees we quantified the antimicrobial peptides defensin, abaecin, and hymenoptaecin, and the enzymes phenoloxidase and lysozyme, related to humoral and cellular immune response (EVANS and SPIVAK, 2010).

At the beginning of the infection the expression of abaecin and defensin was higher in the infected group in 26º ±2ºC. However, the production of AMPs decrease in 32º ±2ºC after 24 hours and in both temperatures after 48 hours. The increase of the temperature during the first 24 hours reflected in a significant improvement of the abaecin and hymenoptaecin expression and decrease of lysozyme and phenoloxidase on the non-infected groups (Figure 2-A1, C1;E1).

Most of the genes (ABA, HYM, LYS and PO) had a different expression caused by the increase on temperature at 24 hours. However this difference was not maintained throughout the experiment (48 hours). These findings suggest that the temperature has an influence on the immune response, but it is quickly regulated by the honey bee's thermoregulatory ability (Figure 2).

We observed a decreased expression of LYS and PO caused by the improvement of temperature. The presence of ABPV increased the expression of these enzymes but only at 24h 32ºC (Figure 2D and E).

Our findings suggest that the immune related genes are not overexpressed in response to the infection. In an experimental scale, we observed that there is a decrease of ABPV expression in a temperature lower than the colony usual and the immune related genes are not overexpressed in response to the infection. The colony environment is kept at 32-34ºC, and the thermal fluctuation is actually described as a defense mechanism (behavioral fever), when the worker bees can achieve until 45ºC around an invader (EVANS and SPIVAK, 2010).

The treatment of honey bees with simulated heat waves showed a surprisingly positive effect at colony level and decreased the load of *Deformed wings virus* (DWV), an Iflavirus highly spread in managed colonies (BORDIER, et al., 2017). This study also showed that honey bees have a remarkable ability of thermoregulation of the colony temperature, however, it was observed higher recruitment to foraging activity, which could increase the exposure to other environmental stressors and pathogens. Despite to seem an interesting way to control the viral load, our finds shown that

honey bee virus have a different response to temperature changes, with make the improvement of temperatures an inappropriate approach to deal with viral infections.

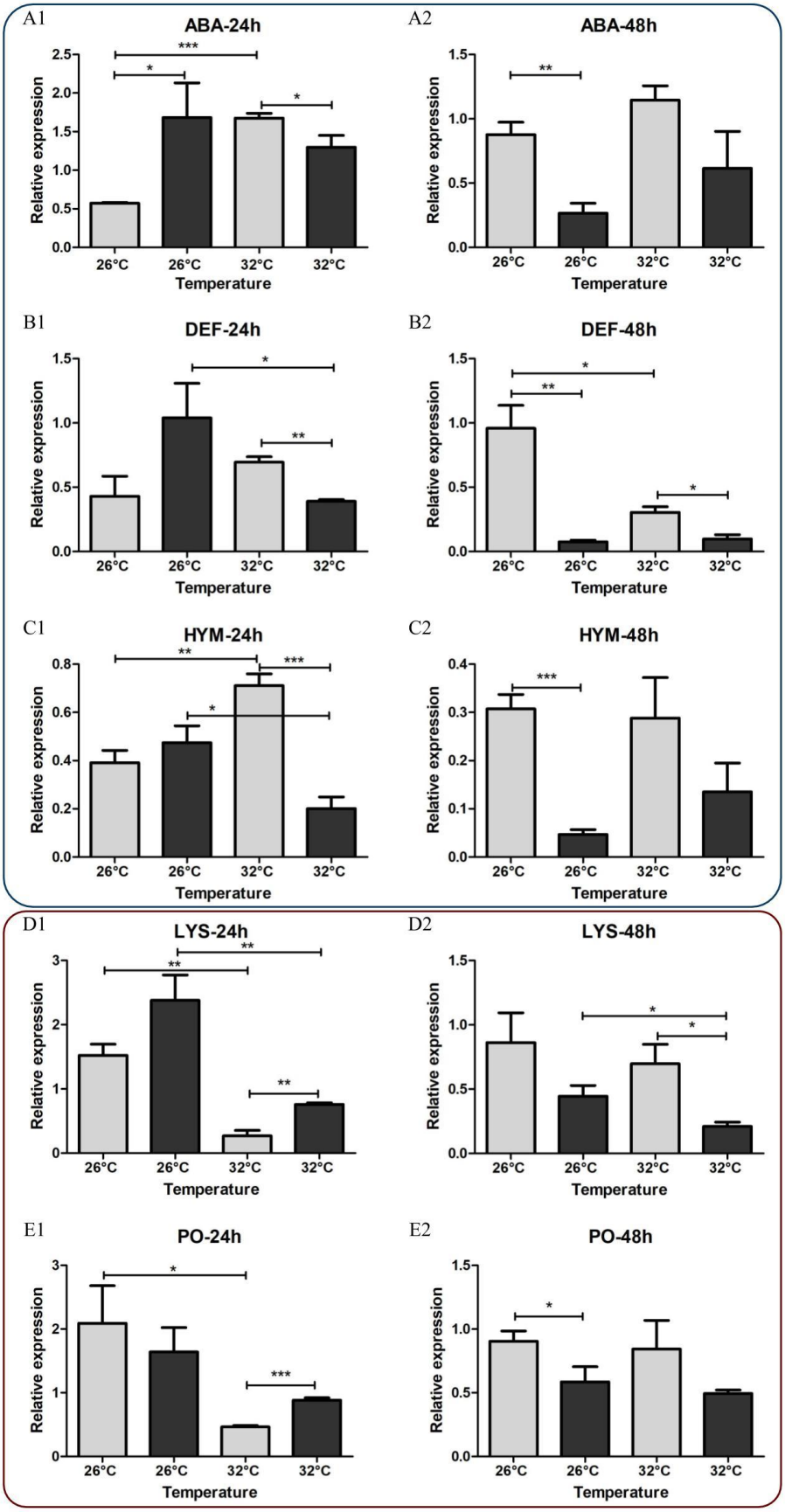
A1
ABA-24h
Relative expression
Temperature
26°C
26°C
32°C
32°C
A2
ABA-48h
B1
DEF-24h
B2
DEF-48h
C1
HYM-24h
C2
HYM-48h
D1
LYS-24h
D2
LYS-48h
E1
PO-24h
E2
PO-48h

Figure 2- The relative expression of genes involved in the humoral (blue) and cellular (red) immune response of worker bees between infected (dark gray) and uninfected (light gray) groups under two temperatures (26 ±2ºC and 32 ±2ºC) for 24h (1) and 48h (2). In each treatment, two pools containing two worker bees each were used. A) Quantification of relative expression of abaecin (ABA). B) Quantification of relative expression of defensin (DEF). C) Quantification of relative expression of hymenoptaecin (HYM). D) Quantification of relative expression of lysozyme (LYS). E) Quantification of relative expression of phenoloxidase (PO).

According to proposed by Azzami et al. (2012), ABPV does not induce a humoral or cellular immune response. They did not observe the presence of AMPs in the hemolymph of worker bees artificially infected by injection of a purified virus. In their work, the formation of nodules in the digestive tract and in the hemocoel was not observed. In our study was performed an artificial infection with a viral suspension obtained from bees previously identified with ABPV. In addition, we used a non-invasive method of infection (feeding), which causes a lower viremia compared to the pathogen injection made by Azzami, et al (2012). Thus, in this work we observed that ABPV negatively influences the expression of genes related to immune response, which is consistent with the absence of a physiological response against infection. The use of interfering RNA is a mechanism of control of viral infections that could be employed by the immune system of bees (BRUTSCHER, DAUGHENBAUGH, and FLENNIKEN, 2015), and future research on the expression of genes related to this pathway is necessary in presence of ABPV.

We also evaluated the proteomic profile of the worker bees in each of the experimental conditions. The figure 3-B shows the number of proteins identified at 32°C and 26°C in the absence of the virus (group 0h). Among these, 14% were differentially expressed between the two temperatures after the induction time (-log p-value > 1.3) (Figure 3-A). The up and down regulated protein presented a highly correlation, suggesting that they are involved in related biological process (Figure 3-C and D).

The differentially abundant proteins were grouped in order to perform an analysis of enrichment of biological processes based on GO annotations, as shown in Figure 3-E.

The most down-regulated protein on the high temperature was hemolymph juvenile hormone binding (GB42702) and histone acetyltransferase (GB47991), which could indicate a delay in honey bee development.

Glycosyl hydrolase (GB43247) and malic oxidoreductase (GB49967) were up-regulated at high temperature, indicating an increase in oligosaccharide hydrolysis and pyruvate formation processes. We also observed the overrepresentation of GO related to carbohydrate metabolism and energy production in the set of up-regulated proteins at high temperature. The heat shock protein alpha-crystallin (GB45906) was the most up-regulated in response to temperature increase (6.87 log_2Fold change). The heat shock pathway presented a mutually antagonistic relationship with humoral and cellular immune response in honey bees (MCKINSTRY et al., 2017). This relationship is unique among invertebrates and could explain the decreased expression of phenoloxidase and lysozyme in the high-temperature groups observed in this work (Figure 2).

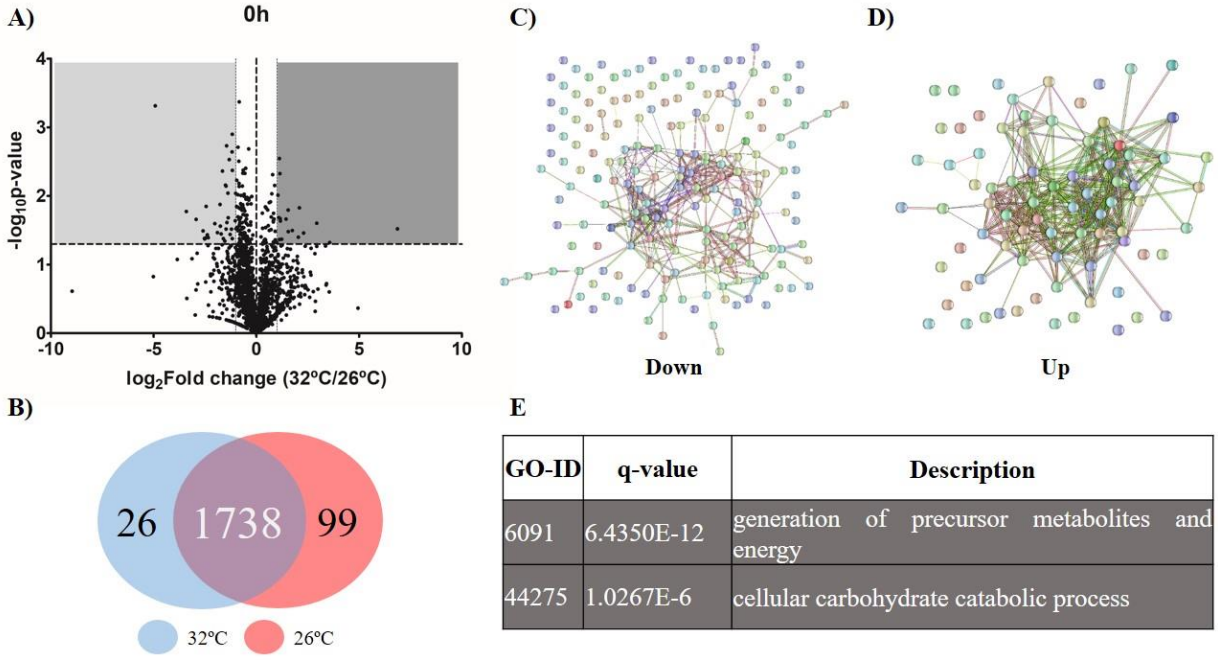

GO-ID	q-value	Description
6091	6.4350E-12	generation of precursor metabolites and energy
44275	1.0267E-6	cellular carbohydrate catabolic process

Figure 3- Influence of the temperature upon the expression of proteins in non-infected worker bees. A) Volcano-plot graph correlating the negative logarithm of the p-value with the logarithm of base two of the ratio between the expression of proteins in the group 0h at 32ºC versus group 0h at 26ºC . The data above the horizontal dotted axis have significant different expression between the groups (t-test, p-value < 0.05). The highlighted quadrants contain proteins up-regulated 2-fold or more (dark gray) and down-regulated 2-fold or more (light gray). B) Venn diagram. Proteins identified in group 0h in each of the conditions. PPI (Protein-Protein Interaction) network of the down-regulated (C) and up-regulated (D) proteins, with PPI p-value < 1.0e-16. E) Overrepresented proteins between the up-regulated set (FDR corrected p-value < 0.05) and their GO-ID (Gene Ontology Identificator) and biological process. There were no overrepresented proteins between the down-regulated set.

The enrichment of the energetic metabolism could explain our observation of a decreased expression of ABPV at lower temperature. This suggest that the lower viral load was a consequence of the temperature upon the host basic metabolism. We evaluate the proteome profile of infected *vs*. non-infected worker bees on both temperatures after 24h and 48h of incubation (Figure 4). Between the identified proteins in both conditions, the amount of differentially abundant (-log p-value > 1,3) was: 2.6% in the group 24h incubation, 26ºC; 2.3% in the group 24h incubation, 32ºC; 20.2% in the group 48h incubation, 26ºC and 4.3% in the group 48h incubation, 32ºC.

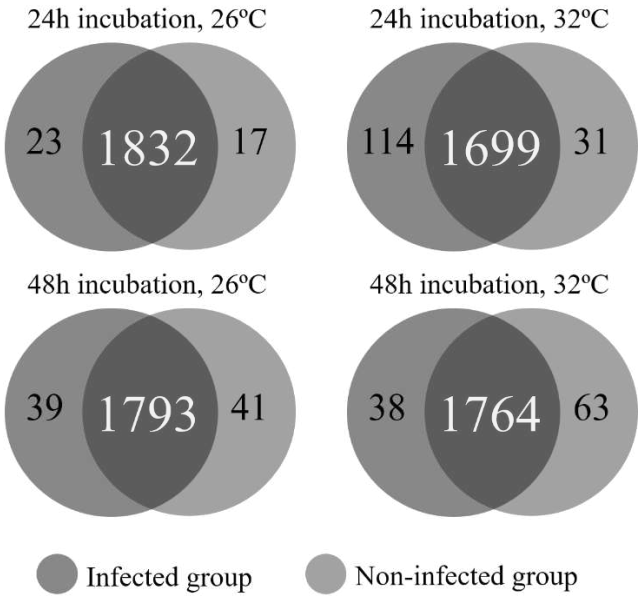

Figure 4- Venn diagram. Proteins identified in the infected (dark grey) and non-infected (light grey) groups after 24h and 48h of incubation at 26 ±2ºC and 32 ±2ºC in workers of honey bees.

At the first 24 hours of incubation we observer that the down-regulated proteins are related to translation process and biosynthesis of the host's macromolecules (GB54433, GB55150). This finds are consistent with the replication mechanism of Dicistrovirus, that is IRES-mediated and requires fewer factors than canonical cap-dependent translation initiation, allowing the virus to usurp the translational machinery of the host (KEER and JAN, 2016).

The group with a longer time of exposure to ABPV (48h) presented a large amount of highly up-regulated proteins, like glycoside hydrolase (GB53565) and EF-hand calcium binding proteins (GB55432), important in process of muscle contraction and well function of Voltage-gated sodium

channels (Figure 6-A). In Figure 6-D are shown the overrepresented GO terms, related to cytoplasm organization and muscle system process. With the down-regulated set, we observed that the identified proteins formed a highly correlated network (Figure 5-B2). The infection decreased the expression of proteins related to metabolism of ATP (GB51580), chaperonin GroES-like (GB48857) and t-SNARES proteins (GB46404).

This finds are consistent with the phenotype observed in highly infected honey bees (trembling and paralysis) and could lead to a mechanism of action by interference on the vesicular transport and muscle contraction.

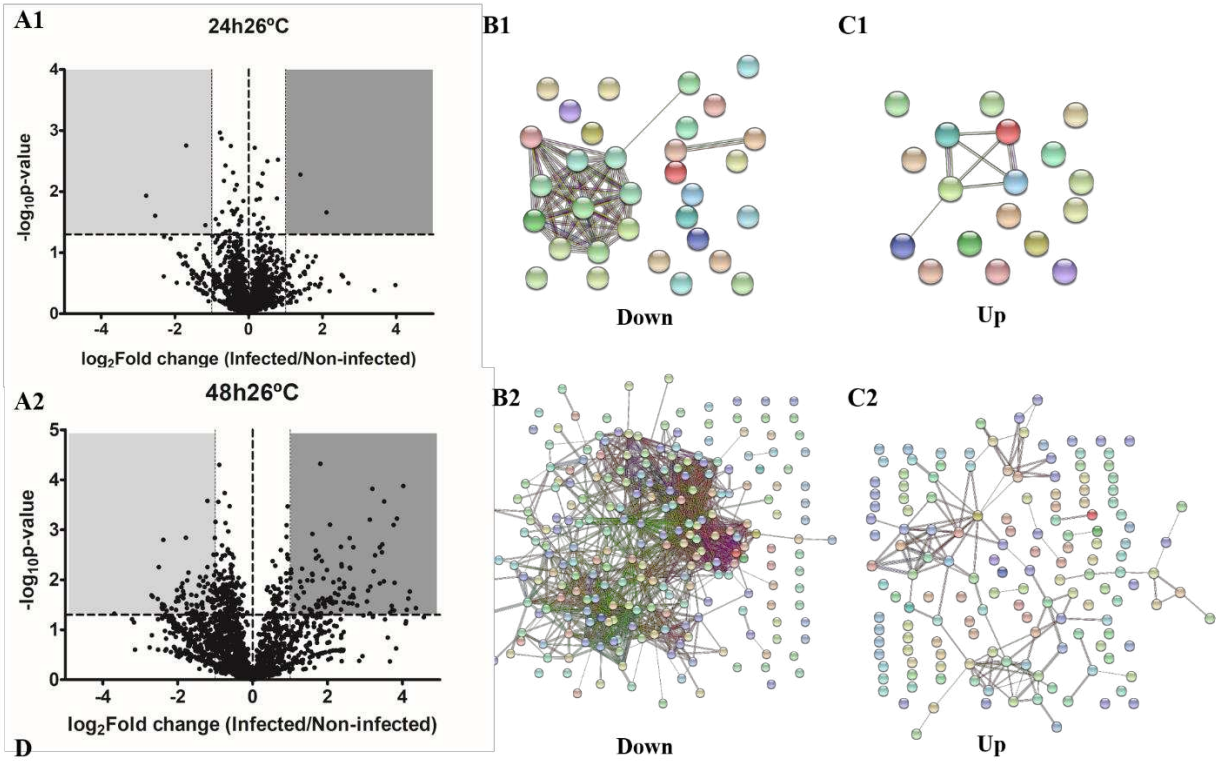

Experiment group	GO-ID	q-value	Description
24h at 26ºC	6412	7.2618E-7	translation
24h at 26ºC	34645	2.0403E-4	cellular macromolecule biosynthetic process
48h at 26ºC	46034	0,025	ATP metabolic process
48h at 26ºC	7028	3.5393E-3	Cytoplasm organization
48h at 26ºC	3012	5.5649E-3	Muscle system process

Figure 5- Influence of the ABPV infection under 26 ±2ºC upon the expression of proteins in worker bees. A) Volcano-plot graph correlating the negative logarithm of the p-value with the logarithm of base two of the ratio between the expression of proteins in the groups at 26ºC infected vs. non-infected for 24h (1) and

for 48h (2). The data above the horizontal dotted axis have significant different expression between the groups (t-test, p-value < 0.05). The highlighted quadrants contain proteins up-regulated 2-fold or more (dark gray) and down-regulated 2-fold or more (light gray). Protein-Protein Interaction network (PPI) of the down-regulated proteins on 24h group (B1, PPI p-value 1.96e-10) and 48h group (B2, PPI p-value < 1.0e-16); and up-regulated proteins on 24h group (C1, PPI p-value 0.0416) and 48h group (C2, PPI p-value < 1.0e-16). D) Overrepresented proteins between the down-regulated set (light grey) and the up-regulated set (dark gray) (FDR corrected p-value < 0.05) and their GO-ID (Gene Ontology Identificator) and biological process. There were no overrepresented proteins between the up-regulated set in the group 24h at 26ºC.

Despite the high viral load observed at 32 ±2ºC (Figure 1), there were no overrepresented GO terms on the differentially abundant proteins between infected and non-infected groups at that temperature (Figure 6). Between the up-regulated proteins at 32 ±2ºC are heat shock proteins (GB54222, GB45494), glycoside hydrolase (GB54549), chaperone (GB46263) and EF-hand calcium binding proteins (GB44903), suggesting that the immune response trigged by ABPV is related to environmental temperature and could be mediated by HSP pathway. Indeed Cevallos and Sarnow (2010) observed a low production of infectious *Cricket Paralysis Virus*, a Dicistrovirus like ABPV, in Drosophila S2 cells at high temperature, even though the amounts of viral protein and RNA had increased. This suggests that a heat shock-induced factor could inhibit virion formation.

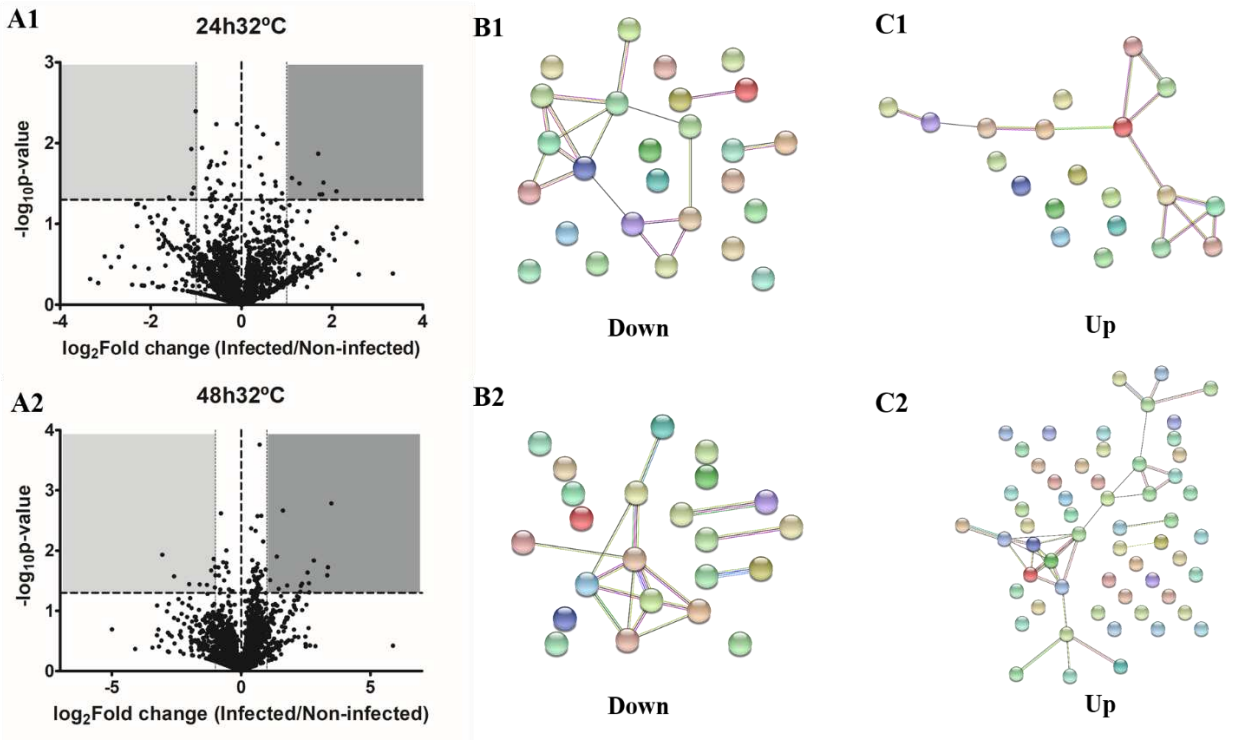

Figure 6- Influence of the ABPV infection under 32 ±2ºC upon the expression of proteins in honey bees. A) Volcano-plot graph correlating the negative logarithm of the p-value with the logarithm of base two of the ratio between the expression of proteins in the groups at 32ºC infected vs. non-infected for 24h (1) and for 48h (2). The data above the horizontal dotted axis have significant different expression between the groups (t-test, p-value < 0.05). The highlighted quadrants contain proteins up-regulated 2-fold or more (dark gray) and down-regulated 2-fold or more (light gray). Protein-Protein Interaction network (PPI) of the down-regulated proteins on 24h group (B1, PPI p-value 2.64e-06) and 48h group (B2, PPI p-value 7.86e-05); and up-regulated proteins on 24h group (C1, PPI p-value 4.71e-07) and 48h group (C2, PPI p-value 3.02e-05). There were no overrepresented proteins between the down or up-regulated sets in the groups at 32ºC.

Conclusion

We observed that the temperature variation presented a high impact on the physiology of the worker bees, mainly affecting the metabolism of carbohydrates and energy production. ABPV infection did not promote the expression of genes involved in the humoral and cellular response; on the opposite, the expression of these genes was lower in infected groups and also in those maintained at 32 ±2ºC. We also observed that ABPV causes changes in the energy metabolism of the host and usurps its cellular machinery to favor viral biosynthesis, which could causes the typical symptoms of paralysis and trembling. Among the physiological changes caused by the infection is

the depletion of targets on the energetic metabolism, the vesicular transport process and muscular system, and essential chaperonins in the process of proteostasis. The evidences found in this work suggests that the typical symptoms of ABPV infection are due to interference in the transport of neurotransmitters and the functioning of calcium-binding proteins vital in the process of muscle contraction and synapse. The metabolism of ATP was also impaired due to the infection, which justifies the delay in the development of larvae infected by this pathogen (AZZAMI et al., 2012).

Although the viral load was higher in the group at 32 ±2ºC, the proteins differentially expressed at 26 ±2ºC were more correlated, and we observed the overrepresentation of processes related to the characteristics generated by the virus on the groups at low temperature. The production of HSPs was increased as a result of the infection at the higher temperature, suggesting that these proteins act in the control of the infection and the formation of new infectious virus. The high mortality of the group placed at 36 ±2ºC suggests that the ABPV can break the immunological barrier of the honey bee in response to temperature variation. These results suggest climate change and temperature variations may cause damage to the response worker bees against ABPV.

References

AZZAMI, K; RITTER, W; TAUTZ, J; BEIER, H. Infection of honey bees with acute bee paralysis virus does not trigger humoral or cellular immune responses. **Archives of virology**, v. 157, n. 4, p. 689-702, 2012.

BAILEY, L; GIBBS, A. J. Acute infection of bees with paralysis virus. **Journal of insect pathology**, v. 6, n. 4, p. 395–407, 1964.

BAILEY, L; GIBBS, A. J; WOODS, R. D. Two viruses from adult honey bees (*Apis mellifera* Linnaeus). **Virology**, v. 21, p. 390-395, 1963.

BAKER, A; SCHROEDER, D. Occurrence and genetic analysis of picorna-like viruses infecting worker bees of *Apis mellifera* L. populations in Devon, South West England. **Journal of Invertebrate Pathology,** v. 98, p. 239-242, 2008.

BERÉNYI, O; BAKONYI, T; DERAKHSHIFAR, I; KÖGLBERGER, H; NOWOTNY, N. Occurrence of six honeybee viruses in diseased austrian apiaries. **Invertebrate Microbiology**, v. 72, p. 2414-2420, 2006.

BORDIER, C; DECHATRE, H; SUCHAIL, S; PERUZZI, M; SOUBEYRAND, S; PIOZ, M; PÉLISSIER, M; CRAUSER, D; Le CONTE, Y; ALAUX, C. Colony adaptive response to simulated heat waves and consequences at the individual level in honeybees (*Apis mellifera*). **Scientific Reports**, v. 7, n. 3760, 2017.

BRUTSCHER, L. M; DAUGHENBAUGH, K. F; FLENNIKEN, M. L. Antiviral defense mechanisms in honey bees. **Current Opinion in Insect Science**, v. 10, p. 71-82, 2015.

CALDERONE, N. W. Insect pollinated crops, insect pollinators and US agriculture: Trend analysis of aggregate data for the period 1992-2009. **PLoS ONE**, v. 7, n. 5, p. e37235, 2012.

CEVALLOS, R. C; SARNOW, P. Temperature Protects Insect Cells from Infection by *Cricket Paralysis Virus*. **American Society for Microbiology,** v. 84, p. 1652-1655, 2010.

CHANPANITKITCHOTE, P; CHEN, Y; EVANS, J. D; LI, W; LI J; HAMILTON, M; CHANTAWANNAKUL, P. *Acute bee paralysis virus* occurs in the Asian honey bee *Apis cerana* and parasitic mite *Tropilaelaps mercedesae*. **Journal of Invertebrate Pathology**, v. 151, p. 131-136, 2018.

COX, J; HEIN, M. Y; LUBER, C. A; PARON, I; NAGARAJ, N; MANN, M. Accurate proteome-wide label-free quantification by delayed normalization and maximal peptide ratio extraction, termed MaxLFQ. **Molecular and Cellular Proteomics**, v. 13, p. 2513-2526, 2014.

de SOUZA, G. B; MENDES, T. A. O; FONTES, P. P; BARROS, V. A; GONÇALVES, A. B; FERREIRA, T. F; COSTA, M. D. B. L; ALVES, M. S; FIETTO, L. G. Genome-wide identification and expression analysis of dormancyassociated gene 1/auxin repressed protein (DRM1/ARP) gene family in Glycine max. **Progress in Biophysics and Molecular Biology**, v. 146, p. 134-141, 2019.

de MIRANDA, J. R; CORDONI, G; BUDGE, G. The Acute bee paralysis virus-Kashmir bee virus-Israeli acute paralysis virus complex. **Journal of Invertebrate Pathology**, v. 103, p. S30-S47, 2010.

DeGRANDI-HOFFMAN, G; CHEN, Y. Nutrition, immunity and viral infections in honey bees. **Current Opinion in Insect Science**, v. 10, p. 170-175, 2015.

EVANS, J. D. and WHEELER, D. E. Gene expression and the evolution of insect polyphenisms. **BioEssays**, v. 21, 2001.

EVANS, J. D; ARONSTEIN, K; CHEN, Y. P; HETRU, C; IMLER, J. L; JIANG, H; KANOST, M; THOMPSON, G. J; ZOU, Z; HULTMARK, D. Immune pathways and defence mechanisms in honey bees Apis mellifera. **Insect Molecular Biology**, v. 15, p. 645-656, 2006.

EVANS, J. D; SPIVAK, M. Socialized medicine: individual and communal disease barriers in honey bees. **Journal of Invertebrate Pathology**, v. 103, p. S62-S72, 2010.

FLORES, J. M; GIL-LEBRERO, S; GÁMIZ, V; RODRÍGUES, M. I;ORTIZ, M. A; QUILES, F. J. Effect of the climate change on honey bee colonies in a temperate Mediterranean zone assessed through remote hive weight monitoring system in conjunction with exhaustive colonies assessment. **Science of the Total Environment**, v. 653, p. 1111–1119, 2019.

FORGÁCH, P; BAKONYI, T; TAPASZTI, Z; NOWOTNY, N; RUSVAI, M. Prevalence of pathogenic bee viruses in Hungrarian apiaries: Situation before joining the European Union. **Journal of Invertebrate Pathology**, v. 98, n. 2, p. 235-238, 2008.

FOSTER, L. J; HOOG, C. L; MANN, M. Unbiased quantitative proteomics of lipid rafts reveals high specificity for signaling factors. **Proceedings of the National Academy of Sciences**, v. 100, n. 10, p. 5813-5818, 2003.

GALLAI, N; SALLES, J. M; SETTELE, J; VAISSIÈRE, B.E. Economic valuation of the vulnerability of world agriculture confronted with pollinator decline. **Ecological economics**, v.6, n. 8, p. 810-821, 2009.

GOULSON, D; NICHOLLS, E; BOTÍAS, C; ROTHERAY, E. L. Bee declines driven by combined Stress from parasites, pesticides, and lack of flowers. **Science**, v. 347, n. 6229, 2015.

GOVAN, V. A; LEAT, N; ALISOPP, M; DAVISON, S. Analysis of the complete genome sequence of acute bee paralysis virus shows that it belongs to the novel group of insect-infecting rna viruses. **Virology**, v. 277, p. 457-463, 2000.

KERR, C. H; JAN, E. Commandeering the ribosome: lessons learned from dicistroviruses about translation. **Journal of Virology**, v. 90, n. 12, p. 5538-5540, 2016.

Le CONTE, Y; NAVAJAS, M. Climate changes: impacto on honey bee populations and diseases. **Revue Scientifique et Technique-Office**, v. 27, n. 2, p. 499-510, 2008.

LOURENÇO, A. P; MACKERT, M; CRISTINO, A. S; SIMÕES, Z. L. P. Validation of reference genes for gene expression studies in the honey bee, *Apis mellifera*, by quantitative real-time RT-PCR. **Apidologie**, v. 39, n. 3, p. 372-385, 2008.

MAERE, S; HEYMANS, K; KUIPER, M. BiNGO: a Cytoscape plugin to assess overrepresentation of gene ontology categories in biological networks. **Bioinformatics**, v. 21, n. 16, p. 3448–3449, 2005.

MCAFEE, A; CHAN, Q; W; T; EVANS, J; FOSTER, L; J. A *Varroa destructor* protein atlas reveals molecular underpinnings of developmental transitions and sexual differentiation. **Molecular and Cellular Proteomics**, v. 16, n. 12, p. 2125-2137, 2017.

MCCARTHY, F. M; WANG, N; MAGEE, G. B; NANDURI,B; LAWRENCE, M. L; CAMON, E. B; BARRELL, D. G; HILL, D. P; DOLAN, M. E; WILLIAMS, W. P; LUTHE, D. S; BRIDGES, S. M; BURGESS, S. C. AgBase: a functional genomics resource for agriculture. **BMC Genomics**, v. 7, n. 229, 2006.

MCKINSTRY, M; CHUNG, C; TROUNG, H; JOHNSON, B. A; SNOW, J. W. The heat shock response and humoral immune response are mutually antagonistic in honey bees. **Scientific Reports,** v. 7, n. 8850, 2017.

MCMENAMIN, A. J; FLENNIKEN, M. L. Recently identified bee viruses and their impact on bee pollinators. **Current Opinion in Insect Science**, v. 26, p. 120-129, 2018.

POTTS, S. G; BIESMEIJER, J. C; KREMEN, C;NEUMANN, P;SCHWEIGER, O. KUNIN, W. E. Global pollinator declines: Trends, impacts and drivers. **Trends in Ecology and Evolution**, v. 25, p. 345-353, 2010.

REDDY, P. V. R; VERGHESE A; RAJAN, V. V. Potential impact of climate change on honeybees (*Apis* spp.) and their pollination services. **Pest Management in Horticultural Ecosystems**, v. 18, n. 2 p. 121-127, 2012.

REYNALDI, F. J; SGUAZZA, G. H; PECORARO, M. R; TIZZANO, M. A; GALOSI, C.M. First repost of viral infections that affect argentine honeybees. **Environmental Microbiology Reports**, v. 2, n. 6, p. et al; 2010.

SEITZ, N; TRAYNOR, K. S; STEINHAUER, N; RENNICH, K; WILSON, M. E; ELLIS, J. D; ROSE, R; TARPY, D. R; SAGILI, R. R; CARON, D. M; DELAPLANE, K. S; RANGEL, J; LEE, K; BAYLIS, K; WILKES, J. T; SKINNER, J. A; PETTIS, J. S; vanENGELSDORP, D. A national survey of managed honey bee 2014–2015 annual colony losses in the USA. **Journal of Apicultural Research**, v. 54, n. 4, p. 292-304, 2016.

SHANNON, P; MARKIEL, A; OZIER, O; BALIGA, N. S; WANG, J. T; RAMAGE, D; AMIN, N; SCHWIKOWSKI, B; IDEKER, T. Cytoscape: a software environment for integrated models of biomolecular interaction networks. **Genome Research**, v. 13, n. 11, p. 2498-2504, 2003.

SZKLARCZYK, D; GABLE, A. L; LYON, D; JUNGE, A; WYDER, S; HUERTA-CEPAS, J; SIMONOVIC, M; DONCHEVA, N. T; MORRIS, J. H; BORK, P; JENSEN, L. J; MERING, C. V. STRING v11: protein-protein association networks with increased coverage, supporting functional discovery in genome-wide experimental datasets. **Nucleic Acids Research**, v. 47, p. D607-D613, 2019.

TEHEL, A; BROWN, M. J. F. AND PAXTON, R. J. Impact of managed honey bee viruses on wild bees. **Current Opinion in Virology**, v. 19, p. 16-22, 2016.

TEIXEIRA E. W; CHEN, Y; MESSAGE, D; PETTIS, J; EVANS, J. D. Virus infection in Brazilian honey bees. **Journal of Invertebrate Pathology**, v. 99, p. 117-119, 2008.

TENTCHEVA, D; GAUTHIER, L; ZAPPULLA, Z; DAINAT, B; COUSSERANS, F; COLIN, M. E; BERGOIN, M. Prevalence and seasonal variations of six bee viruses in *Apis mellifera* L. and *Varroa destructor* mite populations in France. **Applied and environmental microbiology**, v. 70, n. 12, p. 7185-7191, 2004.

TYANOVA, S; TEMU, T; COX, J. The MaxQuant computational platform for mass spectrometry-based shotgun proteomics. **Nature**, v. 11, n. 12, p. 2301-2319, 2018.

YANG, X; COX-FOSTER, D. L. Impact of an ectoparasite on the immunity and pathology of an invertebrate: Evidence for host immunosuppression and viral amplification. **Proceedings of the National Academy of Sciences**, v. 102, n. 21, p. 7470-7475, 2005.

Supplementary material

Table 2- Proteins identified on the Group 0h (32ºC *vs*. 26ºC)

Down-regulated			Up-regulated		
ID	**log2foldchange**	**-log10p-value**	**ID**	**log2foldchange**	**-log10p-value**
gnl|Amel_4.5|GB53349-PA	-0,835151437	3,370506135	gnl|Amel_4.5|GB54753-PA	1,122179735	2,545881198
gnl|Amel_4.5|GB42702-PA	-4,924316817	3,313077078	gnl|Amel_4.5|GB52013-PA	1,146210211	2,325324039
gnl|Amel_4.5|GB46652-PA	-1,172783318	2,899103906	gnl|Amel_4.5|GB46230-PA	0,791549674	2,311398635
gnl|Amel_4.5|GB43739-PA	-1,451522046	2,731803236	gnl|Amel_4.5|GB47610-PA	0,891296633	2,153075265
gnl|Amel_4.5|GB51788-PA	-0,894668558	2,710051012	gnl|Amel_4.5|GB44462-PA	0,752014531	2,032608997
gnl|Amel_4.5|GB53579-PA	-0,371054635	2,685630858	gnl|Amel_4.5|GB48308-PA	1,053504094	2,01115774
gnl|Amel_4.5|GB48634-PA	-1,182863335	2,642281277	gnl|Amel_4.5|GB50600-PA	0,687340956	1,915088932
gnl|Amel_4.5|GB50099-PA	-1,323666877	2,530675081	gnl|Amel_4.5|GB51091-PA	0,627049123	1,904695063
gnl|Amel_4.5|GB43575-PA	-0,853764821	2,504986181	gnl|Amel_4.5|GB50128-PA	0,436552278	1,841240067
gnl|Amel_4.5|GB49629-PA	-0,522461718	2,404332565	gnl|Amel_4.5|GB55215-PA	2,093428794	1,827213712
gnl|Amel_4.5|GB46071-PA	-0,644166199	2,37601231	gnl|Amel_4.5|GB51089-PA	0,47989293	1,823530116
gnl|Amel_4.5|GB41927-PA	-1,170310464	2,37298699	gnl|Amel_4.5|GB43540-PA	0,549968537	1,796628472
gnl|Amel_4.5|GB51107-PA	-1,651068221	2,362547316	gnl|Amel_4.5|GB52073-PA	1,549165299	1,795489325
gnl|Amel_4.5|GB54747-PA	-0,656202825	2,331842288	gnl|Amel_4.5|GB49948-PA	0,289321172	1,748649876
gnl|Amel_4.5|GB49158-PA	-0,55788033	2,330019185	gnl|Amel_4.5|GB45838-PA	0,834842001	1,748030923
gnl|Amel_4.5|GB45688-PA	-0,953717244	2,228814516	gnl|Amel_4.5|GB47181-PA	0,7207039	1,695232451
gnl|Amel_4.5|GB52656-PA	-0,846196919	2,182100891	gnl|Amel_4.5|GB50761-PA	1,090360577	1,683856735
gnl|Amel_4.5|GB45137-PA	-1,502565418	2,15840834	gnl|Amel_4.5|GB55496-PA	1,152629841	1,67162479
gnl|Amel_4.5|GB50450-PA	-1,480976081	2,144908908	gnl|Amel_4.5|GB41028-PA	0,860716693	1,663767702
gnl|Amel_4.5|GB42809-PA	-0,684303131	2,144293442	gnl|Amel_4.5|GB43117-PA	1,446193742	1,663422089
gnl|Amel_4.5|GB55533-PA	-0,839281129	2,13853562	gnl|Amel_4.5|GB53727-PA	0,82493176	1,639614676
gnl|Amel_4.5|GB53077-PA	-1,383905633	2,041203696	gnl|Amel_4.5|GB40735-PA	1,169302589	1,636429122
gnl|Amel_4.5|GB41781-PA	-1,008791412	2,038206628	gnl|Amel_4.5|GB44983-PA	0,824043408	1,622671446
gnl|Amel_4.5|GB53853-PA	-0,59249737	2,025756633	gnl|Amel_4.5|GB51218-PAgnl|Amel_4.5|GB47127-PA;gnl|Amel_4.5|GB43027-PA	2,939158941	1,603712662
gnl|Amel_4.5|GB47134-PA	-0,900478192	2,017958165	gnl|Amel_4.5|GB47604-PA	0,579545046	1,568628822
gnl|Amel_4.5|GB48552-PA	-0,750149987	2,007379348	gnl|Amel_4.5|GB51746-PA	0,454046634	1,539985126
gnl|Amel_4.5|GB53799-PA	-0,593102403	1,995478378	gnl|Amel_4.5|GB54693-PA	0,303941916	1,529568161
gnl|Amel_4.5|GB55693-PA	-0,228428013	1,992061448	gnl|Amel_4.5|GB45906-PA	6,865656143	1,520487109
gnl|Amel_4.5|GB52739-PA	-0,45624762	1,979778501	gnl|Amel_4.5|GB49306-PA	0,719275696	1,509911875
gnl|Amel_4.5|GB54862-PA	-0,358944357	1,96461807	gnl|Amel_4.5|GB40302-PA	0,627428611	1,498258575
gnl|Amel_4.5|GB46564-PA	-0,506040561	1,954969006	gnl|Amel_4.5|GB41338-PA	1,750010146	1,496631966
gnl|Amel_4.5|GB54929-PA	-0,370289397	1,938934625	gnl|Amel_4.5|GB48163-PA	0,912845013	1,485900014
gnl|Amel_4.5|GB40057-PA	-0,760648632	1,887584831	gnl|Amel_4.5|GB43704-PA	1,55008923	1,481533817
gnl|Amel_4.5|GB44422-PA	-0,260321633	1,884484013	gnl|Amel_4.5|GB48745-PA	2,300388217	1,459968993
gnl|Amel_4.5|GB47405-PA	-0,427510579	1,882445701	gnl|Amel_4.5|GB48641-PA	0,227327391	1,403818411
gnl|Amel_4.5|GB50170-PA	-1,768326849	1,876644313	gnl|Amel_4.5|GB55489-PA	2,042060477	1,40014896
gnl|Amel_4.5|GB56025-PA	-0,738403619	1,873530043	gnl|Amel_4.5|GB41143-PA	1,234277431	1,370376642
gnl|Amel_4.5|GB50970-PA	-0,661275217	1,871434391	gnl|Amel_4.5|GB45280-PA	0,422446236	1,368331546
gnl|Amel_4.5|GB56035-PA	-0,667388162	1,854933576	gnl|Amel_4.5|GB52468-PA	1,125294406	1,366263752
gnl|Amel_4.5|GB42970-PA	-2,44786574	1,847800054	gnl|Amel_4.5|GB55828-PA	0,446838651	1,359863753
gnl|Amel_4.5|GB53080-PA	-0,95827387	1,845959014	gnl|Amel_4.5|GB51042-PA	0,916124536	1,359616533
gnl|Amel_4.5|GB50421-PA	-0,891772843	1,835113512	gnl|Amel_4.5|GB44842-PA	0,377386455	1,351795144
gnl|Amel_4.5|GB47545-PA;gnl|Amel_4.5|GB51305-PA	-0,736458818	1,826810511	gnl|Amel_4.5|GB49313-PA	0,421946915	1,340488331
gnl|Amel_4.5|GB49522-PA	-0,626114823	1,81964181	gnl|Amel_4.5|GB50902-PA	0,954660716	1,336360205
gnl|Amel_4.5|GB50106-PA	-0,803205855	1,81783339	gnl|Amel_4.5|GB50973-PA	0,827743371	1,328552948
gnl|Amel_4.5|GB43573-PA	-0,598448902	1,796827584	gnl|Amel_4.5|GB46565-PA	0,988530386	1,322266805
gnl|Amel_4.5|GB47629-PA	-0,704773506	1,792093702	gnl|Amel_4.5|GB43247-PA	3,56599384	1,321851696
gnl|Amel_4.5|GB47436-PA	-0,566850588	1,781396595	gnl|Amel_4.5|GB46360-PA	0,483296547	1,318849027
gnl|Amel_4.5|GB47991-PA	-3,410441578	1,774105792	gnl|Amel_4.5|GB42297-PA	0,313500118	1,318032458

gnl|Amel_4.5|GB47336-PA	-0,648830253	1,730400341
gnl|Amel_4.5|GB54041-PA	-0,545871565	1,719887723
gnl|Amel_4.5|GB46774-PA	-0,462472245	1,719786805
gnl|Amel_4.5|GB53626-PA	-0,895956939	1,696879323
gnl|Amel_4.5|GB40445-PA	-0,760453034	1,683854595
gnl|Amel_4.5|GB40865-PA	-1,371053663	1,683056703
gnl|Amel_4.5|GB48470-PA	-0,482595708	1,66591799
gnl|Amel_4.5|GB52060-PA	-2,933384405	1,65949582
gnl|Amel_4.5|GB52999-PA	-0,845029406	1,658880304
gnl|Amel_4.5|GB43708-PA	-0,816200218	1,657155474
gnl|Amel_4.5|GB50183-PA	-1,02781617	1,638833954
gnl|Amel_4.5|GB49117-PA	-0,54608262	1,631646602
gnl|Amel_4.5|GB49583-PA	-0,273483421	1,621367544
gnl|Amel_4.5|GB42698-PA	-1,436339968	1,61441209
gnl|Amel_4.5|GB48905-PA	-0,806183972	1,610400204
gnl|Amel_4.5|GB41871-PA	-0,690565351	1,610336349
gnl|Amel_4.5|GB52994-PA	-0,777759188	1,605096166
gnl|Amel_4.5|GB47462-PA	-0,492294019	1,603419967
gnl|Amel_4.5|GB44002-PA	-2,023459307	1,596826935
gnl|Amel_4.5|GB55701-PA	-0,824723742	1,582421257
gnl|Amel_4.5|GB46066-PA	-0,280859416	1,576608306
gnl|Amel_4.5|GB55639-PA	-0,410697895	1,576432991
gnl|Amel_4.5|GB47906-PA	-0,821428277	1,565701622
gnl|Amel_4.5|GB48020-PA	-1,755104684	1,560935768
gnl|Amel_4.5|GB50259-PA	-0,924551862	1,544330831
gnl|Amel_4.5|GB49422-PA	-0,683371373	1,543342534
gnl|Amel_4.5|GB51283-PA	-0,613259927	1,539211523
gnl|Amel_4.5|GB50516-PA	-0,991713053	1,522519452
gnl|Amel_4.5|GB54611-PA	-0,692430541	1,520319996
gnl|Amel_4.5|GB49902-PA	-1,475665937	1,51835614
gnl|Amel_4.5|GB42794-PA	-1,212739009	1,516211043
gnl|Amel_4.5|GB40461-PA	-0,816727696	1,505305535
gnl|Amel_4.5|GB45720-PA	-0,35632217	1,495926187
gnl|Amel_4.5|GB41443-PA	-0,896532836	1,493246217
gnl|Amel_4.5|GB53621-PA	-2,593557468	1,490942781
gnl|Amel_4.5|GB51258-PA	-1,894111806	1,466715069
gnl|Amel_4.5|GB41183-PA	-0,595391164	1,466587631
gnl|Amel_4.5|GB41207-PA	-0,553550978	1,462473378
gnl|Amel_4.5|GB50750-PA	-0,720098003	1,459855575
gnl|Amel_4.5|GB40800-PA	-0,7509108	1,458077349
gnl|Amel_4.5|GB44721-PA	-0,559289459	1,448863219
gnl|Amel_4.5|GB48979-PA	-1,715194496	1,447129564
gnl|Amel_4.5|GB42264-PA	-0,80251078	1,439423384
gnl|Amel_4.5|GB48674-PA	-1,279314942	1,439233547
gnl|Amel_4.5|GB50889-PA	-2,389142769	1,433941437
gnl|Amel_4.5|GB41068-PA	-0,172043408	1,430222989
gnl|Amel_4.5|GB51884-PA	-0,600730523	1,426824975
gnl|Amel_4.5|GB54984-PA	-0,669448628	1,41951459
gnl|Amel_4.5|GB48333-PA	-0,448810191	1,413415382
gnl|Amel_4.5|GB52253-PA	-2,341611831	1,393051563
gnl|Amel_4.5|GB45960-PA	-2,454645743	1,391756017
gnl|Amel_4.5|GB41867-PA	-0,502078004	1,390485977
gnl|Amel_4.5|GB49628-PA	-0,423393588	1,389790992
gnl|Amel_4.5|GB47284-PA	-0,419313579	1,385228503
gnl|Amel_4.5|GB54701-PA	-0,644229475	1,382211306
gnl|Amel_4.5|GB44573-PA	-2,52388314	1,381790568
gnl|Amel_4.5|GB47331-PA	-0,821790007	1,379978842
gnl|Amel_4.5|GB52262-PA	-1,606944947	1,378767397
gnl|Amel_4.5|GB51579-PA	-1,176060508	1,378610076
gnl|Amel_4.5|GB44039-PA	-0,479451557	1,376433422
gnl|Amel_4.5|GB40824-PA	-2,514347481	1,375253579

gnl|Amel_4.5|GB50709-PA;gnl|Amel_4.5|GB48335-PA	-0,242903384	1,371907151
gnl|Amel_4.5|GB47103-PA	-0,49944363	1,355478606
gnl|Amel_4.5|GB53625-PA	-1,536959847	1,343622367
gnl|Amel_4.5|GB48852-PA	-0,489171468	1,342307415
gnl|Amel_4.5|GB50044-PA	-0,80987896	1,340840751
gnl|Amel_4.5|GB40713-PA	-0,757492432	1,340391623
gnl|Amel_4.5|GB44340-PA	-0,339416683	1,33904863
gnl|Amel_4.5|GB45047-PA	-0,312315898	1,319567098
gnl|Amel_4.5|GB52095-PA	-0,860757028	1,308845421
gnl|Amel_4.5|GB43819-PA	-0,359826493	1,304238498

Table 3- Proteins identified on the Group 24h 26ºC (infected *vs*. non-infected)

Down-regulated			Up-regulated		
ID	**log2foldchange**	**-log10p-value**	**ID**	**log2foldchange**	**-log10p-value**
gnl|Amel_4.5|GB45303-PA	-0,781296381	2,965523186	gnl|Amel_4.5|GB43548-PA	0,162797522	2,717105711
gnl|Amel_4.5|GB44586-PA	-0,734155723	2,869836901	gnl|Amel_4.5|GB42981-PA	0,791408235	2,522917588
gnl|Amel_4.5|GB54433-PA	-1,696142462	2,755343045	gnl|Amel_4.5|GB48147-PA	0,506727146	2,497844251
gnl|Amel_4.5|GB40735-PA	-0,485607907	2,748066607	gnl|Amel_4.5|GB47103-PA	0,378703568	2,296239303
gnl|Amel_4.5|GB45910-PA	-0,629480776	2,427148344	gnl|Amel_4.5|GB48020-PA	1,401478646	2,279479431
gnl|Amel_4.5|GB50333-PA	-0,424473298	2,312371554	gnl|Amel_4.5|GB47629-PA	0,253407716	2,131233672
gnl|Amel_4.5|GB45152-PA	-0,671089056	2,178070792	gnl|Amel_4.5|GB54321-PA	0,341575736	2,092044826
gnl|Amel_4.5|GB54446-PA	-0,323174452	2,110546234	gnl|Amel_4.5|GB44175-PA	0,765701732	1,888372409
gnl|Amel_4.5|GB53194-PA	-0,375681205	2,030605752	gnl|Amel_4.5|GB48240-PA	0,302013779	1,884903624
gnl|Amel_4.5|GB42233-PA	-2,780730185	1,933853318	gnl|Amel_4.5|GB50106-PA	0,210118892	1,867317408
gnl|Amel_4.5|GB47299-PA	-0,148205364	1,847354834	gnl|Amel_4.5|GB55602-PA	2,107341709	1,660753167
gnl|Amel_4.5|GB47747-PA	-0,53048741	1,82315722	gnl|Amel_4.5|GB42862-PA	0,141818926	1,622350882
gnl|Amel_4.5|GB54692-PA	-0,315406457	1,716097705	gnl|Amel_4.5|GB54549-PA	0,387767574	1,571582834
gnl|Amel_4.5|GB48244-PA	-0,457035768	1,688574176	gnl|Amel_4.5|GB51598-PA	0,298563978	1,487960378
gnl|Amel_4.5|GB41150-PA	-0,373789213	1,671831541	gnl|Amel_4.5|GB43280-PA	0,243997011	1,467408018
gnl|Amel_4.5|GB44531-PA	-0,718780696	1,670279974	gnl|Amel_4.5|GB50057-PA	0,522632713	1,406379116
gnl|Amel_4.5|GB44444-PA	-0,413154532	1,629644716	gnl|Amel_4.5|GB45831-PA	0,33698314	1,378383238
gnl|Amel_4.5|GB55150-PA	-2,535821202	1,605129678	gnl|Amel_4.5|GB46750-PA	0,148705163	1,318156392
gnl|Amel_4.5|GB40673-PA	-0,204276634	1,593730907			
gnl|Amel_4.5|GB48810-PA	-0,894434089	1,550949882			
gnl|Amel_4.5|GB47604-PA	-0,248212126	1,529200195			
gnl|Amel_4.5|GB41084-PA	-0,201259517	1,519058241			
gnl|Amel_4.5|GB53065-PA	-0,817272729	1,464378512			
gnl|Amel_4.5|GB42616-PA	-0,272721011	1,458053536			
gnl|Amel_4.5|GB49854-PA	-1,173332372	1,449884126			
gnl|Amel_4.5|GB40261-PA	-0,514962017	1,357507299			
gnl|Amel_4.5|GB49024-PA	-0,622441186	1,345322581			
gnl|Amel_4.5|GB47016-PA	-0,400425629	1,311038917			
gnl|Amel_4.5|GB48201-PA	-0,323340674	1,309800307			
gnl|Amel_4.5|GB47505-PA;gnl|Amel_4.5|GB47408-PA;gnl|Amel_4.5|GB44765-PA;gnl|Amel_4.5|GB44339-PA	-0,703308514	1,308832765			

Table 4- Proteins identified on the Group 48h 26ºC (infected *vs*. non-infected)

Down-regulated			Up-regulated		
ID	**log2foldchange**	**-log10p-value**	**ID**	**log2foldchange**	**-log10p-value**
gnl|Amel_4.5|GB46986-PA	-0,88853	4,299431	gnl|Amel_4.5|GB40566-PA	1,808526	4,320085
gnl|Amel_4.5|GB50044-PA	-0,74509	3,735009	gnl|Amel_4.5|GB46749-PA	4,024227	3,877921
gnl|Amel_4.5|GB55895-PA	-1,20518	3,5783	gnl|Amel_4.5|GB47990-PA	3,200674	3,820938

gnl|Amel_4.5|GB49240-PA	-0,9142	3,559927	gnl|Amel_4.5|GB50076-PA	3,513342	3,565841
gnl|Amel_4.5|GB51963-PA	-0,61318	3,47075	gnl|Amel_4.5|GB49775-PA	0,934808	3,470088
gnl|Amel_4.5|GB50595-PA	-0,98815	3,158756	gnl|Amel_4.5|GB46914-PA	3,854119	3,225732
gnl|Amel_4.5|GB50265-PA	-0,72269	3,135081	gnl|Amel_4.5|GB55328-PA	3,132369	3,201303
gnl|Amel_4.5|GB54446-PA	-0,64882	2,968355	gnl|Amel_4.5|GB46297-PA	2,068073	3,102156
gnl|Amel_4.5|GB50451-PA	-1,78154	2,84236	gnl|Amel_4.5|GB55231-PA	3,765989	3,097206
gnl|Amel_4.5|GB47573-PA	-1,007	2,83671	gnl|Amel_4.5|GB48831-PA	0,910023	3,093995
gnl|Amel_4.5|GB53010-PA	-2,38404	2,799034	gnl|Amel_4.5|GB54355-PA	1,596622	2,917119
gnl|Amel_4.5|GB43815-PA	-0,8168	2,688825	gnl|Amel_4.5|GB40976-PA	0,904678	2,858039
gnl|Amel_4.5|GB52728-PA	-0,66103	2,609733	gnl|Amel_4.5|GB50995-PA	2,594268	2,833663
gnl|Amel_4.5|GB52013-PA	-0,66658	2,579956	gnl|Amel_4.5|GB43248-PA	3,461845	2,706425
gnl|Amel_4.5|GB52120-PA	-0,61908	2,53482	gnl|Amel_4.5|GB47839-PA	2,356419	2,660145
gnl|Amel_4.5|GB49448-PA	-0,96486	2,509846	gnl|Amel_4.5|GB44502-PA	2,689836	2,651364
gnl|Amel_4.5|GB53626-PA	-0,55061	2,507834	gnl|Amel_4.5|GB41927-PA	3,397541	2,64946
gnl|Amel_4.5|GB53887-PA	-1,04093	2,503044	gnl|Amel_4.5|GB52598-PA	0,756842	2,595347
gnl|Amel_4.5|GB49956-PA	-0,73269	2,489166	gnl|Amel_4.5|GB49117-PA	1,689966	2,582089
gnl|Amel_4.5|GB46052-PA	-0,79897	2,480335	gnl|Amel_4.5|GB45763-PA	3,453752	2,550935
gnl|Amel_4.5|GB44462-PA	-0,51074	2,445868	gnl|Amel_4.5|GB45537-PA	0,924357	2,505159
gnl|Amel_4.5|GB44464-PA	-0,83742	2,416059	gnl|Amel_4.5|GB49220-PA	3,26922	2,491067
gnl|Amel_4.5|GB51335-PA	-0,58139	2,30196	gnl|Amel_4.5|GB41867-PA	1,762192	2,475785
gnl|Amel_4.5|GB46120-PA	-0,9999	2,292357	gnl|Amel_4.5|GB45968-PA	0,934446	2,434995
gnl|Amel_4.5|GB54363-PA	-0,53712	2,279717	gnl|Amel_4.5|GB40320-PA	1,693516	2,428668
gnl|Amel_4.5|GB43848-PA	-1,20442	2,252566	gnl|Amel_4.5|GB41392-PA	0,951196	2,414691
gnl|Amel_4.5|GB53947-PA	-2,50415	2,252184	gnl|Amel_4.5|GB46564-PA	1,848541	2,375101
gnl|Amel_4.5|GB47284-PA	-0,58847	2,219653	gnl|Amel_4.5|GB48823-PA	0,537188	2,372217
gnl|Amel_4.5|GB42141-PA	-0,75601	2,174918	gnl|Amel_4.5|GB45700-PA	2,374112	2,310895
gnl|Amel_4.5|GB44704-PA	-0,97844	2,167736	gnl|Amel_4.5|GB43890-PA	0,607148	2,281734
gnl|Amel_4.5|GB43750-PA	-0,5697	2,150391	gnl|Amel_4.5|GB52947-PA	2,380738	2,267071
gnl|Amel_4.5|GB51009-PA	-1,71205	2,144732	gnl|Amel_4.5|GB46962-PA	2,596336	2,242936
gnl|Amel_4.5|GB43618-PA	-0,56497	2,143702	gnl|Amel_4.5|GB43052-PA	2,610581	2,225233
gnl|Amel_4.5|GB50873-PA	-0,88961	2,11506	gnl|Amel_4.5|GB47584-PA	1,32063	2,221299
gnl|Amel_4.5|GB50598-PA	-0,83161	2,105289	gnl|Amel_4.5|GB55063-PA	1,025114	2,207751
gnl|Amel_4.5|GB44153-PA	-1,0293	2,090291	gnl|Amel_4.5|GB47960-PA	1,985067	2,196085
gnl|Amel_4.5|GB40100-PA	-0,53719	2,059905	gnl|Amel_4.5|GB53013-PA	3,230718	2,171782
gnl|Amel_4.5|GB45334-PA	-1,2489	2,059818	gnl|Amel_4.5|GB54380-PA	1,033714	2,138268
gnl|Amel_4.5|GB52121-PA	-0,84521	2,054019	gnl|Amel_4.5|GB45688-PA	0,994504	2,133854
gnl|Amel_4.5|GB51396-PA	-1,40786	2,052917	gnl|Amel_4.5|GB48248-PA	0,896429	2,128485
gnl|Amel_4.5|GB53333-PA	-0,60749	2,050269	gnl|Amel_4.5|GB49353-PA	1,588582	2,123902
gnl|Amel_4.5|GB47604-PA	-0,6788	2,042322	gnl|Amel_4.5|GB51467-PA;gnl|Amel_4.5|GB48148-PA	1,598635	2,098596
gnl|Amel_4.5|GB44983-PA	-0,37539	2,039541	gnl|Amel_4.5|GB53937-PA	1,01177	2,027917
gnl|Amel_4.5|GB51884-PA	-0,53341	2,021044	gnl|Amel_4.5|GB45429-PA	0,741009	2,02706
gnl|Amel_4.5|GB47433-PA	-0,76317	2,017734	gnl|Amel_4.5|GB50973-PA	1,892417	2,025718
gnl|Amel_4.5|GB49497-PA	-0,91964	2,016154	gnl|Amel_4.5|GB52343-PA	2,315274	2,002887
gnl|Amel_4.5|GB55382-PA	-0,90621	2,002698	gnl|Amel_4.5|GB55215-PA	1,463823	1,988978
gnl|Amel_4.5|GB47723-PA	-1,74709	1,986095	gnl|Amel_4.5|GB54990-PA	0,905074	1,982183
gnl|Amel_4.5|GB47106-PA	-1,31682	1,979058	gnl|Amel_4.5|GB50099-PA	1,595123	1,978469
gnl|Amel_4.5|GB46617-PA	-0,41791	1,947971	gnl|Amel_4.5|GB43434-PA	3,507648	1,968879
gnl|Amel_4.5|GB54653-PA	-0,54993	1,931952	gnl|Amel_4.5|GB42426-PA	1,267528	1,963748
gnl|Amel_4.5|GB43990-PA	-0,4205	1,931543	gnl|Amel_4.5|GB48833-PA	0,757099	1,955053
gnl|Amel_4.5|GB43187-PA	-1,87074	1,928574	gnl|Amel_4.5|GB49013-PA	2,159399	1,951784
gnl|Amel_4.5|GB40460-PA	-0,59987	1,92388	gnl|Amel_4.5|GB41772-PA	3,791812	1,938969
gnl|Amel_4.5|GB55010-PA	-1,19276	1,921829	gnl|Amel_4.5|GB42427-PA	2,444843	1,936434
gnl|Amel_4.5|GB40887-PA	-0,22755	1,91597	gnl|Amel_4.5|GB46268-PA	3,396935	1,927743
gnl|Amel_4.5|GB45264-PA	-1,02743	1,915595	gnl|Amel_4.5|GB44422-PA	0,55325	1,870231
gnl|Amel_4.5|GB41798-PA	-0,78671	1,904788	gnl|Amel_4.5|GB40461-PA	3,149253	1,86538
gnl|Amel_4.5|GB53727-PA	-0,69871	1,903605	gnl|Amel_4.5|GB54549-PA	2,448477	1,853301
gnl|Amel_4.5|GB51192-PA	-0,44845	1,902555	gnl|Amel_4.5|GB45855-PA	1,304883	1,851987
gnl|Amel_4.5|GB41604-PA	-0,71487	1,899412	gnl|Amel_4.5|GB52500-PA	0,405555	1,850329
gnl|Amel_4.5|GB52739-PA	-0,37951	1,897088	gnl|Amel_4.5|GB45913-PA	0,921704	1,849537

gnl|Amel_4.5|GB49079-PA	-0,6686	1,895854	gnl|Amel_4.5|GB54281-PA	0,570359	1,849202
gnl|Amel_4.5|GB47574-PA	-1,43629	1,894581	gnl|Amel_4.5|GB47880-PA	1,003536	1,845792
gnl|Amel_4.5|GB48922-PA	-1,41161	1,882041	gnl|Amel_4.5|GB43053-PA	2,327509	1,826821
gnl|Amel_4.5|GB43540-PA	-0,64785	1,878525	gnl|Amel_4.5|GB48699-PA	0,595851	1,820215
gnl|Amel_4.5|GB42698-PA	-1,07758	1,878274	gnl|Amel_4.5|GB45951-PA	2,699858	1,816336
gnl|Amel_4.5|GB43706-PA	-0,75322	1,876328	gnl|Amel_4.5|GB44501-PA	0,694328	1,81205
gnl|Amel_4.5|GB49287-PA	-0,60002	1,875205	gnl|Amel_4.5|GB42425-PA	0,381405	1,80094
gnl|Amel_4.5|GB41028-PA	-0,50527	1,862547	gnl|Amel_4.5|GB43302-PA	3,083471	1,781277
gnl|Amel_4.5|GB47268-PA	-0,29482	1,859773	gnl|Amel_4.5|GB55327-PA	4,198986	1,765908
gnl|Amel_4.5|GB46985-PA	-0,68754	1,856244	gnl|Amel_4.5|GB51598-PA	0,47535	1,755389
gnl|Amel_4.5|GB48844-PA	-1,28184	1,855358	gnl|Amel_4.5|GB48216-PA	0,477338	1,752022
gnl|Amel_4.5|GB49643-PA	-1,90277	1,853234	gnl|Amel_4.5|GB43300-PA	1,367532	1,748648
gnl|Amel_4.5|GB55639-PA	-0,69388	1,852134	gnl|Amel_4.5|GB53945-PA	0,922186	1,743841
gnl|Amel_4.5|GB55853-PA	-1,00226	1,8465	gnl|Amel_4.5|GB48492-PA	0,767813	1,741627
gnl|Amel_4.5|GB52324-PA	-0,4495	1,842277	gnl|Amel_4.5|GB54861-PA	2,197726	1,730475
gnl|Amel_4.5|GB48628-PA	-0,82062	1,841777	gnl|Amel_4.5|GB42556-PA	0,735124	1,722017
gnl|Amel_4.5|GB42723-PA	-0,85759	1,827618	gnl|Amel_4.5|GB49389-PA	2,288852	1,700196
gnl|Amel_4.5|GB51539-PA	-0,83379	1,814041	gnl|Amel_4.5|GB46066-PA	2,671706	1,698539
gnl|Amel_4.5|GB40592-PA	-0,96974	1,802598	gnl|Amel_4.5|GB50242-PA	0,579241	1,684265
gnl|Amel_4.5|GB49974-PA	-2,01828	1,794787	gnl|Amel_4.5|GB44749-PA	1,167678	1,683338
gnl|Amel_4.5|GB54343-PA	-1,12843	1,793356	gnl|Amel_4.5|GB51086-PA	0,691829	1,678289
gnl|Amel_4.5|GB48841-PA	-0,74366	1,78165	gnl|Amel_4.5|GB52999-PA	0,702977	1,654281
gnl|Amel_4.5|GB49047-PA	-0,63898	1,781486	gnl|Amel_4.5|GB54654-PA	2,609137	1,652118
gnl|Amel_4.5|GB51551-PA	-0,87906	1,780606	gnl|Amel_4.5|GB55250-PA	2,699627	1,651316
gnl|Amel_4.5|GB40718-PA	-0,70016	1,77482	gnl|Amel_4.5|GB55348-PA	2,079076	1,63969
gnl|Amel_4.5|GB46534-PA	-0,8708	1,774782	gnl|Amel_4.5|GB50219-PA	1,222197	1,636711
gnl|Amel_4.5|GB50355-PA	-0,66778	1,772049	gnl|Amel_4.5|GB52059-PA	1,866865	1,631115
gnl|Amel_4.5|GB47904-PA	-1,85714	1,769034	gnl|Amel_4.5|GB55432-PA	4,159303	1,625766
gnl|Amel_4.5|GB43905-PA	-0,84012	1,766951	gnl|Amel_4.5|GB41945-PA	0,62368	1,618453
gnl|Amel_4.5|GB48641-PA	-0,70074	1,765637	gnl|Amel_4.5|GB53549-PA	0,728992	1,616178
gnl|Amel_4.5|GB42918-PA	-0,55059	1,763525	gnl|Amel_4.5|GB48191-PA	1,99754	1,60564
gnl|Amel_4.5|GB44869-PA	-1,06897	1,761113	gnl|Amel_4.5|GB42693-PA	0,531555	1,6048
gnl|Amel_4.5|GB48111-PA	-0,61251	1,761091	gnl|Amel_4.5|GB46014-PA	1,995915	1,591973
gnl|Amel_4.5|GB54508-PA	-1,3185	1,747626	gnl|Amel_4.5|GB41773-PA	1,763289	1,583089
gnl|Amel_4.5|GB45099-PA	-0,69687	1,74507	gnl|Amel_4.5|GB47906-PA	2,129594	1,569021
gnl|Amel_4.5|GB48527-PA	-0,92773	1,742222	gnl|Amel_4.5|GB43869-PA	1,915731	1,567561
gnl|Amel_4.5|GB54192-PA	-1,0074	1,737497	gnl|Amel_4.5|GB55214-PA	3,055135	1,566172
gnl|Amel_4.5|GB47304-PA	-0,81748	1,736709	gnl|Amel_4.5|GB46420-PA	0,633852	1,559525
gnl|Amel_4.5|GB54423-PA	-0,71083	1,720169	gnl|Amel_4.5|GB41332-PA	0,896713	1,556527
gnl|Amel_4.5|GB53132-PA	-0,56586	1,711079	gnl|Amel_4.5|GB43184-PA	2,437736	1,55407
gnl|Amel_4.5|GB51733-PA	-0,69515	1,710189	gnl|Amel_4.5|GB52467-PA	2,07305	1,553663
gnl|Amel_4.5|GB44586-PA	-1,83953	1,709303	gnl|Amel_4.5|GB53125-PA	2,229171	1,553023
gnl|Amel_4.5|GB49632-PA	-0,72035	1,708637	gnl|Amel_4.5|GB52789-PA	0,656807	1,552332
gnl|Amel_4.5|GB45736-PA	-0,47719	1,70689	gnl|Amel_4.5|GB55564-PA	2,567984	1,534101
gnl|Amel_4.5|GB55827-PA	-1,63695	1,699677	gnl|Amel_4.5|GB49597-PA	2,556872	1,529367
gnl|Amel_4.5|GB47629-PA	-0,27906	1,695008	gnl|Amel_4.5|GB50757-PA	2,136549	1,526237
gnl|Amel_4.5|GB48663-PA	-0,78838	1,692271	gnl|Amel_4.5|GB40877-PA	2,66689	1,526096
gnl|Amel_4.5|GB48857-PA	-2,69798	1,688719	gnl|Amel_4.5|GB41025-PA	1,870583	1,521943
gnl|Amel_4.5|GB44211-PA	-0,95005	1,686938	gnl|Amel_4.5|GB46227-PA	0,553082	1,520959
gnl|Amel_4.5|GB51042-PA	-0,67838	1,686548	gnl|Amel_4.5|GB47933-PA	1,915974	1,5159
gnl|Amel_4.5|GB45720-PA	-0,24383	1,681975	gnl|Amel_4.5|GB48604-PA	0,706043	1,513747
gnl|Amel_4.5|GB45087-PA	-1,50263	1,679534	gnl|Amel_4.5|GB54368-PA	0,809843	1,507667
gnl|Amel_4.5|GB46263-PA	-1,90748	1,669112	gnl|Amel_4.5|GB54222-PA	1,697323	1,501663
gnl|Amel_4.5|GB50158-PA	-2,66481	1,659861	gnl|Amel_4.5|GB46774-PA	1,096973	1,497401
gnl|Amel_4.5|GB44404-PA	-0,8069	1,652191	gnl|Amel_4.5|GB52161-PA	1,745646	1,492263
gnl|Amel_4.5|GB50596-PA	-0,69614	1,651413	gnl|Amel_4.5|GB54507-PA	0,793194	1,486215
gnl|Amel_4.5|GB50974-PA	-0,56202	1,643382	gnl|Amel_4.5|GB55325-PA	2,793775	1,485777
gnl|Amel_4.5|GB44056-PA	-0,68827	1,642821	gnl|Amel_4.5|GB44198-PA	1,74684	1,48463
gnl|Amel_4.5|GB55919-PA	-2,00491	1,642199	gnl|Amel_4.5|GB46360-PA	3,717182	1,478271
gnl|Amel_4.5|GB41427-PA	-1,19334	1,640272	gnl|Amel_4.5|GB46567-PA	1,759924	1,46472
gnl|Amel_4.5|GB51710-PA	-0,8951	1,63377	gnl|Amel_4.5|GB40865-PA	1,931548	1,456736
gnl|Amel_4.5|GB55077-PA	-0,56232	1,633526	gnl|Amel_4.5|GB42769-PA	1,72373	1,450006

gnl|Amel_4.5|GB42604-PA	-1,8489	1,632051
gnl|Amel_4.5|GB49554-PA	-0,66533	1,630831
gnl|Amel_4.5|GB40769-PA	-0,79103	1,628824
gnl|Amel_4.5|GB53256-PA	-0,78742	1,620597
gnl|Amel_4.5|GB46071-PA	-0,37096	1,620285
gnl|Amel_4.5|GB53566-PA	-0,52571	1,619953
gnl|Amel_4.5|GB46404-PA	-2,53382	1,615941
gnl|Amel_4.5|GB41778-PA	-1,08413	1,615715
gnl|Amel_4.5|GB54714-PA	-0,40037	1,605935
gnl|Amel_4.5|GB55298-PA	-1,18226	1,604836
gnl|Amel_4.5|GB42793-PA	-0,5237	1,599844
gnl|Amel_4.5|GB54747-PA	-0,93982	1,599394
gnl|Amel_4.5|GB50817-PA	-1,19276	1,59563
gnl|Amel_4.5|GB55537-PA	-0,98936	1,593445
gnl|Amel_4.5|GB41207-PA	-0,43902	1,577099
gnl|Amel_4.5|GB55701-PA	-1,97369	1,575678
gnl|Amel_4.5|GB41711-PA	-0,5742	1,574854
gnl|Amel_4.5|GB42874-PA	-0,5029	1,573467
gnl|Amel_4.5|GB47478-PA	-0,82618	1,569563
gnl|Amel_4.5|GB40267-PA	-1,03034	1,567257
gnl|Amel_4.5|GB41027-PA	-2,04617	1,565815
gnl|Amel_4.5|GB42862-PA	-0,57156	1,561403
gnl|Amel_4.5|GB47661-PA	-1,10924	1,559617
gnl|Amel_4.5|GB47331-PA	-0,3133	1,558075
gnl|Amel_4.5|GB54692-PA	-0,6811	1,552861
gnl|Amel_4.5|GB51206-PA	-1,34769	1,550644
gnl|Amel_4.5|GB40770-PA	-0,68839	1,547043
gnl|Amel_4.5|GB41770-PA	-1,06026	1,545159
gnl|Amel_4.5|GB49495-PA	-0,81792	1,538172
gnl|Amel_4.5|GB52497-PA	-0,76733	1,525957
gnl|Amel_4.5|GB54590-PA	-0,7003	1,525002
gnl|Amel_4.5|GB50210-PA	-0,3496	1,5242
gnl|Amel_4.5|GB48373-PA;gnl|Amel_4.5|GB48374-PA	-1,76135	1,520794
gnl|Amel_4.5|GB48610-PA	-2,41734	1,512884
gnl|Amel_4.5|GB52074-PA	-1,36984	1,512004
gnl|Amel_4.5|GB52073-PA	-0,57399	1,51131
gnl|Amel_4.5|GB44068-PA	-1,34881	1,506725
gnl|Amel_4.5|GB48124-PA	-1,49916	1,499389
gnl|Amel_4.5|GB44449-PA	-1,6309	1,49826
gnl|Amel_4.5|GB51736-PA	-2,37217	1,497898
gnl|Amel_4.5|GB46887-PA	-0,46508	1,497312
gnl|Amel_4.5|GB55680-PA	-0,56982	1,497241
gnl|Amel_4.5|GB47500-PA	-0,86545	1,496868
gnl|Amel_4.5|GB49161-PA	-0,8835	1,49366
gnl|Amel_4.5|GB50854-PA	-0,90967	1,492809
gnl|Amel_4.5|GB48103-PA	-0,4753	1,472277
gnl|Amel_4.5|GB44847-PA	-2,34711	1,471487
gnl|Amel_4.5|GB51543-PA	-1,47577	1,460995
gnl|Amel_4.5|GB54587-PA	-0,55728	1,460963
gnl|Amel_4.5|GB55782-PA	-1,06898	1,459915
gnl|Amel_4.5|GB53201-PA	-0,62068	1,456466
gnl|Amel_4.5|GB48914-PA	-2,42605	1,446484
gnl|Amel_4.5|GB49347-PA	-0,65689	1,444651
gnl|Amel_4.5|GB49534-PA	-1,00799	1,444149
gnl|Amel_4.5|GB45761-PA	-1,33195	1,437003
gnl|Amel_4.5|GB47227-PA	-1,05573	1,436245
gnl|Amel_4.5|GB50450-PA	-1,75255	1,433612
gnl|Amel_4.5|GB44783-PA	-2,16376	1,429605
gnl|Amel_4.5|GB42560-PA	-0,34871	1,420657
gnl|Amel_4.5|GB46170-PA	-0,6557	1,420434
gnl|Amel_4.5|GB45673-PA	1,374807	1,449914
gnl|Amel_4.5|GB53565-PA	4,358862	1,432875
gnl|Amel_4.5|GB51783-PA	0,613019	1,422206
gnl|Amel_4.5|GB53579-PA	1,519846	1,411325
gnl|Amel_4.5|GB41858-PA	1,071659	1,409592
gnl|Amel_4.5|GB50170-PA	2,359425	1,403585
gnl|Amel_4.5|GB50519-PA	4,119239	1,399451
gnl|Amel_4.5|GB55329-PA	3,732491	1,397566
gnl|Amel_4.5|GB53435-PA	3,77482	1,388181
gnl|Amel_4.5|GB54588-PA	1,577376	1,386285
gnl|Amel_4.5|GB50064-PA	1,554046	1,379185
gnl|Amel_4.5|GB40934-PA	0,56541	1,370846
gnl|Amel_4.5|GB44533-PA	0,540038	1,346054
gnl|Amel_4.5|GB47266-PA	0,567763	1,34536
gnl|Amel_4.5|GB55499-PA	3,672915	1,344117
gnl|Amel_4.5|GB50183-PA	1,825956	1,335233
gnl|Amel_4.5|GB47310-PA	0,862703	1,33492
gnl|Amel_4.5|GB54862-PA	1,280108	1,333879
gnl|Amel_4.5|GB46310-PA	2,091935	1,332595
gnl|Amel_4.5|GB50235-PA	0,423802	1,3313
gnl|Amel_4.5|GB54381-PA	3,135939	1,324597
gnl|Amel_4.5|GB48079-PA	1,584695	1,32448
gnl|Amel_4.5|GB46298-PA	1,738763	1,320073
gnl|Amel_4.5|GB42701-PA	1,804963	1,31594
gnl|Amel_4.5|GB40009-PA	1,543505	1,308174

gnl|Amel_4.5|GB50952-PA	-2,40413	1,416151
gnl|Amel_4.5|GB50975-PA	-0,74021	1,41427
gnl|Amel_4.5|GB47299-PA	-0,73639	1,408605
gnl|Amel_4.5|GB44039-PA	-0,28514	1,407759
gnl|Amel_4.5|GB45545-PA	-0,46423	1,400345
gnl|Amel_4.5|GB46339-PA	-2,04417	1,39564
gnl|Amel_4.5|GB41150-PA	-0,65096	1,39028
gnl|Amel_4.5|GB50123-PA	-0,51611	1,38424
gnl|Amel_4.5|GB55536-PA	-2,29567	1,382615
gnl|Amel_4.5|GB49948-PA	-1,58929	1,380704
gnl|Amel_4.5|GB40705-PA	-1,59844	1,379112
gnl|Amel_4.5|GB40535-PA	-0,55649	1,378687
gnl|Amel_4.5|GB41741-PA	-0,71259	1,374342
gnl|Amel_4.5|GB42845-PA	-0,71512	1,372351
gnl|Amel_4.5|GB47430-PA	-0,8641	1,36762
gnl|Amel_4.5|GB49313-PA	-0,58823	1,363234
gnl|Amel_4.5|GB48201-PA	-1,59254	1,360591
gnl|Amel_4.5|GB49422-PA	-1,55569	1,358943
gnl|Amel_4.5|GB42835-PA	-1,50871	1,357869
gnl|Amel_4.5|GB55062-PA	-0,69667	1,352607
gnl|Amel_4.5|GB50555-PA	-0,14306	1,346843
gnl|Amel_4.5|GB48351-PA	-1,58965	1,344095
gnl|Amel_4.5|GB55220-PA	-1,54852	1,341191
gnl|Amel_4.5|GB50728-PA	-1,58348	1,331629
gnl|Amel_4.5|GB48745-PA	-1,67151	1,328356
gnl|Amel_4.5|GB40716-PA	-0,38847	1,327466
gnl|Amel_4.5|GB54606-PA	-1,30874	1,323453
gnl|Amel_4.5|GB49629-PA	-0,66229	1,323302
gnl|Amel_4.5|GB41154-PA	-0,77124	1,322646
gnl|Amel_4.5|GB42871-PA	-1,00698	1,320955
gnl|Amel_4.5|GB41068-PA	-1,01021	1,320441
gnl|Amel_4.5|GB51580-PA	-3,692	1,320384
gnl|Amel_4.5|GB54417-PA;gnl|Amel_4.5|GB53986-PA	-1,76261	1,32008
gnl|Amel_4.5|GB42234-PA	-1,37619	1,319818
gnl|Amel_4.5|GB49999-PA	-0,36712	1,31834
gnl|Amel_4.5|GB49784-PA	-0,96764	1,313918
gnl|Amel_4.5|GB40349-PA	-1,36733	1,312606
gnl|Amel_4.5|GB54817-PA	-0,51917	1,311451
gnl|Amel_4.5|GB49959-PA	-1,49099	1,311221
gnl|Amel_4.5|GB45419-PA	-0,34947	1,310563
gnl|Amel_4.5|GB51683-PA	-0,91785	1,310444
gnl|Amel_4.5|GB45635-PA	-1,22889	1,307462
gnl|Amel_4.5|GB44966-PA	-2,33483	1,303569
gnl|Amel_4.5|GB41663-PA	-0,53813	1,301929
gnl|Amel_4.5|GB45280-PA	-0,74508	1,300963
gnl|Amel_4.5|GB49471-PA	-0,48215	1,300962

Table 5- Proteins identified on the Group 24h 32ºC (infected *vs*. non-infected)

Down-regulated			**Up-regulated**		
ID	**log2foldchange**	**-log10p-value**	**ID**	**log2foldchange**	**-log10p-value**
gnl|Amel_4.5|GB52644-PA	-1,00975	2,395731	gnl|Amel_4.5|GB44298-PA	0,345789	2,201296
gnl|Amel_4.5|GB47576-PA	-0,0966	2,234334	gnl|Amel_4.5|GB44133-PA;gnl|Amel_4.5|GB44074-PA	0,478497	2,108656
gnl|Amel_4.5|GB54611-PA	-0,55142	2,23433	gnl|Amel_4.5|GB53579-PA	0,792716	1,995372
gnl|Amel_4.5|GB45731-PA	-0,86696	1,941583	gnl|Amel_4.5|GB54549-PA	1,694854	1,868968
gnl|Amel_4.5|GB44153-PA	-1,10389	1,927742	gnl|Amel_4.5|GB44878-PA	0,414928	1,819702

gnl|Amel_4.5|GB44882-PA	-0,34344	1,882046	gnl|Amel_4.5|GB40976-PA	0,175185	1,712239
gnl|Amel_4.5|GB47407-PA;gnl|Amel_4.5|GB47406-PA;gnl|Amel_4.5|GB47382-PA;gnl|Amel_4.5|GB44318-PA	-0,66559	1,774142	gnl|Amel_4.5|GB43052-PA	0,444033	1,609704
gnl|Amel_4.5|GB48244-PA	-0,38135	1,751473	gnl|Amel_4.5|GB41793-PA	1,115731	1,568456
gnl|Amel_4.5|GB47176-PA	-0,53395	1,727845	gnl|Amel_4.5|GB52782-PA	0,749374	1,521816
gnl|Amel_4.5|GB52684-PA	-0,69071	1,726046	gnl|Amel_4.5|GB52074-PA	1,807337	1,511379
gnl|Amel_4.5|GB50663-PA	-0,71354	1,703926	gnl|Amel_4.5|GB54222-PA	1,279536	1,501503
gnl|Amel_4.5|GB48929-PA	-0,76549	1,561704	gnl|Amel_4.5|GB41427-PA	0,489174	1,500885
gnl|Amel_4.5|GB50355-PA	-0,50588	1,53561	gnl|Amel_4.5|GB47990-PA	0,754927	1,471809
gnl|Amel_4.5|GB40240-PA	-0,45406	1,504171	gnl|Amel_4.5|GB48574-PA	2,096486	1,404921
gnl|Amel_4.5|GB40492-PA	-0,16815	1,486118	gnl|Amel_4.5|GB51653-PA	0,896079	1,378511
gnl|Amel_4.5|GB49234-PA	-1,05039	1,448029	gnl|Amel_4.5|GB46263-PA	1,781355	1,366663
gnl|Amel_4.5|GB44608-PA	-0,69729	1,439253	gnl|Amel_4.5|GB42427-PA	1,728713	1,365119
gnl|Amel_4.5|GB51192-PA	-0,57996	1,39194	gnl|Amel_4.5|GB55328-PA	0,432321	1,347656
gnl|Amel_4.5|GB52211-PA	-1,09395	1,375472	gnl|Amel_4.5|GB41773-PA	0,43659	1,30497
gnl|Amel_4.5|GB42792-PA	-0,64611	1,366458			
gnl|Amel_4.5|GB44967-PA	-0,2273	1,353628			
gnl|Amel_4.5|GB51224-PA	-0,64271	1,344094			
gnl|Amel_4.5|GB49937-PA	-1,59549	1,329646			
gnl|Amel_4.5|GB54192-PA	-0,31268	1,32132			
gnl|Amel_4.5|GB50226-PA	-0,696	1,314261			
gnl|Amel_4.5|GB51963-PA	-0,58371	1,302076			

Table 6- Proteins identified on the Group 48h 32ºC (infected *vs*. non-infected)

Down-regulated			**Up-regulated**		
ID	**log2foldchange**	**-log10p-value**	**ID**	**log2foldchange**	**-log10p-value**
gnl|Amel_4.5|GB50355-PA	-0,78149	2,6191	gnl|Amel_4.5|GB45496-PA	0,71507	3,759212
gnl|Amel_4.5|GB50555-PA	-0,57063	2,001991	gnl|Amel_4.5|GB49013-PA	3,489584	2,784369
gnl|Amel_4.5|GB49584-PA	-3,0492	1,930214	gnl|Amel_4.5|GB45495-PA	1,6187	2,666631
gnl|Amel_4.5|GB41798-PA	-1,06133	1,863378	gnl|Amel_4.5|GB46587-PA	0,781085	2,577489
gnl|Amel_4.5|GB46069-PA	-0,69166	1,807218	gnl|Amel_4.5|GB52581-PA;gnl|Amel_4.5|GB50783-PA	0,632408	2,572145
gnl|Amel_4.5|GB42845-PA	-0,57097	1,793715	gnl|Amel_4.5|GB55232-PA	0,38708	2,368979
gnl|Amel_4.5|GB48255-PA	-1,00093	1,729548	gnl|Amel_4.5|GB50106-PA	0,558585	2,327651
gnl|Amel_4.5|GB52028-PA	-0,57422	1,727619	gnl|Amel_4.5|GB48219-PA	0,85257	2,151688
gnl|Amel_4.5|GB52428-PA	-0,87804	1,721671	gnl|Amel_4.5|GB48929-PA	1,380114	1,900939
gnl|Amel_4.5|GB47043-PA	-1,15674	1,671073	gnl|Amel_4.5|GB47407-PA;gnl|Amel_4.5|GB47406-PA;gnl|Amel_4.5|GB47382-PA;gnl|Amel_4.5|GB44318-PA	0,429604	1,841553
gnl|Amel_4.5|GB41358-PA	-0,48853	1,645159	gnl|Amel_4.5|GB44483-PA	2,81339	1,83614
gnl|Amel_4.5|GB50995-PA	-0,99473	1,589527	gnl|Amel_4.5|GB48843-PA	0,642688	1,782557
gnl|Amel_4.5|GB40746-PA	-0,85615	1,588264	gnl|Amel_4.5|GB44903-PA	3,357086	1,724296
gnl|Amel_4.5|GB43713-PA	-2,59321	1,574324	gnl|Amel_4.5|GB54814-PA	0,616535	1,717953
gnl|Amel_4.5|GB55388-PA	-0,6573	1,506636	gnl|Amel_4.5|GB48216-PA	0,585469	1,716991
gnl|Amel_4.5|GB45128-PA	-2,00984	1,443101	gnl|Amel_4.5|GB53032-PA	0,568397	1,690647
gnl|Amel_4.5|GB48661-PA	-1,60319	1,439112	gnl|Amel_4.5|GB53360-PA	0,472611	1,689361
gnl|Amel_4.5|GB41715-PA	-1,3224	1,431383	gnl|Amel_4.5|GB54653-PA	0,949812	1,687582
gnl|Amel_4.5|GB47500-PA	-1,01458	1,388819	gnl|Amel_4.5|GB44967-PA	0,567495	1,665449
gnl|Amel_4.5|GB41143-PA	-0,46961	1,356291	gnl|Amel_4.5|GB48784-PA	0,758868	1,653026
gnl|Amel_4.5|GB41979-PA	-0,46045	1,353462	gnl|Amel_4.5|GB41303-PA	0,449972	1,650139
gnl|Amel_4.5|GB43088-PA	-0,80271	1,353129	gnl|Amel_4.5|GB44886-PA	2,570008	1,635557
gnl|Amel_4.5|GB48634-PA	-0,33025	1,327505	gnl|Amel_4.5|GB55452-PA	0,81949	1,592447
			gnl|Amel_4.5|GB53860-PA	3,333308	1,590271

gnl|Amel_4.5|GB55091-PA	0,493895	1,575739
gnl|Amel_4.5|GB50727-PA	0,719321	1,561734
gnl|Amel_4.5|GB51564-PA	0,65346	1,558949
gnl|Amel_4.5|GB48841-PA	0,666871	1,539053
gnl|Amel_4.5|GB43353-PA	0,552776	1,521658
gnl|Amel_4.5|GB40865-PA	1,120104	1,510506
gnl|Amel_4.5|GB50831-PA	0,527227	1,510113
gnl|Amel_4.5|GB42698-PA	0,317628	1,502755
gnl|Amel_4.5|GB50663-PA	0,319052	1,501978
gnl|Amel_4.5|GB52315-PA	0,302639	1,492831
gnl|Amel_4.5|GB50885-PA	0,599496	1,49142
gnl|Amel_4.5|GB50032-PA	0,312823	1,486967
gnl|Amel_4.5|GB51089-PA	0,273759	1,484242
gnl|Amel_4.5|GB43464-PA	2,620593	1,458943
gnl|Amel_4.5|GB40618-PA	0,63209	1,456694
gnl|Amel_4.5|GB49220-PA	2,360364	1,450383
gnl|Amel_4.5|GB52999-PA	0,653503	1,439966
gnl|Amel_4.5|GB54194-PA	0,679364	1,427345
gnl|Amel_4.5|GB47946-PA	1,779043	1,421429
gnl|Amel_4.5|GB53024-PA	2,312916	1,416529
gnl|Amel_4.5|GB42809-PA	0,6215	1,384724
gnl|Amel_4.5|GB50780-PA	0,616142	1,378321
gnl|Amel_4.5|GB48492-PA	0,759925	1,369032
gnl|Amel_4.5|GB48248-PA	1,455045	1,365544
gnl|Amel_4.5|GB42608-PA	0,56265	1,347011
gnl|Amel_4.5|GB44882-PA	0,409593	1,333593
gnl|Amel_4.5|GB55139-PA	0,12767	1,331156
gnl|Amel_4.5|GB42537-PA	0,529149	1,329444
gnl|Amel_4.5|GB40539-PA	0,458304	1,324635
gnl|Amel_4.5|GB48544-PA	2,295424	1,315793
gnl|Amel_4.5|GB50924-PA	0,532926	1,312292
gnl|Amel_4.5|GB42597-PA	0,678678	1,310007
gnl|Amel_4.5|GB51086-PA	0,54199	1,30753
gnl|Amel_4.5|GB45105-PA	2,631914	1,306463

Title

3. Antiviral activity of synthetic xanthenones against honey bee ABPV identified by molecular docking and virtual screening

Authors and Affiliations:

Luana Lucas Dutra[1], Ananda Pereira Aguilar[1], Kyung-Mee Moon[2], Flavia de Oliveira Souza[3], Poliane Alfenas-Zerbini[3], Ângelo de Fátima[4], Sergio Antonio Fernandes[5], Leonard Foster[2], Weyder Cristiano Santana[6], Tiago Antônio de Oliveira Mendes[1*]

1 Department of Biochemistry and Molecular Biology, Universidade Federal de Viçosa, Viçøsa, Minas Gerais, Brazil.

2 Department of Biochemistry and Molecular Biology, University of British Columbia, Vancouver, British Columbia, Canada.

3 Department of Microbiology, Universidade Federal de Viçosa, Viçøsa, Minas Gerais, Brazil.

4 Department of Chemitry, Universidade Federal de Minas Gerais, Belo Horizonte, Minas Gerais, Brazil.

5 Department of Chemistry, Universidade Federal de Viçosa, Viçøsa, Minas Gerais, Brazil.

6 Department of Enthomology, Universidade Federal de Viçosa, Viçøsa, Minas Gerais, Brazil.

***Correspondent author: tiagoaomendes@ufv.br**

Abstract

Acute bee paralysis virus (ABPV) is one of the major threats to honey bees. Although widely distributed asymptomatically in colonies, this pathogen can become highly lethal. The characteristic symptoms of this infection include trembling, paralysis, and death in a few days. In this work, we evaluated the protein profile of honey bees workers artificially infected by ABPV and observed the detriment of neurotransmitter transport, which may explain the development of the pathology in response to environmental stresses. In order to find compounds to control infection, we selected four synthetic xanthenones that had a high binding affinity with the viral 3C-protease and evaluated the expression of ABPV after treatment with these molecules. Compound

2 promoted a significant reduction of viral expression and increased energetic metabolism of the host.

Introduction

Pollinator insects play a crucial role in the world economy and in agricultural production. Bees contribute to approximately 80% of insect-mediated pollination, and their decline has drawn the attention of researchers worldwide (GALLAI et al., 2009; POTTS et al., 2010; SHEPHERD et al., 2018).

The abusive use of pesticides, climate changes, lack of flowers variety are some examples of environmental conditions that present risk to managed and wild bees (GOULSON et al., 2015). Also, a recent study also evaluates the damage caused by extremely low-frequency electromagnetic fields over the behavior and cognitive abilities of honey bees (SHEPHERD et al., 2018). Besides that, there are many diseases that threaten the health of honey bees at the individual and colony levels, like the microsporidia *Nosema ceranae*, the mite *Varroa destructor*, and several viral diseases (GOULSON et al., 2015). Most of the virus identified in *Apis mellifera* present a positive sense single-stranded RNA genome (+ssRNA) and are classified as Dicistroviruses (*Acute bee paralysis virus*- ABPV, *Israeli acute paralysis virus*- IAPV, *Kashmir bee virus*- KBV, *Black queen cell virus*- BQCV), Iflaviruses (*Deformed wing virus*- DWV, *Slow bee paralysis virus*- SBPV, *Sacbrood virus*- SBV, *Varroa destructo virus 1*- VDV-1) or the taxonomically non-classified CBPV (*Chronic bee paralysis virus*) and LSVs (*Lake Sinai viruses*) (BRUTSCHER, DAUGHENBAUGH, and FLENNIKEN, 2015; TEHEL, BROWN, and PAXTON, 2016).

The ABPV was first identified in England by Bailey et al (1963) and was detected in different countries since then, such as United States (EVANS and WHEELER, 2001), France (TENTCHEVA et al., 2004), Austria (BERÉNYI et al., 2006), Brazil (TEIXEIRA et al., 2008), Hungary (FORGÁCH et al., 2008), UK (BAKER and SCHROEDER, 2008), Argentina (REYNALDI et al., 2010) and Thailand (CHANPANITKITCHOTE et al., 2018).

This pathogen usually causes an asymptomatic infection in the colonies, but at high concentrations can produce the classical signs of darkening by losses of hair, trembling, paralysis and death (BAILEY, GIBBS, and WOODS, 1963; BAILEY and GIBBS, 1964). The acute infection is related to the infestation of the *Varroa Destructor* mite, an important vector of this and other bee parasites capable to transmitting the virus through the bite directly into the hemolymph

(BAILEY and GIBBS, 1964; de MIRANDA, CORDONI, BUDGE, 2010). The infestation of this mite causes damage at individual level, by immunosuppression and transmission of diseases, and at collective level, reducing the population of affected colonies (DeGRANDI-HOFFMAN and CHEN, 2015).

Since its discovery, ABPV has been related to large losses in colonies of *A. mellifera* infested with the *Varroa* mite. However, this virus was also found in bees of the genus *Bombus* (BAILEY and GIBBS, 1963) and was recently identified in *Apis cerana* and *Tropilaelaps mercedesae* mite in Asia (CHANPANITKITCHOTE et al., 2018) and in weak colonies of stingless Brazilian bees *Melipona scutellaris* (UEIRA-VIEIRA, et al., 2015).

The study presented by Azzami et al. (2012) evaluated the response to ABPV artificial infection in adult bees and larvae through injection of purified virus. They observed that the ABPV does not induce a humoral or cellular response, like the production of AMPs or melanization, respectively. In addition, the hemolymph was highlighted as a tissue of higher viral proliferation in larvae and adults.

The ABPV genome has a 9470 nucleotide polyadenylated RNA segment (GenBank AF150629) containing two ORFs (open reading frame) that encodes the replicative enzymes (ORF1-non-structural polyprotein), and the four structural capsid proteins (ORF2-structural polyprotein), separated by an intergenic region (IGR) (GOVAN et al., 2000; BONNING, 2009; de MIRANDA, CORDONI, BUDGE, 2010). The polyproteins are cleaved by the viral protease 3C-Pro through mechanisms that are not totally understood. Proteases are present in the most diverse organisms and participate in different physiological processes such as inflammation and degenerative diseases, and also perform a crucial role in pathogens virulence (ZHAI et al., 2015; VIEIRA, SANTOS, and FERREIRA, 2018), which makes these enzymes attractive targets for the development of new drugs.

The application of *in silico* studies in the field of medicinal chemistry has been grown, due to the advancement of biomolecule characterization techniques and also the improvement of computational methods of analyzing these data. Molecular docking is a method widely applied for screening of potential drugs based on the target structure (FERREIRA et al., 2015; VIEIRA, SANTOS, and FERREIRA et al., 2018).

Thus, we used the method of virtual screening of molecules based on the viral cysteine protease structure to search for potential inhibitors. After the selection of the four molecules with

the best binding energy value, we evaluated the antiviral activity of these potential inhibitors in *in vivo* worker bee artificial infection model. The physiologic effects of treatment with an activity compound was also evaluated by label-free proteomics.

Material and methods

Molecular docking study:

The viral cysteine protease (ABPV_PEP) (RefSeq NP_066241.1) was a target for the search of potential inhibitors. We created the structure of ABPV_PEP using the I-tasser online server (ZHANG, 2008) and checked the quality of the model by the online server Verify 3D (BOWIE, LÜTHY and EISENBERG, 1991; LUETHY, BOWIE and EISENBERG, 1992), Procheck (LASKOWSKI et al., 1993; LASKOWSKI et al., 1996) and Errat (COLOVOS and YEATES, 1993).

Automated protein docking of the ABPV_PEP model with the synthetic ligands was performed using AutoDock Vina (TROTT and OLSON, 2010). The synthesis of the ligands molecules was previously reported (da SILVA et al., 2011; da SILVA et al., 2015; REGO et al., 2016; LIBERTO et al., 2017; ABRANCHES et al., 2018). The grid box was centered at 57.7, 57.7 and 58.8 Å in the X, Y and Z coordinate axes, respectively, with size of 50.5 x 49.1 x 45.3 Å. The visualization of ligands and target was performed with the software PyMol (The PyMOL Molecular Graphics System, Version 2.0 Schrödinger, LLC.). The 2D Ligand Interaction Diagram was created with the software Discovery Studio (Dassault Systèmes BIOVIA, Discovery Studio, version 19.1.0.18287, San Diego: Dassault Systèmes, 2019).

Identification of the ABPV:

The identification of ABPV in symptomatic worker bees from an apiary in the city of Passa Quatro-MG (Brazil) was previously described (DUTRA et al., manuscript in preparation). For cDNA synthesis, were extracted the RNA from six honey bees with TRIzol® (Invitrogen) and used the MultiScribe Reverse Transcriptase (Applied Biosystems) enzyme with the oligo dT primer, according to the manufacturer's instructions. The presence of ABPV was confirmed by the amplification of a specific fragment described by TEIXEIRA et al (2008). The fragment (500 bp) was purified and cloned in pGEM-T Easy vector (Promega). The plasmid was purified (Wizard®

Plus SV Minipreps DNA Purification System, Promega), sequenced (Myleus Facility) and the fragment sequence used as a template for the construction of the ABPV-specific RT-qPCR primers (Table 1).

Table 1- Sequence of the primers applied in the PCR

Name	Sequence (5'- 3')	Gene (efficiency %)	Reference
β-actin F	TGCCAACACTGTCCTTTCTG	β-actin (76.3%)	Lourenço et al., 2008
β-actin R	AGAATTGACCCACCAATCCA		
ABPV-F	ACTGCGCTTACGGATTTGAC	171pb Amplicon specific for ABPV (100%)	This work.
ABPV-R	TCTTGGTGTCAAAAAGCTTCG		
ABPV-F	TCTGATGCTGAAGAGAGAAA	500 bp amplicon (identification of ABPV)	Teixeira et al., 2008
ABPV-R	AATCATCATTGCCGGCTCTA		

Extraction of ABPV from Passa Quatro-MG (Brazil):

The extraction of ABPV was performed as described by Bailey, Gibss and Wood (1963). We grounded 10 symptomatic bees from the apiary in Passa Quatro-MG in a mixture of carbon tetrachloride and water (1:4, v/v), followed by a filtration and centrifugation steps was filtered and centrifuged at (3000 rpm for 10 minutes). The organic fraction was discarded.

According to the first description of ABPV (BAILEY and GIBSS, 1964), feeding and injection are both efficient ways to artificially infect worker bees, though ABPV has a higher virulence upon injection. Thus, we firstly infected a group of 36 newly emerged worker bees through the injection of 1 μL of the aqueous fraction, previously described, between the second and the third tergite into the hemocoel of each bee, using a capillary glass coupled to a microinjector (AZZAMI, et al., 2012). The worker bees were collected in the apiary of the Federal University of Viçosa (Brazil) and kept in a plastic container at 32 ±2ºC for 4 days supplied with 50% (w/v) sucrose solution. The food was replaced daily.

Every 24 hours the bees were inspected and those with paralysis and tremors were removed and stored at -20°C. At the end of the fourth day all bees were stored at -20ºC and the virus extraction step was repeated. The aqueous phase (ABPV suspension) was used for artificial infection by feeding.

Artificial infection of honey bees by feeding:

The worker bees were collected from the same colony, all with a similar age (until 12 hours after emerge). They were divided between two Control groups and 4 Treatment groups (Figure 1). Each group was placed in a plastic cage coupled to a 2 mL tube with the respective diet (Table 2). The cages were maintained at 32 ±2ºC for 48 hours. After that, all groups were split in triplicates, and total RNA and protein were extracted with the commercial reagent TRIzol (Invitrogen), according to the manufacturer's instructions (Figure 1).

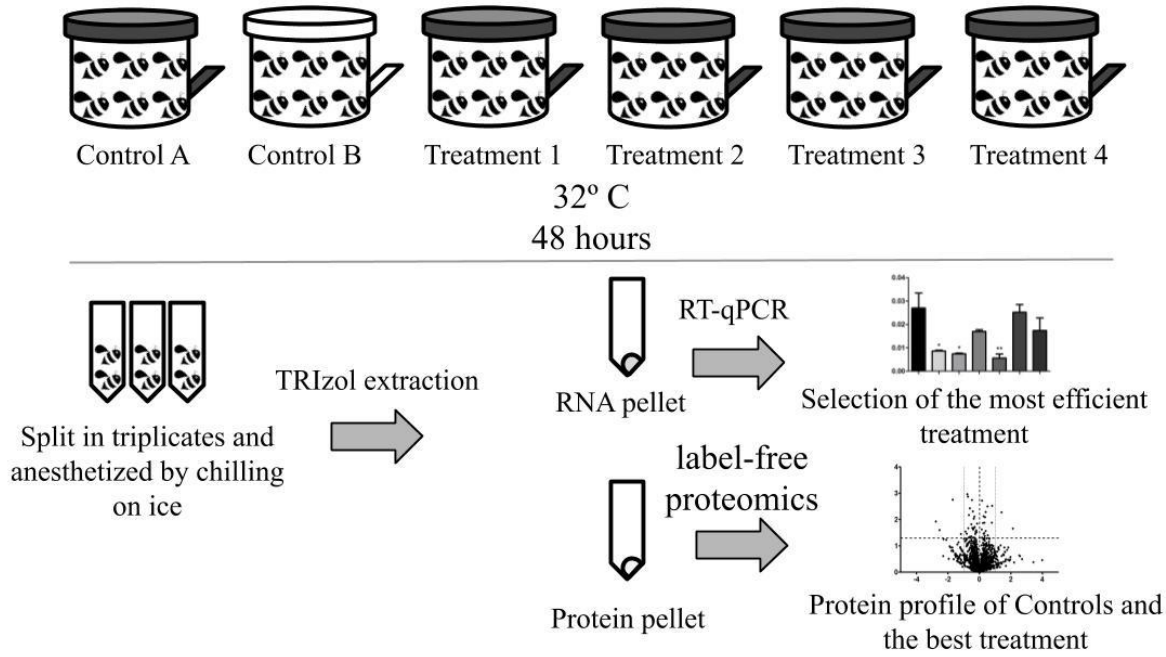

Figure 1- Flowchart executed to evaluate the antiviral activity and physiologic effects of the infection and the treatment with the synthetic compounds selected by molecular docking. The worker bees were divided in: Control A (infected, grey cage lid), Control B (non-infected, white cage lid) and Treatments 1-4 (infected, grey cage lids).

Table 2- Content of the food provided in each group

Group	Diet	DMSO content	Antiviral content	ABPV suspension
Control A (infected)	sucrose 50% w/v	0,40% v/v	-	0,25 ml
Control B (non-infected)	sucrose 50% w/v	0,40% v/v	-	-
Treatments 1-4	sucrose 50% w/v	0,40% v/v	0,30% w/v	0,25 ml

Evaluation of the antiviral activity of the treatments:

The qPCR reaction was done in a 96-well plate using the 7500 Real-Time PCR System (Applied Biosystems, Thermo Fisher Scientific, USA) by the standard curve method applying the GoTaq® qPCR kit Master Mix (Promega, Madison, USA). In these reactions, 1 µL of cDNA with a concentration of 20 ng/µL and 0.5 µL of each primer (2 µM) (Table 1) was applied, a total of 10 µL in each reaction. The thermocycler program was started at 95° C for 10 minutes followed by 40 cycles of 95° C for 15 seconds and 60° C for 1 minute. The quantification was done by a standard curve (log_{10}DNA concentration (ng) vs. *threshold cycle* (Ct) value) obtained for the genes described in Table 1. The R^2 was calculated for each primer, and the reaction efficiency was calculated using the formula: $E = (10^{-1/SLOPE})-1$. The results of ABPV concentration in each group (Table 2) were normalized by the endogenous gene β-actin (Relative expression) (de SOUZA et al., 2019). The Treatment groups were compared to the Control A group by ANOVA test with Dunnett correction of multiple hypothesis (p-value < 0.05) and the graphs were prepared using the GraphPad Prism 5.0 software (GraphPad Inc.)

Effect of treatments on the worker bee protein expression profile:

In order to evaluate the difference of protein expression on each group, we performed a label-free proteomic study. We performed the extraction of RNA with commercial TRIzol® reagent (Invitrogen) according to the manufacturer's instructions. Protein pellets were solubilized in 200 µL solubilization buffer (6M urea/2M thiourea in 0.1M Tris, pH 7.8), vortexed for 10 seconds, sonicated in an ice bath for 5 minutes and vortexed again. After a quick spin (14000 x g for 15 seconds) the tubes were incubated at room temperature for 30 minutes and then centrifuged at 16000 x g for 10 minutes. We discarded the pellets and determined the protein content in each sample by Bradford assay (Bio-Rad). Next, 15 µg of proteins were digested with Lys-C and trypsin, and desalted by STAGE tips, as previously described by Foster et al. (2003). We dried (SpeedVac, Eppendorf, 45 min) and resuspended each sample in 15 µL of 0.1% formic acid. The peptide concentrations were determined by NanoDrop® (Thermo, 280 nm) and the sample analyzed by liquid chromatography-tandem mass spectrometry (LC-MS/MS).

LC-MS/MS data acquisition:

The peptide samples were injected on liquid chromatography coupled to a mass spectrometer as described previously by McAfee and collaborators (2017). For the search performed with MaxQuant (v1.6.3.3) we used the *A. mellifera* genome version 4.5 (Amel 4.5) blasted against the non-redundant protein database for Arthropoda (NCBI) in 2015 plus the manually annotated ABPV proteome from UniProt database, totalizing 15314 entries. The MaxQuant parameters were set by default (TYANOVA, TEMU, and COX, 2018) and the statistical analysis were performed with normalized LFQ intensity values (COX, et al., 2014).

Experiments were carried out in three biological replicates (pools containing 2 worker bees, each) and the differently abundant proteins (t-test, p-value < 0.05) were menstruated by the fold change between the mean of Control A *vs*. Control B or Treated *vs*. Control B. The result was shown as logarithm in base two ($\log_2$ Fold change) versus the negative logarithm of p-value (-log p-value) in a volcano-plot graph created with the software GraphPad Prism 5 (GraphPad Software, Inc, La Jolla, CA, USA).

Bioinformatics analysis:

The Gene Ontology (GO) annotations of the biological process of proteins were acquired with the tool AgBase-GOanna (https://agbase.arizona.edu/, McCARTHY, et al. 2006). The Protein-Protein Interaction (PPI) network was generated for the up and down regulated proteins identified in each experimental group using the STRING database version 11.0 (https://string-db.org/, SZKLARCZYK, et al. 2019). The proteins that have more interactions among themselves than what would be expected for a random set of proteins of similar size presented PPI enrichment p-value < 0.05. The proteins network was represented as a Cytoscape graph (v 3.7.1, SHANNON, et al., 2003) and the statistically overrepresented GOs were determined with the tool Bingo (MAERE, HEYMANS and KUIPER, 2005) by a Hypergeometric Test with the Benjamini & Hochberg's FDR correction (p-values < 0.05).

Results and discussion

Proteomic profile of infected and non-infected honey bees

We evaluated the proteomic profile of honey bee infected (Control A) vs. non-infected (Control B). Between the identified proteins in both conditions (Figure 2-B), 1.6% were differently abundant due to the infection.

The most up-regulated proteins in the infected group was the osteonectin-like calcium-binding protein (GB43302), highly expressed in extracellular matrix in young bees and related to morphogenesis and development (KUCHARSKI and MALESZKA, 2002); the immunoglobulin-like protein (GB42053) that present a MD-related lipid-recognition domain; and the apolipophorin with an protein-protein interaction domain AMR (GB41418). The insect's apolipophorines are homologous to the mammalian ApoE and are relevant to immune process like encapsulation and melanisation (WHITTEN et al., 2004). They presented a weak correlation (Figure 2-D) and no significant pathway enrichment was observed in the biological process (GO) search.

Among the down-regulated proteins, the most differentially expressed were the UDP-glucuronosyl/UDP-glucosyltransferase (GB47303), an ATPase (GB42482), and the member of the t-SNARE protein family synaptosomal nerve-associated protein 25 (SNAP-25) (GB44583), both relevant to vesicular transport. We search for biological process enriched in the infected group based on GO annotation (Figure 2-E) and observed that the transport of neurotransmitter is impaired in reason of the infection.

The intensity of the ABPV infection seems to be related to the viral load and the presence of an environmental trigger like agrochemical exposure, presence of other pathogens or infestation by *Varroa* mite (McMENAMIN et al., 2016; THADURI et al., 2019), and the development of the trembling and paralysis symptoms is not defined by the tissue tropism or the brain regions infected (WANG, MEEUS and SMAGGHE, 2016). We used a non-invasive infection method (feeding) that is known to create an asymptomatic infection (BAILEY and GIBBS, 1963), and our findings suggest that the neurotoxicity observed in high viral concentration could be resulted of an impairment of the host's vesicular transport. Further analysis of protein profile of symptomatic and non-symptomatic worker bees are need.

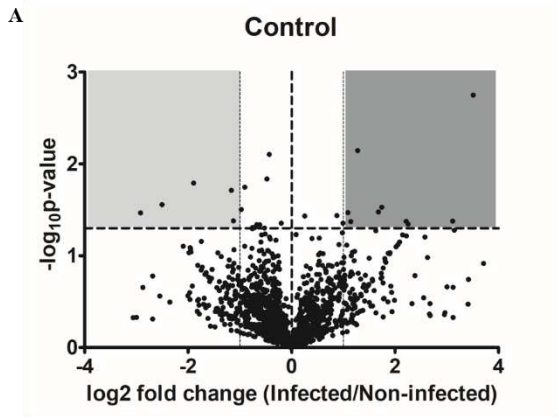

E

GO-ID	q-value	Description
6836	0,007	Neurotransmitter transport
48193	0,007	Golgi vesicle transport

Figure 2- Influence of ABPV infection upon the expression of proteins in the host. A) Volcano-plot graph correlating the negative logarithm of the p-value with the logarithm of base two of the ratio between the expression of proteins in the group Control A (infected) versus Control B (non-infected). The data above the horizontal dotted axis have significant different expression between the groups (t-test, p-value < 0.05). The highlighted quadrants contain proteins up-regulated 2-fold or more (dark gray) and down-regulated 2-fold or more (light gray). B) Venn diagram. Number of proteins identified in the Controls A and B. Protein-Protein Interaction network (PPI) of the down-regulated proteins on Control group (C, PPI p-value 0.611); and up-regulated proteins Control group (D, PPI p-value 0.0378). D) Overrepresented proteins between the down-regulated set (q-value: FDR corrected p-value < 0.05) and their GO-ID (Gene Ontology Identification) and biological process. There were no overrepresented proteins between the up-regulated set.

Molecular docking

The three-dimensional structure of the viral 3C-protease predicted *in silico* presented 96.6% of the residues in allowed regions of the Ramachandran plot and was within the quality parameters evaluated by the Verify 3D, Errat, and Procheck programs. Between the 175 synthetic molecules used as ligands, the five best predicted binding affinity were selected, showing high affinity with the active site region of the model (Figure 3). The selected compounds belong to the class of xanthenones, linear tricyclic structures which generally contain an O-heteroatom and a carbonyl group (KHANNA et al., 2016). These molecules have activity against a broad spectrum of diseases, and inhibitory activity on many enzymatic targets such as protein kinase, reverse transcriptase and glycosidase (MOLINER et al., 2003; VICINI et al., 2009; TARIQ et al., 2019).

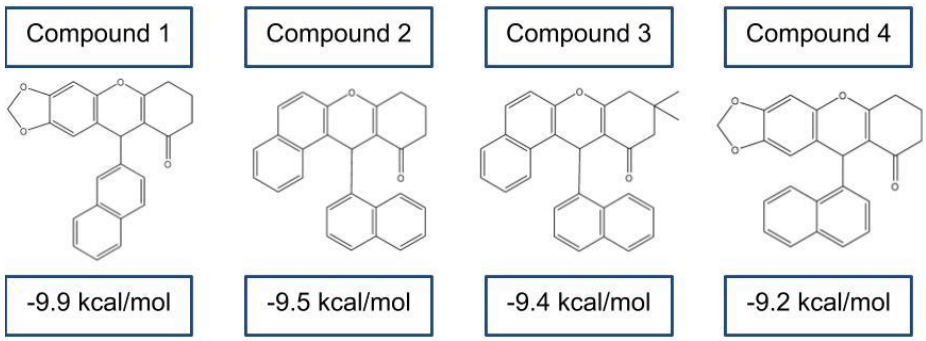

Figure 3- Structure of the four synthetic xanthenones selected by molecular docking and their respective predicted binding affinity to the active site of the viral protease. Their synthesis was described by da Silva et al. (2015).

All the molecules shown a similar conformation after the docking with the ABPV 3C-protease. The Compound 2 (Figure 3) presented a binding affinity of -9.5 kcal/mol inside the active site of the 3C-protease model. There were no predicted polar interactions between the oxygen atoms in the ligand and the residues around it. However, the predicted conformation seems to block the catalytic triad predicted by Govan et al. (2000) (Figure 4).

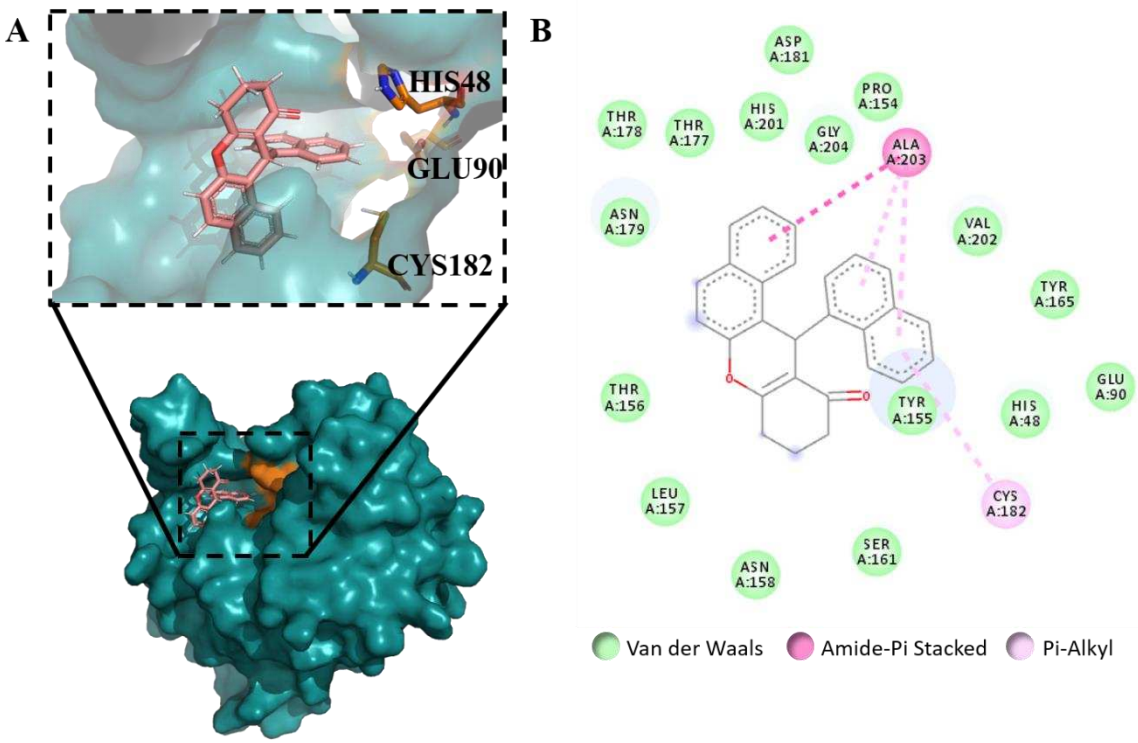

Figure 4- A) Three-dimensional model of ABPV 3C-protease (cyan). Representation of the active site and the three catalytic residues predicted by Govan et al. (2000) (orange) and predicted conformation of Compound 2 (pink). B) 2D Ligand Interaction Diagram of the best predicted conformation of Compound 2

with the macromolecule. The type of interaction between the residues (in circles) and the xanthenone are described below the diagram.

Molecules with conjugated systems exhibit antiviral action through different mechanisms (ONG et al., 2011; ZHOU et al., 2012; CERÓN et al., 2019), and viral proteases are a current target in the search for treatments against many viruses such as HIV (LV, CHU, and WANG, 2015) and DENV (TIMIRI, SINHA, and JAYAPRAKASH, 2016). Thus, the interaction of Compound 2 with the ABPV 3C-protease may be one of the mechanisms responsible for the decrease in viral load observed in this work. Hence, it would be possible to confirm the inhibitory action of this compound by the *in vitro* expression of the viral protease and enzyme inhibition assay, that also enabling the estimation of a minimum inhibitory concentration.

Antiviral activity- RT-qPCR

After the quantification of ABPV and the endogenous gene β-actin on each treatment by RT-qPCR, the concentration of each gene was calculated using a standard curve. Figure 5 shows the relative expression of ABPV in each treatment and Control A. Compound 2 reduced the ABPV expression by 79.4%, and this group was selected for the subsequent step of determining the proteomic profile.

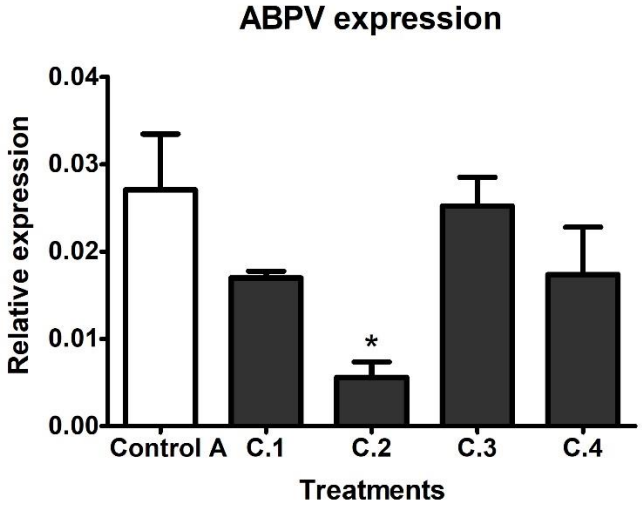

Figure 5- Quantification of ABPV relative expression on each treatment groups. The bar marked with an asterisk was the treatment that had the relative expression of ABPV significantly lower than the Control A group (t-test, p-value < 0.05).

Protein profile of worker bees treated and control

We also evaluated the proteomic profile of the worker bees treated with Compound 2 and the non-infected group Control B, in order to observe the impact of the treatment upon health honey bees. Figure 6-B shows the number of proteins identified at each treatment, and between the proteins identified simultaneously 2.6% were differentially expressed (-log p-value > 1.3). The differently abundant proteins shown no significant correlation (Figure 6-C and D).

The most down-regulated are a nucleotide-binding protein (GB43827), Thiolase-like (GB44420), Alkaline-phosphatase-like (GB44493) and the SNAP 25 (GB44583), the last one also down-regulated in the infected group Control A. However, there were no overrepresented biological processes related to the down-regulated proteins, suggesting that the impairment of vesicular transport is not detectable anymore after the treatment. Between the up-regulated proteins, we observed the overrepresentation of metabolic process and energy production. The Major royal jelly protein 2 precursor (MRJP) (GB55212) was the most up-regulated protein in response to the treatment with Compound 2.

The MRJP family is set by storage proteins mainly related to nutritional function, although these proteins are also related to the immune response in mammals, antibacterial activity against American foulbrood and the caste determination in honey bees (BUTTSTEDT, MORITZ, and ERLER, 2014). Pathogens like IAPV, *Varroa destructor*, and the microsporidia *Nosema ceranae* also promote the impairment of energy metabolism (CHEN et al., 2014; VIDAU et al., 2014; DeGRANDI-HOFFMAN and CHEN, 2015). The improvement of energy production after the treatment could be helpful to control other diseases since the infection by multiple pathogens is common in eusocial insects like honey bees.

A

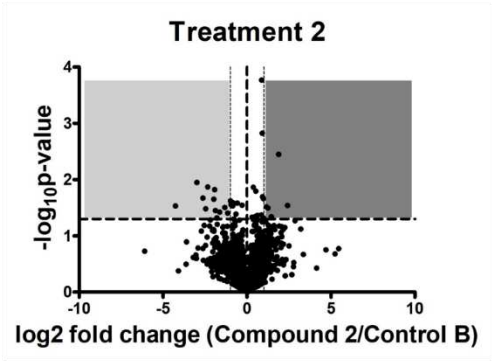

C

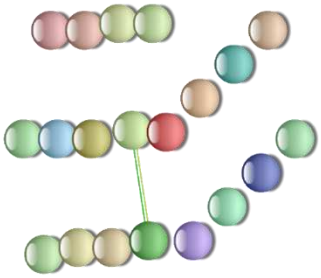

Down

D

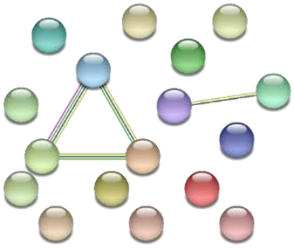

Up

B

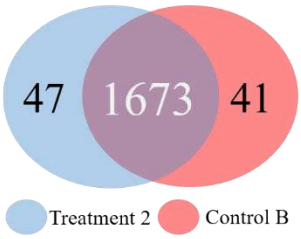

E

GO-ID	q-value	Description
6091	0.03	Generation of precursor metabolites and energy
6082	0.03	Organic acid metabolic process

Figure 6- Influence of the treatment with Compound 2 upon the expression of proteins in the host. A) Volcano-plot graph correlating the negative logarithm of the p-value with the logarithm of base two of the ratio between the expression of proteins in the group Treatment 2 (ABPV+compound 2) versus Control B (non-infected). The data above the horizontal dotted axis have significative different expression between the groups (t-test, p-value <0.05). The highlighted quadrants contain proteins up-regulated 2-fold or more (dark gray) and down-regulated 2-fold or more (light gray). B) Venn diagram. Number of proteins identified in the groups Treatment 2 and Control B. Protein-Protein Interaction network (PPI) of the down-regulated proteins on Treatment 2 group (C, PPI p-value 0.713); and up-regulated proteins on Treatment 2 group (D, PPI p-value 0.0754). E) Overrepresented proteins between the up-regulated set (q-value: FDR corrected p-value < 0,05) and their GO-ID (Gene Ontology Identificator) and biological process. There were no overrepresented proteins between the down-regulated set.

Conclusion

ABPV infection is a significant threat to wild and managed honey bees. Infection usually does not cause symptoms, but when the viral load reaches high levels, this virus can cause severe neurological damage and massive death in the colony. Several factors can promote the proliferation of this virus in the host by mechanisms not yet clarified. In this work, we have identified that the process of vesicular transport of neurotransmitters is decreased in response to infection, a suggestion of the development of the pathology at the molecular level. In order to propose a method of infection control, we performed a virtual screening for inhibitors of viral 3C-protease. We selected four xanthenones from which Compound 2 promoted a significant reduction of the ABPV concentration. The treatment promoted the energy metabolism and the expression of the MRJP

family, a condition usually impaired due to different infections. Thus, Compound 2 showed inhibition of the ABPV expression and improvement of energy metabolism of the host, and it is likely to promote more powerful tolerance against other pathogens as well.

References

ABRANCHES, P. A. S; de PAIVA, W. F; de FÁTIMA, A; MARTINS, F. T; FERNANDES, S. A. Calix[n]arene-catalyzed three-component Povarov reaction: microwave-assisted synthesis of julolidines and mechanistic insights. **The Journal of Organic Chemistry**, v. 83, p. 1761-1771, 2018.

AZZAMI, K; RITTER, W; TAUTZ, J; BEIER, H. Infection of honey bees with *Acute bee paralysis virus* does not trigger humoral or cellular immune responses. **Archives of virology**, v. 157, n. 4, p. 689-702, 2012.

BAILEY, L; GIBBS, A. J. Acute infection of bees with paralysis virus. **Journal of insect pathology**, v. 6, n. 4, 1964.

BAILEY, L; GIBBS, A. J; WOODS, R. D. Two viruses from adult honey bees (*Apis mellifera* Linnaeus). **Virology**, v. 21, p. 390-395, 1963.

BAKER, A; SCHROEDER, D. Occurrence and genetic analysis of picorna-like viruses infecting worker bees of *Apis mellifera* L. populations in Devon, South West England. **Journal of Invertebrate Pathology,** v. 98, p. 239-242, 2008.

BERÉNYI, O; BAKONYI, T; DERAKHSHIFAR, I; KÖGLBERGER, H; NOWOTNY, N. Occurrence of six honeybee viruses in diseased Austrian apiaries. **Invertebrate Microbiology**, v. 72, p. 2414-2420, 2006.

BONNING, B. C. The *Dicistroviridae*: an emerging family of invertebrate viruses. **Virologica Sinica**, v. 24, n. 5, p. 415-427, 2009.

BOWIE, J. L; LÜTHY, R; EISENBERG, D. A method to identify protein sequences that fold into a known three-dimensional structure. **Science**, v. 253, n. 5016, p. 164-170, 1991.

BRUTSCHER, L. M; DAUGHENBAUGH, K. F; FLENNIKEN, M. L. Antiviral defense mechanisms in honey bees. **Current Opinion in Insect Science**, v. 10, p. 71-82, 2015.

BUTTSTEDT, A; MORITZ, R. F. A; ERLER, S. Origin and function of the major royal jelly proteins of the honeybee (*Apis mellifera*) as members of the yellow gene family. **Biological Reviews**, v. 89, p. 255-269, 2014.

CERÓN, S; NORTH, B. J; TAYLOR, S. A; LEIB, D. A. The STING agonist 5,6-dimethylxanthenone-4-acetic acid (DMXAA) stimulates an antiviral state and protects mice against herpes simplex virus induced neurological disease. **Virology**, v. 529, p. 23-28, 2019.

CHANPANITKITCHOTE, P; CHEN, Y; EVANS, J. D; LI, W; LI J; HAMILTON, M; CHANTAWANNAKUL, P. *Acute bee paralysis virus* occurs in the Asian honey bee *Apis cerana* and parasitic mite *Tropilaelaps mercedesae*. **Journal of Invertebrate Pathology**, v. 151, p. 131-136, 2018.

CHEN, Y; PETTIS, J. S; CORONA, M; CHEN, W. P; LI, C. J; SPIVAK, M; VISSCHER, P. K; DEGRANDI-HOFFMAN, G; BONCRISTIANI, H; ZHAO, Y; VANENGELSDORP, D; DELAPLANE, K; SOLTER, L; DRUMMOND, F; KRAMER, M; LIPKIN, W. I; PALACIOS, G; HAMILTON, M. C; SMITH, B; HUANG, S. K; ZHENG, H. Q; LI, J. L; ZHANG, X; ZHOU, A. F; WU, L. Y; ZHOU, J. Z; LEE, M. L; TEIXEIRA, E. W; LI, Z. G; EVANS, J. D. *Israeli acute paralysis virus*: epidemiology, pathogenesis and implications for honey bee health. **PLoS Pathogens**, v. 10, n. 7, 2014.

COLOVOS, C; YEATES, T. O. Verification of protein structures: patterns of nonbonded atomic interactions. **Protein Science**, v. 2, n. 9, p. 1511-1519, 1993.

COX, J; HEIN, M. Y; LUBER, C. A; PARON, I; NAGARAJ, N; MANN, M. Accurate proteome-wide label-free quantification by delayed normalization and maximal peptide ratio extraction, termed MaxLFQ. **Molecular and Cellular Proteomics**, v. 13, p. 2513-2526, 2014.

da SILVA, D. L; FERNANDES, S. S; SABINO, A. A; de FÁTIMA, A. p-Sulfonic acid calixarenes as efficient and reusable organocatalysts for the synthesis of 3,4-dihydropyrimidin-2(1H)-ones/-thiones. **Tetrahedron Letters**, v. 52, p. 6328-6330, 2011.

da SILVA, D. L; TERRA, B. S; LAGE, M. R; RUIZ, A. L. T. G; da SILVA C. C; de CARVALHO, J. E; CARNEIRO, J. W. M; MARTINS, F. T; FERNANDES, S. A; de FÁTIMA, A. Xanthenones: calixarenes-catalyzed syntheses, anticancer activity and QSAR studies. **Organic and Biomolecular Chemistry**, v. 13, n. 11, p. 3280–3287, 2015.

de SOUZA, G. B; MENDES, T. A. O; FONTES, P. P; BARROS, V. A; GONÇALVES, A. B; FERREIRA, T. F; COSTA, M. D. B. L; ALVES, M. S; FIETTO, L. G. Genome-wide identification and expression analysis of dormancyassociated gene 1/auxin repressed protein (DRM1/ARP) gene family in Glycine max. **Progress in Biophysics and Molecular Biology**, v. 146, p. 134-141, 2019.

de MIRANDA, J. R; CORDONI, G; BUDGE, G. The *Acute bee paralysis virus-Kashmir bee virus-Israeli acute paralysis virus* complex. **Journal of Invertebrate Pathology**, v. 103, p. S30-S47, 2010.

DeGRANDI-HOFFMAN, G; CHEN, Y. Nutrition, immunity and viral infections in honey bees. **Current Opinion in Insect Science**, v. 10, p. 170-175, 2015.

EVANS, J. D. and WHEELER, D. E. Gene expression and the evolution of insect polyphenisms. **BioEssays**, v. 21, 2001.

EVANS, J. D; ARONSTEIN, K; CHEN, Y. P; HETRU, C; IMLER, J. L; JIANG, H; KANOST, M; THOMPSON, G. J; ZOU, Z; HULTMARK, D. Immune pathways and defence mechanisms in honey bees *Apis mellifera*. **Insect Molecular Biology**, v. 15, p. 645-656, 2006.

FERREIRA, L. G; dos SANTOS, R. N; OLIVIA, G; ANDRICOPULO, A. D. Molecular docking and structure-based drug design strategies. **Molecules**, v. 20, p. 13384-13421, 2015.

FORGÁCH, P; BAKONYI, T; TAPASZTI, Z; NOWOTNY, N; RUSVAI, M. Prevalence of pathogenic bee viruses in Hungrarian apiaries: situation before joining the European Union. **Journal of Invertebrate Pathology**, v. 98, n. 2, p. 235-238, 2008.

FOSTER, L. J; HOOG, C. L; MANN, M. Unbiased quantitative proteomics of lipid rafts reveals high specificity for signaling factors. **Proceedings of the National Academy of Sciences**, v. 100, n. 10, p. 5813-5818, 2003.

GALLAI, N; SALLES, J. M; SETTELE, J; VAISSIÈRE, B.E. Economic valuation of the vulnerability of world agriculture confronted with pollinator decline. **Ecological economics**, v.6, n. 8, p. 810-821, 2009.

GOULSON, D; NICHOLLS, E; BOTÍAS, C; ROTHERAY, E. L. Bee declines driven by combined stress from parasites, pesticides, and lack of flowers. **Science**, v. 347, n. 6229, 2015.

GOVAN, V. A; LEAT, N; ALISOPP, M; DAVISON, S. Analysis of the complete genome sequence of *Acute bee paralysis virus* shows that it belongs to the novel group of insect-infecting RNA viruses. **Virology**, v. 277, p. 457-463, 2000.

KHANNA, R; DALAI, A; KUMAR, R; KAMBOJ, R. C. Synthesis of xanthenones: a review. **Medicinal Chemistry and Drug Discovery**, v. 4, p. 840-851, 2016.

KUCHARSKI, R; MALESZKA, R. Evaluation of differential gene expression during behavioral development in the honeybee using microarrays and northern blots. **Genome Biology**, v. 3, n. 2, 2002.

LASKOWSKI, R. A; MACARTHUR, M. W; MOSS, D. S; THORNTON, J. M. PROCHECK - a program to check the stereochemical quality of protein structures. **Journal of Applied Crystallography**, v. 26, p. 283-291, 1993.

LASKOWSKI, R. A; RULLMANNN, J. A; MACARTHUR, M. W; KAPTEIN, R; THORNTON, J. M. AQUA and PROCHECK-NMR: programs for checking the quality of protein structures solved by NMR. **Journal of Biomolecular NMR**, v. 8, p. 477-486, 1996.

LIBERTO, N. A; SIMÕES, J. B; SILVA, S. P; da SILVA, C. J; MODOLO, L. V; de FÁTIMA, A; SILVA, L. M; DERITA, M; ZACCHINO, S; ZUÑIGA, O. M. P; ROMANELI, G. P; FERNANDES, S. A. Quinolines: microwave-assisted synthesis and their antifungal, anticancer and radical scavenger properties. **Bioorganic and Medicinal Chemistry**, v. 25, p. 1153-1162, 2017

LOURENÇO, A. P; MACKERT, M; CRISTINO, A. S; SIMÕES, Z. L. P. Validation of reference genes for gene expression studies in the honey bee, *Apis mellifera*, by quantitative real-time RT-PCR. **Apidologie**, v. 39, n. 3, p. 372-385, 2008.

LÜTHY, R; BOWIE, J. U; EISENBERG, D. Assessment of protein models with three-dimensional profiles. **Nature**, v. 356, n. 6364, p. 83-85, 1992.

LV, Z; CHU, Y; WANG, Y. HIV protease inhibitors: a review of molecular selectivity and toxicity. **HIV/AIDS-Research and Palliative Care**, v. 7, p. 95–104, 2015.

MAERE, S; HEYMANS, K; KUIPER, M. BiNGO: a Cytoscape plugin to assess overrepresentation of gene ontology categories in biological networks. **Bioinformatics**, v. 21, n. 16, p. 3448–3449, 2005.

MCAFEE, A; CHAN, Q; W; T; EVANS, J; FOSTER, L; J. A *Varroa destructor* protein atlas reveals molecular underpinnings of developmental transitions and sexual differentiation. **Molecular and Cellular Proteomics**, v. 16, n. 12, p. 2125-2137, 2017.

MCCARTHY, F. M; WANG, N; MAGEE, G. B; NANDURI,B; LAWRENCE, M. L; CAMON, E. B; BARRELL, D. G; HILL, D. P; DOLAN, M. E; WILLIAMS, W. P; LUTHE, D. S; BRIDGES, S. M; BURGESS, S. C. AgBase: a functional genomics resource for agriculture. **BMC Genomics**, v. 7, n. 229, 2006.

MCKINSTRY, M; CHUNG, C; TROUNG, H; JOHNSON, B. A; SNOW, J. W. The heat shock response and humoral immune response are mutually antagonistic in honey bees. **Scientific Reports,** v. 7, n. 8850, 2017.

MCMENAMIN, A. J; BRUTSCHER, L. M; GLENNY, W; FLENNIKEN, M. L. Abiotic and biotic factors affecting the replication and pathogenicity of bee viruses. **Current Opinion in Insect Science,** v. 16, p. 14-21, 2016.

MOLINER, E; MORO, S; SARNOS, S; ZAGOTTO, G; ZANOTTI, G; PINNAS, L. A; BATTISTUTTA, R. Inhibition of protein kinase CK2 by anthraquinone-related compounds, **The Journal of Biological Chemistry**, v. 278, n. 3, p. 1831-1836, 2003.

ONG, E.B; WATANABE, N; SAITO, A; FUTAMURA, Y; ABD EL GALIL, K. H; KOITO, A; NAJIMUDIN, N; OSADA, H. Vipirinin, a coumarin-based HIV-1 Vpr inhibitor, interacts with a hydrophobic region of VPR. **The Journal of Biological Chemistry**, v. 286, n. 16, p. 14049-14056, 2011.

POTTS, S. G; BIESMEIJER, J. C; KREMEN, C;NEUMANN, P;SCHWEIGER, O. KUNIN, W. E. Global pollinator declines: Trends, impacts and drivers. **Trends in Ecology and Evolution**, v. 25, p. 345-353, 2010.

REGO, Y. F; da SILVA, C. M; da SILVA D. L; da SILVA, J. G; RUIZ, A. L. T. G; de CARVALHO, J. E; FERNANDES, S. A; de FÁTIMA, A. Phthalazine-triones: calix[4]rene-assisted synthesis using green solvents and their anticancer activities against human cancer cells. **Arabian Journal of Chemistry**, *In press*, DOI: http://dx.doi.org/10.1016/j.arabjc.2016.04.007, 2016.

REYNALDI, F. J; SGUAZZA, G. H; PECORARO, M. R; TIZZANO, M. A; GALOSI, C.M. First repost of viral infections that affect argentine honeybees. **Environmental Microbiology Reports**, v. 2, n. 6, p. et al; 2010;

SHANNON, P; MARKIEL, A; OZIER, O; BALIGA, N. S; WANG, J. T; RAMAGE, D; AMIN, N; SCHWIKOWSKI, B; IDEKER, T. Cytoscape: a software environment for integrated models of biomolecular interaction networks. **Genome Research**, v. 13, n. 11, p. 2498-2504, 2003.

SHEPHERD, S; LIMA, M. A. P; OLIVEIRA, E. E; SHARKH, S. M; JACKSON, C. W; NEWLAND, P. L. Extremely low frequency electromagnetic fields impair the cognitive and motor abilities of honey bee. **Scientific Reports**, v. 8, n. 7928, 2018.

SZKLARCZYK, D; GABLE, A. L; LYON, D; JUNGE, A; WYDER, S; HUERTA-CEPAS, J; SIMONOVIC, M; DONCHEVA, N. T; MORRIS, J. H; BORK, P; JENSEN, L. J; MERING, C. V. STRING v11: protein-protein association networks with increased coverage, supporting functional discovery in genome-wide experimental datasets. **Nucleic Acids Research**, v. 47, p. D607-D613, 2019.

TARIQ, Q. U; MALIK, S; KHAN, A; NASEER, M. M; KHAN, S. U; ASHRAF, A; ASHRAF, M; RAFIQ, M; MAHMOOD, K; TAHIR, M. N; SHAFIQ, Z. Xanthenone-based hydrazones as potent α-glucosidase inhibitors: synthesis, solid state self-assembly and *in silico* studies. **Bioorganic Chemistry**, v. 84, p. 372-383, 2019.

TEHEL, A; BROWN, M. J. F. AND PAXTON, R. J. Impact of managed honey bee viruses on wild bees. **Current Opinion in Virology**, v. 19, p. 16-22, 2016.

TEIXEIRA E. W; CHEN, Y; MESSAGE, D; PETTIS, J; EVANS, J. D. Virus infection in Brazilian honey bees. **Journal of Invertebrate Pathology**, v. 99, p. 117-119, 2008.

TENTCHEVA, D; GAUTHIER, L; ZAPPULLA, Z; DAINAT, B; COUSSERANS, F; COLIN, M. E; BERGOIN, M. Prevalence and seasonal variations of six bee viruses in *Apis mellifera* L. and *Varroa destructor* mite populations in France. **Applied and environmental microbiology**, v. 70, n. 12, p. 7185-7191, 2004.

THADURIS, S; STEPHAN, J. G; de MIRANDA, J. R; LOCKE, B. Disentangling host-Parasite pathogen interactions in a *Varroa* resistant honeybee population reveals virus tolerance as an independent, naturally adapted survival mechanism. **Scientific Reports**, v. 9, n. 6221, 2019.

TIMIRI, A. K; SINHA, B. N; JAYAPRAKASH, V. Progress and prospects on DENV protease inhibitors, **European Journal of Medicinal Chemistry,** v. 117, p. 125-143, 2016.

TROTT, O; OLSON, A. J. AutoDock Vina: improving the speed and accuracy of docking with a new scoring function, efficient optimization, and multithreading. **Journal of Computational Chemistry**, v. 31, p. 455-491, 2010.

TYANOVA, S; TEMU, T; COX, J. The MaxQuant computational plataform for mass spectrometry-based shotgun proteomics. **Nature**, v. 11, n. 12, p. 2301-2319, 2018.

UEIRA-VIEIRA, C; ALMEIDA, L. O; de ALMEIDA, F. C; AMARAL, I. M. R; BRANDEBURGO, M. A. M; BONETTI, A. M. Scientific note on the first molecular detection of the *Acute bee paralysis virus* in Brazilian stingless bees. **Apidologie**, v. 46, n. 5, p. 628-639, 2015.

VICINI, P; INCERTI, M; COLLA, P. L; LODDO, R. Anti-HIV evaluation of benzo[d]isothiazole hydrazones. **European Journal of Medicinal Chemistry,** v. 44, n. 4, p. 1801-1807, 2009.

VIDAU, C; PANEK, J; TEXIER, C; BIRON, D. G; BELZUNCES, L. P; GALL, M. L; BROUSSARD, C; DELBAC, F; ALAOUI, H. E. Differential proteomic analysis of midguts from *Nosema ceranae*-infected honeybees reveals manipulation of key host functions. **Journal of Invertebrate Pathology**, v. 121, p. 89-96, 2014.

VIEIRA, R. P; SANTOS, V. C; FERREIRA, R. S. Structure-based approaches targeting parasite cysteine proteases. **Current Medicinal Chemistry**, v. 25, p. 1-18, 2018.

WANG H; MEEUS, I; SMAGGHE, G; *Israeli acute paralysis virus* associated paralysis symptoms, viral tissue distribution and Dicer-2 induction in bumblebee workers (*Bombus terrestris*). **Journal of General Virology**, v. 97, p. 1981-1989, 2016.

WHITTEN, M. M. A; TEW, I. F; LEE, B. L; RATCLIFFE, N. A. A novel role for an insect apolipoprotein (Apolipophorin III) in β-1,3-glucan pattern recognition and cellular encapsulation reactions. **The Journal of Immunology**, v. 172, p. 2177-2185, 2004.

ZHAI, Y; ZHAO, X; CUI, Z; WANG, M; WANG, Y; LI, L; SUN, Q; YANG, X; ZENG, D; LIU, Y; SUN, Y; LOU, Z; SHANG, L; YIN, Z. Cyanohydrin as an anchoring group for potent and selective inhibitors of enterovirus 71 3C protease. **Journal of Medicinal Chemistry**, v. 59, p. 9414-9420, 2015.

ZHANG, Y. I-TASSER server for protein 3D structure prediction. **BMC Bioinformatics**, v. 9, n. 40, 2008.

ZHOU, T; SHI, Q; CHEN, C. H; HUANG, L; HO, P; MORRIS-NATSCHKE, S. L; LEE, K. H. Anti-AIDS agents 85. Design, synthesis, and evaluation of 1R,2R-dicamphanoyl-3,3-dimethyldihydropyrano-[2,3-c]xanthen-7(1H)-one (DCX) derivatives as novel anti-HIV agents. **European Journal of Medicinal Chemistry**, v. 47, p. 86-96, 2012.

Supplementary material

Table 3- Proteins identified on the Group Control (Control A *vs*. Control B)

Down-regulated			Up-regulated		
ID	**log2foldchange**	**-log10p-value**	**ID**	**log2foldchange**	**-log10p-value**
gnl|Amel_4.5|GB46365-PA	-0,432091169	2,103522661	gnl|Amel_4.5|GB53186-PA	3,509722735	2,75004473
gnl|Amel_4.5|GB49629-PA	-0,475894706	1,835677263	gnl|Amel_4.5|GB50170-PA	1,276440477	2,146388784
gnl|Amel_4.5|GB51262-PA	-1,893133273	1,791268713	gnl|Amel_4.5|GB43247-PA	1,743006333	1,529055201
gnl|Amel_4.5|GB52158-PA	-0,904883951	1,746513664	gnl|Amel_4.5|GB44549-PA	1,678708768	1,477867848
gnl|Amel_4.5|GB52530-PA	-1,166121204	1,712351444	gnl|Amel_4.5|GB40934-PA	1,087078212	1,469520288
gnl|Amel_4.5|GB44583-PA	-2,506213857	1,557542358	gnl|Amel_4.5|GB52531-PA	0,876705922	1,43779196
gnl|Amel_4.5|GB42871-PA	-0,97116426	1,504459693	gnl|Amel_4.5|GB49377-PA	0,25381955	1,432648519
gnl|Amel_4.5|GB47303-PA	-2,919788967	1,467219261	gnl|Amel_4.5|GB42053-PA	3,114569623	1,377175706
gnl|Amel_4.5|GB42482-PA	-1,125437048	1,379677002	gnl|Amel_4.5|GB41418-PA	2,216064217	1,375016705
gnl|Amel_4.5|GB43548-PA	-0,201950193	1,355629626	gnl|Amel_4.5|GB53578-PA	1,142920341	1,373454618
gnl|Amel_4.5|GB44869-PA	-0,674969827	1,338924847	gnl|Amel_4.5|GB46562-PA	0,992018396	1,355025499
gnl|Amel_4.5|GB47478-PA	-0,61556952	1,33675773	gnl|Amel_4.5|GB43302-PA	2,251674209	1,343940966

gnl|Amel_4.5|GB44777-PA	-0,711351944	1,308777041
gnl|Amel_4.5|GB41068-PA	-0,757132955	1,306771258
gnl|Amel_4.5|GB55977-PA	-0,524048577	1,303295769

Table 4- Proteins identified on the Group Treatment 2 (Treatment 2 *vs*. Control B)

Down-regulated			**Up-regulated**		
ID	**log2foldchange**	**-log10p-value**	**ID**	**log2foldchange**	**-log10p-value**
gnl|Amel_4.5|GB44420-PA	-2,98605	1,949866	gnl|Amel_4.5|GB45545-PA	0,868896	3,768684
gnl|Amel_4.5|GB44726-PA	-2,34363	1,870883	gnl|Amel_4.5|GB41332-PA	0,90086	2,82524
gnl|Amel_4.5|GB46707-PA	-1,92904	1,820455	gnl|Amel_4.5|GB42929-PA	1,872419	2,449342
gnl|Amel_4.5|GB44493-PA	-2,6266	1,671581	gnl|Amel_4.5|GB52999-PA	0,372093	1,863809
gnl|Amel_4.5|GB46006-PA	-1,98627	1,650112	gnl|Amel_4.5|GB54747-PA	0,519996	1,79556
gnl|Amel_4.5|GB41852-PA	-0,98713	1,621511	gnl|Amel_4.5|GB42648-PA	0,921965	1,692901
gnl|Amel_4.5|GB44467-PA	-0,82645	1,58789	gnl|Amel_4.5|GB44222-PA	0,974988	1,663168
gnl|Amel_4.5|GB55285-PA	-0,58344	1,582072	gnl|Amel_4.5|GB55212-PA;gnl|Amel_4.5|GB55211-PA	2,410962	1,538776
gnl|Amel_4.5|GB42467-PA	-0,94972	1,552076	gnl|Amel_4.5|GB42526-PA	1,148359	1,515194
gnl|Amel_4.5|GB48289-PA	-0,29757	1,545946	gnl|Amel_4.5|GB40783-PA	1,248423	1,493684
gnl|Amel_4.5|GB43827-PA	-4,26513	1,532151	gnl|Amel_4.5|GB43540-PA	0,851541	1,370821
gnl|Amel_4.5|GB43902-PA	-0,85285	1,530757	gnl|Amel_4.5|GB49999-PA	0,613812	1,362955
gnl|Amel_4.5|GB53195-PA	-1,32423	1,505855	gnl|Amel_4.5|GB51356-PA	0,501657	1,345946
gnl|Amel_4.5|GB44583-PA	-2,45805	1,48062	gnl|Amel_4.5|GB43618-PA	1,441914	1,340076
gnl|Amel_4.5|GB46978-PA	-1,88801	1,448917	gnl|Amel_4.5|GB55729-PA	0,293467	1,331507
gnl|Amel_4.5|GB49220-PA	-1,63209	1,421822	gnl|Amel_4.5|GB40718-PA	0,970882	1,318348
gnl|Amel_4.5|GB55329-PA	-1,1575	1,403788			
gnl|Amel_4.5|GB51282-PA	-0,65811	1,387899			
gnl|Amel_4.5|GB47431-PA	-1,79885	1,317522			
gnl|Amel_4.5|GB45267-PA	-0,80241	1,301228			

4. Conclusão geral

Neste trabalho foi possível avaliar o efeito da temperatura sobre a fisiologia e a resposta imunológica de abelhas operárias (*Apis melliferas*) artificialmente infectadas pelo ABPV. O aumento da temperatura promoveu maior multiplicação viral e também exerceu influência sobre a expressão de genes relacionados a resposta humoral (defensina, himenoptaecina e abaecina) e celular (fenol oxidase e lisozima). A resposta contra o ABPV não parece ser mediada pelos genes estudados, que foram menos expressos em condições de maior viremia. Observou-se também que este patógeno causa prejuízos sobre o metabolismo energético do hospedeiro e também sobre os processos celulares de tradução e transporte vesicular. Proteínas envolvidas na via de choque térmico foram mais expressas nas condições de maior carga viral, indicando que esta via pode estar envolvida na resposta imunológica contra o ABPV. O grupo mantido a uma temperatura acima do ideal (36 ±2ºC) apresentou alta mortalidade, evidenciando a influência da temperatura sobre o desenvolvimento e sobrevivência das abelhas.

Também foi avaliado o efeito de antivirais sintéticos contra o ABPV *in vivo*. A infecção de abelhas recém emergidas via alimentação se mostrou bastante eficiente e observou-se que o Composto 2 foi o mais promissor dentre as moléculas sintéticas computacionalmente selecionadas. O tratamento com este composto favoreceu o metabolismo energético das operárias e foi capaz de reduzir a expressão relativa de ABPV em 79,4%.

ANEXO I

Relatório descritivo

USO DE XANTENONA SINTÉTICA E EXTRATO ETANÓLICO DE EUTERPE EDULIS EM SOLUÇÃO DE SACAROSE PARA O CONTROLE DA INFECÇÃO POR VÍRUS CAUSADOR DE PARALISIA (ABPV) EM ABELHAS

CAMPO TÉCNICO DA INVENÇÃO

1. A presente invenção refere-se ao uso de soluções de sacarose contendo a molécula sintética 12-(naftalen-1-il)-2,3,4,12-tetrahidro-1H-5-oxatetrafen-1-ona (Composto 2) ou o extrato etanólico de *Euterpe edulis* como aditivos alimentares para abelhas a fim de controlar a infecção causada pelo *Acute bee paralysis virus* (ABPV). Este vírus, quando encontrado em altas concentrações, pode provocar a morte das abelhas em poucos dias. O ABPV é um patógeno encontrado em vários países e é uma das principais infecções virais na América do Sul, o que torna o seu controle uma ação importante para a manutenção de colônias em apiários. Uso de antivirais como aditivos alimentares é uma abordagem fácil e não invasiva que se mostrou eficiente na redução da carga viral de ABPV em escala experimental e pode ser aplicada no setor apícola.

ESTADO DA TÉCNICA

2. As mortes de abelhas são um alarmante problema econômico e ambiental que tem preocupado pesquisadores, produtores e governos. Não há uma causa definida para as perdas massivas de colônias ou para os casos de *Colony Collapse Disorder* (CCD), todavia estes casos estão relacionadas a um conjunto de fatores que atuam enfraquecendo as abelhas e as tornando mais suscetíveis à infecções (GOULSON, D. *et al*. Bee declines driven by combined stress from parasites, pesticides, and lack of flowers. Science, v. 347, p. 1-16, 2015).

3. Em geral, doenças virais são a maior ameaça para as abelhas domesticadas ao redor do mundo e mais de 20 vírus já foram identificados em *Appis mellifera*. A maior parte destes patógenos compartilham semelhanças como genoma +ssRNA e um vetor em comum: o ácaro *Varroa destructor* (TEHEL, A., BROWN, M. J. F., PAXTON, R. J. Impact of managed honey bee viruses on wild bees. Current Opinion in Virology, v. 19, p. 16-22, 2016).

4. Dentre os vírus encontrados em abelhas o *Acute bee paralysis virus* (ABPV) apresenta distribuição global e é a principal infecção viral na América do Sul (de MIRANDA, J. R., CORDONI, G., BUDGE, G. The *Acute bee paralysis virus-Kashmir bee virus-Israeli acute paralysis virus* complex. Journal of Invertebrate Pathology, v. 103, p. S30–S47, 2010). A infestação por varroa está intimamente relacionada à intensidade da infecção por ABPV, que quando ocorre em altas concentrações provoca sérios danos neurológicos e morte das abelhas em poucos dias (DEGRANDI-HOFFMAN, G., CHEN, Y. Nutrition, immunity and viral infections in honey bees. Current Opinion in Insect Science, v. 10, p. 170-176, 2015).

5. Devido à gravidade deste ectoparasita, foram desenvolvidos diversos métodos acaricidas para conter as infestações por varroa e, consequentemente, os patógenos transmitidos por ele. Uso de acaricidas comerciais (derivados de organofosforados e piretróides), criação de armadilhas no interior da colônia, inserção de predadores ou linhagens de varroa com baixa virulência são exemplos de técnicas que apresentam moderada eficiência e alguns efeitos colaterais como contaminação dos produtos apícolas, efeito tóxico sobre as abelhas ou pouca efetividade em larga escala. O método amplamente utilizado é a aplicação periódica de ácido fórmico, que apresenta eficácia superior a 90% se aplicado de forma correta (ROSENKRANZ, P., AUMEIER, P., ZIEGELMANN, B. Biology and control of *Varroa destructor*. Journal of Invertebrate Pathology, v. 103, p. S96-S119, 2010).

6. Até o momento não são usados tratamentos químicos contra a infecção por ABPV ou outros vírus em abelhas. Porém, o extrato natural de *Laurus nobilis* apresentou eficiente ação antiviral, diminuindo a carga viral de Black queen cell virus (BQCV) sem alterar a expressão proteica do hospedeiro (AURORI, A. C. et al. Bay laureal (*Laurus nobilis*) as potential antiviral treatment in naturally BQCV infected honeybees. Virus Research, v. 222, p. 29-33, 2016). O uso de ribonucleases artificiais foi capaz de inativar o ABPV por meio da degradação do material genético sem detrimento da capsula viral antes da infecção, entretanto este estudo não avaliou as moléculas antivirais após serem metabolizados pelo hospedeiro (FEDOROVA, A. A. et al. Inactivation of a non-enveloped RNA vírus by artificial ribonucleases: Honey bees and *Acute bee paralysis virus* as a new experimental model for in vivo antiviral activity assessment, Antiviral Research, v. 91, p. 267-277, 2011).

7. Tendo em vista as limitações para controle do varroa e o grande impacto do ABPV sobre a saúde das abelhas e qualidade da produção apícola, a presente invenção busca atuar diretamente

sobre o vírus. As xantenonas sintéticas e as antocianinas que compõe o extrato etanólico de *E. edulis* foram selecionadas computacionalmente devido à seu potencial ação inibitória sobre a protease viral, enzima essencial para o processo de replicação do vírus. A aplicação dos compostos estudados na alimentação através de uma solução de sacarose contendo cada um dos antivirais se mostrou um método eficiente no controle da carga viral em escala experimental.

DESCRIÇÃO DAS FIGURAS

8. Figura 1: Estrutura das quatro xantenonas sintéticas selecionadas por ancoragem molecular e seus respectivos valores de energia de ligação ao sítio ativo da protease viral. A molécula denominada "Composto 2" (12-(naftalen-1-il)-2,3,4,12-tetrahidro-1H-5-oxatetrafen-1-ona) promoveu grande redução da expressão de ABPV, sendo esta a substância sintética cujo uso é requerido nesta invenção.

9. Figura 2: Composição do extrato etanólico do fruto de *Euterpe edulis* (ao centro). As três antocianinas principais encontradas no extrato são: cianidina-3-O-glicosídeo (37,8%); cianidina-3-O-rutinosídeo (53,0%) e cianidina-3-O-sambubiosídeo (2,8%). Os valores de energia de ligação ao sítio ativo da protease viral também estão representados.

10. Figura 3: Organização dos grupos de tratamentos da infecção artificial de abelhas com ABPV. A) Recipiente plástico acoplado ao tubo contendo a solução de tratamento. Foram colocadas seis abelhas em cada recipiente. B) Distribuição dos 16 grupos: dois grupos controle (abelhas operárias infectadas e não infectadas) e sete grupos alimentados com as soluções de sacarose 50% contendo os potenciais antivirais sintéticos, extrato etanólico de própolis e de *E. edulis*. Cada tratamento foi avaliado em duas concentrações diferentes.

11. Figura 4: Eletroforese em gel de agarose 1% com o produto da amplificação por PCR. Confirmação da infecção por ABPV via alimentação. Canaleta 1: grupo Controle B (controle negativo); canaleta 2: grupo Controle A (controle positivo) após 48 h; canaleta 3: grupo Controle A após 72h; e canaleta 4: abelhas sintomáticas de Passa Quatro-MG (controle positivo da reação de PCR).

12. Figura 5: Resultado do RT-qPCR. Gráfico representando a expressão do ABPV em relação ao gene endógeno β-actina em cada um dos grupos tratados e no grupo controle. As barras marcadas com asterisco são os tratamentos que tiveram a expressão relativa de ABPV significativamente menor que o grupo controle (teste-t, p-valor < 0,05).

DESCRIÇÃO DETALHADA DA INVENÇÃO

13. A presente invenção trata do uso de solução de sacarose (50% m/v) contendo a xantenona sintética (Composto 2) ou o extrato etanólico de *E. edulis* (0,3% m/v) como aditivos alimentares de ação antival contra o patógeno de abelha ABPV. O processo de seleção destes aditivos seguiu as seguintes etapas:

Modelagem computacional da protease viral

14. Para a construção do modelo da protease viral utilizou-se a sequência do genoma de ABPV definida no banco de dados National Center for Biotechnology Information (NCBI) como região da protease-C3G (NP_066241.1). O modelo foi desenvolvido pelo servidor online I-tasser (YANG, J., ZHANG, Y. I-TASSER server: New development for protein structure and function predictions. Nucleic Acids Research, v. 43, p. W174-W181, 2015), software considerado o estado-da-arte para a predição de estrutura de proteínas. A qualidade do modelo foi avaliada por parâmetros internos do referido software de modelagem e também pelos programas Verify 3D (http://servicesn.mbi.ucla.edu/Verify3D/), Procheck (http://servicesn.mbi.ucla.edu/PROCHECK/) e Errat (http://servicesn.mbi.ucla.edu/ERRAT/), que mensuram a qualidade estereoquímica do modelo com base em estruturas experimentais de proteínas.

Estudo de ancoragem molecular

15. Utilizando o modelo da protease viral como alvo foi realizado estudo de ancoragem entre o alvo e ligantes naturais e sintéticos descritos na literatura. Dentre um conjunto de 187 moléculas foram selecionadas aquelas com melhor afinidade de ligação pelo sítio ativo da protease.

16. As moléculas sintéticas de maior afinidade pela protease viral pertencem à classe das xantenonas (Figura 1) e foram sintetizadas e caracterizadas por da Silva e colaboradores (da SILVA, D. L., *et al*. Xanthenones: Calixarenes-catalyzed syntheses, anticancer activity and QSAR studies. Organic and Biomolecular Chemistry, v. 13, p. 3280-3287, 2015).

17. O extrato etanólico do fruto de *Euterpe edulis* continha as moléculas de maior afinidade pela enzima alvo (Figura 2). O preparo do extrato foi descrito por Novello e colaboradores (NOVELLO, A., et al. Chemical characterization, antioxidant and antiatherogenic activity of anthocyanin-rich extract from *Euterpe edulis* mart. in mice. Journal of Food and Nutrition Research, v. 54, p. 101-112, 2015).

18. Para o preparo do extrato utilizou-se 3,0 kg de frutos maduros de *Euterpe edulis*, lavados em água corrente por 3 vezes e submersos em água morna (45-60ºC) por 1 hora, a fim de facilitar a remoção da polpa. Em seguida os frutos são colocados em solução clorada (40 ppm) por 30 minutos e lavados com água potável por aspersão. Adicionou-se solução de etanol 80% e ácido cítrico 0,3% (solvente extrator, pH 3,8). Frutos e solvente foram homogeneizados em batedeira caseira por 4 minutos, na proporção de 2:1 (100 g de fruto bruto: 50 ml de solvente). A polpa foi peneirada e filtrada por gaze para a separação das fibras e sementes, cujo peso correspondeu a cerca de 91% do fruto bruto. Essa relação varia de acordo com o teor de maturidade dos frutos. O extrato foi armazenado em frasco âmbar à -80ºC até o congelamento. Em seguida o material foi liofilizado, obtendo-se um extrato seco que foi utilizado nas etapas que seguem.

Identificação do ABPV no Estado de Minas Gerais

19. Para confirmar a presença do vírus em abelhas sintomáticas coletadas em Passa Quatro-MG foi realizada a extração do RNA total de seis indivíduos (dois por réplica) com o reagente comercial TRIzol (Invitrogen). Em seguida foi sintetizado o cDNA com a enzima MultiScribe Reverse Transcriptase (Applied Biosystems) de acordo com as instruções do fabricante e utilizando o primer oligo dT. Os primers utilizados para a reação de PCR foram descritos por Teixeira e colaboradores (TEIXEIRA, E. W., *et al*. Virus infections in Brazilian honey bees. Journal of Invertebrate Pathology, v. 99, p. 117-119, 2008) e apresentam especificidade pelo ABPV identificado no Brasil, gerando um amplicon de 500 pb (ABPV-F 5'-TCTGATGATGCTGAAGAGAGAAA-3'; ABPV-R 5'-AATCATCATTGCCGGCTCTA-3'). Após a amplificação por PCR o fragmento foi purificado com o kit GFX PCR DNA and Gel Band Purification (Amersham Biosciences), de acordo com instruções do fabricante e inserido no vetor pGEM-T Easy (Promega). Nesta etapa foi utilizado 5 µl de 2X Rapid Ligation Buffer, 1 µl pGEM-T Easy (50 ng), 3 µl do DNA purificado e 1 µl T4 DNA Ligase, incubados à temperatura ambiente por 1 hora. Em seguida, o vetor contendo o inserto foi colocado em células competentes de *E. coli* DH5□ por transformação com choque térmico (42ºC por 1 minuto seguido de 2 minutos em banho de gelo). Para o cultivo das células transformadas foi utilizado 1 ml de meio Luria-Bertani (LB) (Fisher) líquido. O meio contendo as bactérias foi incubado por 1 hora a 37ºC sob agitação, centrifugado a 13000 g por 10 minutos e descartou-se 900 µl do sobrenadante. As células foram ressuspensas no volume restante e plaqueadas em meio LB sólido contendo ampicilina (100

µg/ml), X-gal (80 µg/ml) e IPTG a 0,5 mM. As placas foram incubadas a 37ºC por 16 horas e as colônias brancas foram selecionadas e cultivadas em LB líquido por 14 horas sob agitação a 37ºC. Os plasmídeos foram purificados (kit Wizard® Plus SV Minipreps DNA Purification System (Promega)) e sequenciados (Myleus Facility). A sequência do fragmento foi molde para a construção dos primers específicos para ABPV utilizados na etapa de qPCR (Tabela 1).

Preparo da solução infecciosa

20. Nesta etapa foram maceradas 10 abelhas sintomáticas coletadas em apiário de Passa Quatro-MG em 10 ml da mistura tetracloreto de carbono e água (1:4, v/v). Em seguida, a mistura foi filtrada em gaze e centrifugada a 3000 rpm por 10 minutos. A fração orgânica foi descartada (BAILEY, L., GIBBS, A. J., WOODS, D. Two Viruses from Adult Honey Bees (Apis mellifera Linnaeus). Virology, v. 21, p. 390-395, 1963). A fim de ampliar a carga viral na solução infecciosa realizou-se uma infecção inicial de abelhas de Viçosa-MG. Para isso foram selecionadas 36 abelhas recém nascidas de colônias cuja ausência de ABPV foi previamente confirmada por RT-PCR. Injetou-se 1 µl da fração aquosa descrita anteriormente no abdome de cada indivíduo, com o auxílio de um capilar de vidro acoplado a um micro injetor. As abelhas foram mantidas em um container plástico acoplado à um tubo de 2 ml contendo uma solução de sacarose 50%, armazenado à 33ºC por 4 dias. O alimento foi reposto diariamente. A cada 24 horas as abelhas eram inspecionadas e aquelas que apresentavam paralisia e tremores eram removidas e armazenadas à -20ºC. Ao final do quarto dia todas as abelhas foram armazenadas à -20ºC. Em seguida, realizou-se novamente a etapa de maceração e obtenção da fase aquosa (solução infecciosa), utilizada para a infecção artificial descrita a seguir.

Infecção artificial de abelhas de Viçosa

21. Os antivirais selecionados computacionalmente foram solubilizados em DMSO de modo que sua concentração final fosse de 0,1% e 0,3% e do solvente fosse de 0,4%. Foram coletadas 96 abelhas recém nascidas e divididas em 16 grupos de 6 indivíduos. Cada grupo foi colocado em um recipiente plástico contendo um tubo de 2 ml com a solução de tratamento (Figura 3A). Cada grupo foi tratado com solução de sacarose 50% + os antivirais em duas concentrações de teste + 250 µl da solução infecciosa (grupos tratados). Foram montados dois grupos controles: Controle A - solução de sacarose 50% + DMSO + 250 µl da solução infecciosa (controle positivo); e Controle

B- solução de sacarose 50% + DMSO (controle negativo). Todos os recipientes foram armazenados à 32ºC por 48 h (Figura 3B). As abelhas foram inspecionadas diariamente e aquelas que apresentavam paralisia e tremores foram removidas e armazenadas à -20ºC. Após 72 horas de infecção todas as abelhas foram armazenadas à -20ºC. A infecção foi confirmada por RT-PCR (Figura 4).

Avaliação da atividade antiviral dos tratamentos

22. A carga viral foi mensurada por RTq-PCR, utilizando os primers descritos na Tabela 1. A extração do RNA total de cada par de abelhas foi realizada utilizando o reagente comercial TRIzol (Invitrogen) de acordo com as instruções do fabricante. A fração contendo DNA+proteínas foi armazenada à -20ºC para o estudo de proteômica realizado posteriormente. O RNA de cada amostra foi quantificado com kit Qubit RNA Assay e o cDNA foi sintetizado a partir de 1,5 µg de RNA. A reação de qPCR foi feita em placa de 96 poços com duas réplicas técnicas e três biológicas, utilizando o equipamento 7500 Real Time PCR System (Applied Biosystems, Thermo Fisher Scientific, USA) pelo método de curva padrão relativa utilizando o kit GoTaq® qPCR Master Mix (Promega, Madison, USA). Nestas reações aplicou-se 1µl de cDNA com concentração de 20 ng/µl e 0,5 µl de cada primer (Tabela 1), totalizando 10 µl em cada reação. O programa no termociclador foi iniciado a 95°C por 10 minutos seguido por 40 ciclos de 95° C por 15 segundos e 60° C por 1 minuto.

23. Tabela 1- Sequência dos primers utilizados para RT-qPCR

Nome	Sequência	Gene	Referência
β-actina F	TGCCAACACTGTCCTTTCTG	gene endógeno β-actina	LOURENÇO, A. P., *et al*. Validation of reference genes for gene expression studies in the honey bee, Apis mellifera, by quantitative real-time RT-PCR. Apidologie, v. 39, p. 372-385, 2008
β-actina R	AGAATTGACCCACCAATCCA		
ABPV-F	ACTGCGCTTACGGATTTGAC	Amplicon de 171pb específico para ABPV	Construído com base na sequência de ABPV encontrado em Passa Quatro-MG
ABPV-R	TCTTGGTGTCAAAAAGCTTCG		

24. A expressão de ABPV e do gene endógeno β-actina foi mensurada em cada tratamento e a concentração de cada gene foi calculada utilizando uma curva padrão. A Figura 5 mostra a expressão relativa de ABPV em cada tratamento e no Controle A. O extrato etanólico de *Euterpe edulis* e o Composto 2 reduziram em 72,5 e 79,4% a expressão de ABPV, respectivamente. O extrato de própolis reduziu em 68,2% a infecção, um resultado já esperado tendo em vista a sua conhecida ação antiviral (controle positivo).

CONCLUSÃO

25. A invenção descrita neste relatório refere-se ao uso de solução de sacarose contendo o composto sintético denominado Composto 2 ou o extrato etanólico de *E. edulis* como aditivos alimentares capazes de reduzir a infecção por ABPV em abelhas operárias.

Desenhos

Figura 1

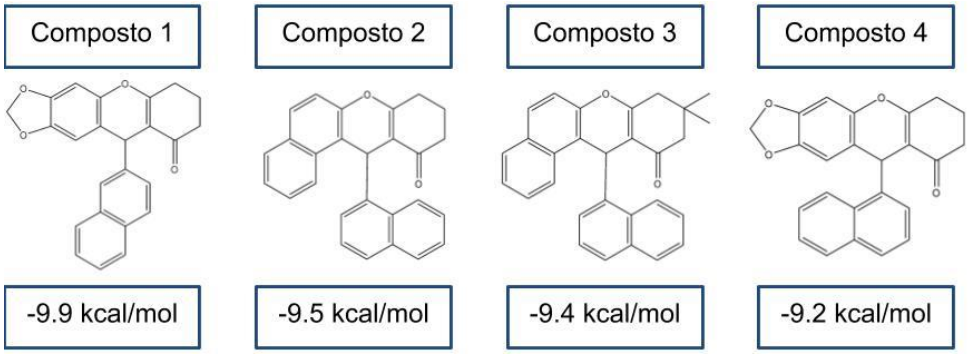

Figura 2

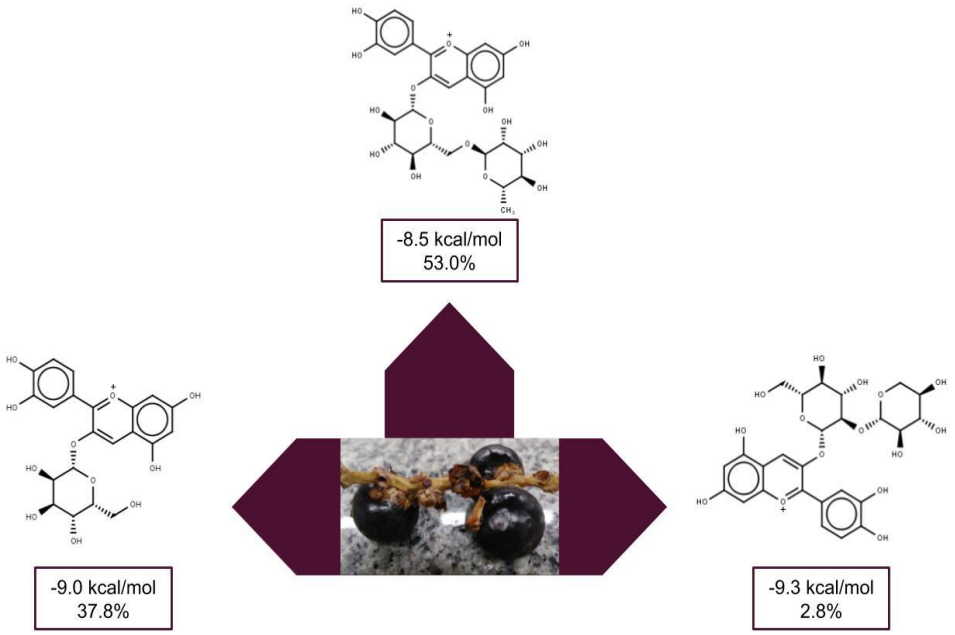

Figura 3

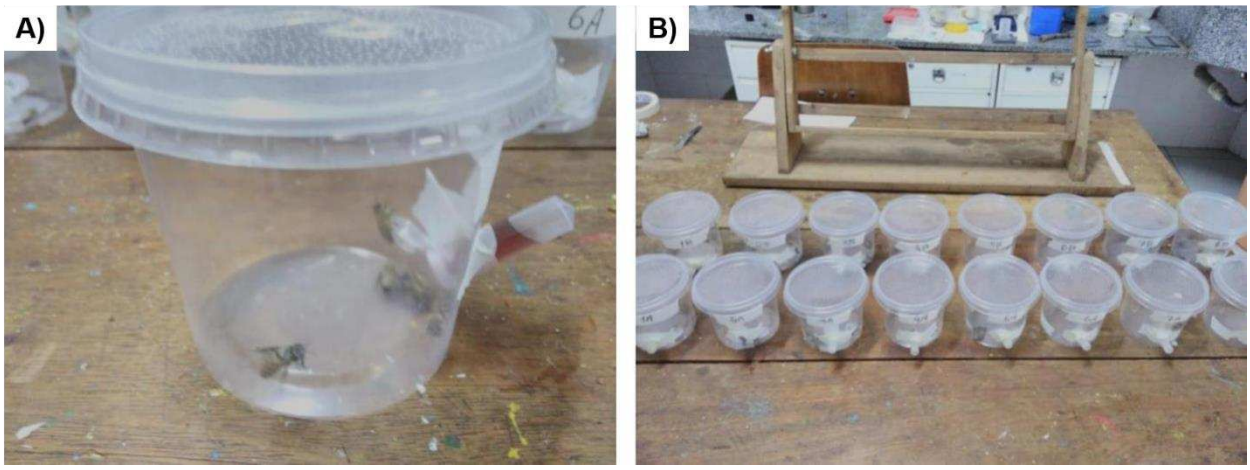

Figura 4

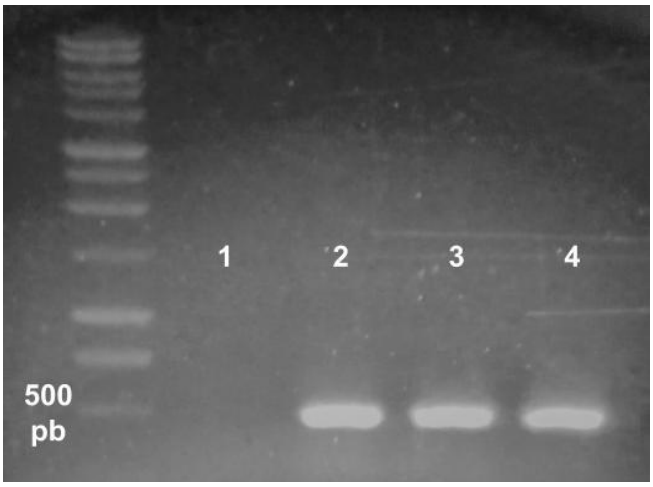

Figura 5

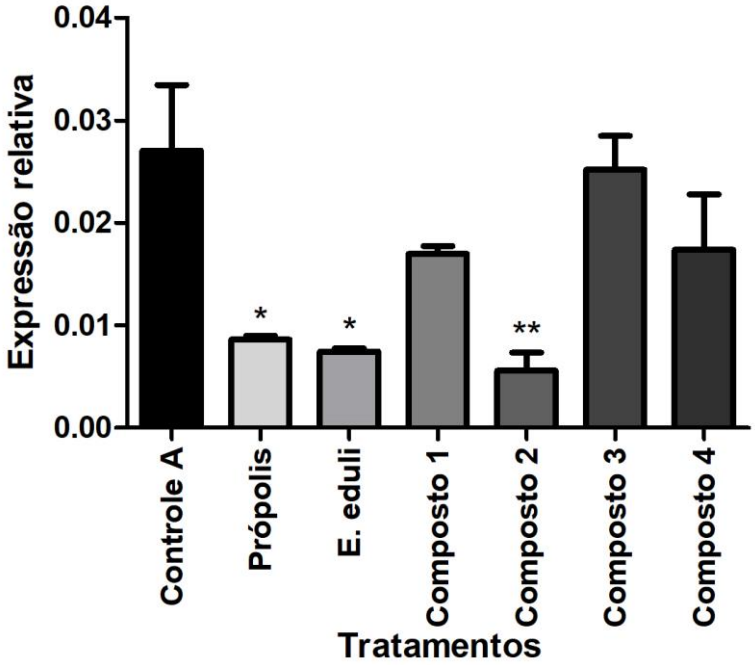
0.04
0.03
0.02
0.01
0.00
Expressão relativa
*
*
**
Controle A
Própolis
E. eduli
Composto 1
Composto 2
Composto 3
Composto 4
Tratamentos